Mechanistic Basis of Electron Transfer to Cytochromes P450 by Natural Redox Partners and Artificial Donor Constructs

10

Peter Hlavica

Abstract

Cytochromes P450 (P450s) are hemoproteins catalyzing oxidative biotransformation of a vast array of natural and xenobiotic compounds. Reducing equivalents required for dioxygen cleavage and substrate hydroxylation originate from different redox partners including diflavin reductases, flavodoxins, ferredoxins and phthalate dioxygenase reductase (PDR)-type proteins. Accordingly, circumstantial analysis of structural and physicochemical features governing donor-acceptor recognition and electron transfer poses an intriguing challenge. Thus, conformational flexibility reflected by togging between closed and open states of solvent exposed patches on the redox components was shown to be instrumental to steered electron transmission. Here, the membrane-interactive tails of the P450 enzymes and donor proteins were recognized to be crucial to proper orientation toward each other of surface sites on the redox modules steering functional coupling. Also, mobile electron shuttling may come into play. While charge-pairing mechanisms are of primary importance in attraction and complexation of the redox partners, hydrophobic and van der Waals cohesion forces play a minor role in docking events. Due to catalytic plasticity of P450 enzymes, there is considerable promise in biotechnological applications. Here, deeper insight into the mechanistic basis of the redox machinery will permit optimization of redox processes via directed evolution and DNA shuffling. Thus, creation of hybrid systems by fusion of the modified heme domain of P450s with proteinaceous electron carriers helps obviate the tedious reconstitution procedure and induces novel activities. Also, P450-based amperometric biosensors may open new vistas in pharmaceutical and clinical implementation and environmental monitoring.

P. Hlavica (✉)
Walther-Straub-Institut für Pharmakologie und
Toxikologie der LMU, Goethestrasse 33,
80336 München, Germany
e-mail: hlavica@lrz.uni-muenchen.de

E.G. Hrycay and S.M. Bandiera (eds.), *Monooxygenase, Peroxidase and Peroxygenase Properties and Mechanisms of Cytochrome P450*, Advances in Experimental Medicine and Biology 851,
DOI 10.1007/978-3-319-16009-2_10,

Keywords
P450 • Redox machinery • Key determinants • Genetic engineering • Biotechnological exploitation

10.1 Introduction

Cytochrome P450 (CYP or P450) enzymes, occurring in organisms from all domains of life [1–5], represent a superfamily of ever-growing *b*-type heme-thiolate proteins [6]. The metalloenzymes are of major importance in both the biosynthesis of endogenous compounds [7, 8] and oxidative clearance of a vast array of drugs, toxins and environmental pollutants characterized by high structural diversity [9, 10]. These processes require the consecutive delivery of two electrons to the ferric P450 catalysts to convert the unreactive atmospheric dioxygen via a generally accepted O-O bond activation cycle to a high-valent iron-oxo species capable of attacking C-H entities and heteroatoms in substrate molecules [11, 12]. Apart from this consensus mechanism, recent data spark particular interest in a "multi-oxidant" concept, providing a rationale for the striking catalytic diversification of P450s [13–15].

Although it would appear that the plethora of *CYP* genes evolved from a common ancestor [16], there exist variations in the nature of the intermediate carrier systems bridging NAD(P)H-derived reducing equivalents to specific terminal P450 acceptors [17]. Thus, in class I P450s comprising bacterial and eukaryotic mitochondrial hemoproteins, a flavin-containing ferredoxin reductase (FdR) usually operates in conjunction with an [Fe_2-S_2] cluster-bearing ferredoxin (Fdx) to shuttle electrons from the reduced cofactor to the heme iron [18]. Noteworthy, in the CYP107H1- and CYP176A1-dependent microbial electron transport chains, unusual FMN-carrying flavodoxins act as functional substitutes for ferredoxins [19–24]. In the class II monooxygenase apparatus comprising microsomal P450 proteins, FAD/FMN prosthetic components in the structure of NADPH-cytochrome P450 oxidoreductase (POR) foster swift electron delivery to the various candidates; here, the NADH-driven cytochrome b_5 (b_5)/b_5 oxidoreductase pair can serve as an alternate redox partner [18]. On the other hand, the unique CYP55A1 enzyme, promoting reductive conversion of nitric oxide to the gaseous nitrous oxide, utilizes NADH as a direct electron supplier without the need for any auxiliary mediator [25]. With other P450s such as human CYP2S1 or bacterial CYP152A/B, the typical O_2/$2e^-$/$2H^+$ proteinaceous systems fail to stimulate catalytic activity, while utilization of H_2O_2 or fatty acid hydroperoxides permits efficient substrate turnover via the peroxygenase main route based on homolytic peroxy O-O bond scission [26–28]. Similarly, biocatalysts such as CYP5A or CYP74, bringing about rearrangement of endoperoxides and hydroperoxides, respectively, require neither oxygen nor an NAD(P)H-type electron source [29, 30].

As can be readily seen, the pronounced P450-dependent specification of the redox machinery creates the challenging task of more detailed analysis of the structural and functional characteristics of the diverse electron transfer entities to improve our understanding of the observed electrochemical phenomena. In this respect, molecular modeling of composite 3D P450 constructs on the basis of the crystal structure, chemical modification and genetic engineering of a broad spectrum of hemoproteins provided an appreciable picture of both the overall topology of key determinants dictating donor docking/orientation and the nature of the driving forces supporting these events [31, 32]; this also helped assess the redox dynamics of the systems [33]. Circumstantial insight into these processes will be beneficial to the development of novel strategies serving to simplify transmission of

reducing power, such as efficient installation of the peroxide shunt pathway to overcome the prohibitive costs for NAD(P)H as the constant electron donor or curtailing of the complex electron transfer conduits [34]; this will give an impetus to exploitation of more flexible P450s in biotechnological areas encompassing the production of fine chemicals, drug processing or degradation of environmental pollutants [35, 36]. The present chapter thus highlights significant breakthroughs in our knowledge about the mechanistic basis of donor/acceptor interactions in the functionally diversified domain of P450s, paving the way for innovative tailoring of versatile redox modules.

10.2 Mechanistic Principles of Electron Transport by Natural Redox Partners of P450s

10.2.1 NADPH-Cytochrome P450 Oxidoreductase (POR)

10.2.1.1 Evolutionary History

Microsomal POR represents a prototypic member of the fairly small family of diflavin redox proteins. The enzyme bears one molecule each of FAD and FMN as cofactors and favors electron transfer from NADPH to eukaryotic P450s or cytochrome *c* as the ultimate acceptors [37, 38]. Precursors of the 78-kDa POR proteins have been hypothesized to arise from ancestral fusion of genes encoding an FMN-binding bacterial flavodoxin and a plant-type FAD-complexed ferredoxin-$NADP^+$ reductase. Subsequent evolutionary steps helped create an α-helical interdomain linker, allowing efficient functional coupling of the two flavins and an N-terminal membrane anchor region (Fig. 10.1) [39–41]. Flavodoxins as such operate in photosynthetic processes or participate in nitrate reduction as well as in methionine and biotin producing pathways [42]. Similarly, ferredoxin-$NADP^+$ reductases display high functional plasticity in supporting auto- and heterotrophic reactions [43].

Analysis of the genetic code for representative PORs from taxonomically diverse eukaryotic species mostly points at the involvement of a single gene in protein expression. Thus, the human gene, located on chromosome 7, contains 16 exons and has been found to be highly polymorphic [44–46]. Likewise, the rat gene carries 16 exons, 15 of which are coding exons. Organization of the latter strictly correlates with functional or structural domains [47]. Moreover, cytogenetic mapping of insect and fungal oxidoreductases suggests them to be single-copy products [48, 49]. Exception to this rule is given by the widespread polyploidy in plants, giving rise to gene duplication and divergence. In this respect, about 54 gene sequences encoding PORs derived from a total of 35 different plant species have as of now been identified, most of the paralogous enzymes at least partially complementing each other [50, 51]. Multiple-alignment studies revealed the majority of full-length POR proteins isolated from mammalian, insect, fungal and plant phyla to share 33–38 % amino acid sequence homology [49].

10.2.1.2 Electrochemical Features of Electron Transfer

The family of POR proteins mediates electron transfer in the NADPH→FAD→FMN→P450 redox system. Here, the flavin cofactors have a vital function in the step-down process from the obligatory two-electron donor NADPH to the one-electron acceptor P450. Using rabbit POR as a probe, flavins were shown to exist as one-electron reduced air-stable blue (neutral) semiquinones ($FMN/FMNH^{\bullet}$, $E_0' = -110\,mV$ and $FAD/FADH^{\bullet}$, $E_0' = -290\,mV$) or two-electron fully reduced red (anionic) forms ($FMNH^{\bullet}/FMNH_2$, $E_0' = -270\,mV$ and $FADH^{\bullet}/FADH_2$, $E_0' = -365\,mV$) equilibrating between these states [52–55]. Noteworthy, no shift from the blue di-semiquinone ($FMNH^{\bullet}$, $FADH^{\bullet}$) toward the red species is observed upon increasing the pH of the reaction media [56]. However, the lipid bilayer of membrane-tethered POR was found to impact the redox potential of the FMN/FAD prosthetic groups: application of anionic phospholipids was shown to drive the E_0' for the red forms of both cofactors to more negative values, favoring

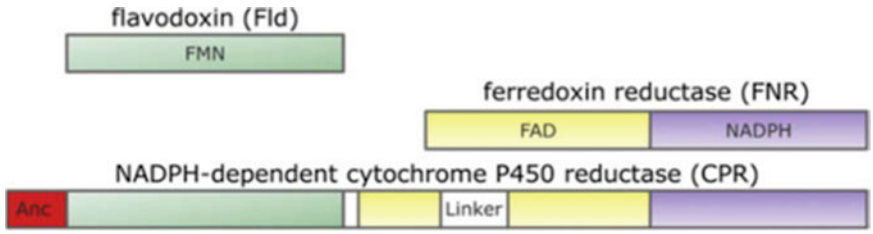

Fig. 10.1 Molecular evolution of NADPH-cytochrome P450 oxidoreductase (POR). The mammalian diflavin protein POR originates from ancestral fusion of the genes of flavodoxin and ferredoxin oxidoreductase with the subsequent creation of a flexible interdomain linker and a membrane anchor serving in proper orientation of the electron donor toward P450s (Data taken from Ref. [51])

electron transfer to P450s [57]. Similarly, structural aberrations in the flavin-binding domains of reductases from different taxa may dramatically affect the redox parameters and abilities to support the catalytic activity of P450s. For example, the redox potential of the $FMNH^{\bullet}/FMNH_2$ pair in yeast POR was shown to be more positive than that for the blue couple. This behavior contrasts the situation in the rat and plant POR species and is similar to the inversion observed with the reductase moiety of the bacterial flavocytochrome CYP102A1 [58, 59].

Elucidation of the precise pathway of flavin-driven redox cycling during electron donation to heme catalytic centers has been fuelled by techniques such as deflavination and reconstitution [60] or dissection of PORs into their component domains [61], permitting more detailed studies on the kinetic and thermodynamic properties of the enzymes. Thus, triggering of the cycle is thought to be brought about by the stable, 635 nm-absorbing FAD-$FMNH^{\bullet}$ semiquinone potentially generated during a priming reaction [62]. Upon hydride transfer from NADPH ($E_0^{'} = -320$ mV) to the latter species, interflavin electron flow proceeds from $FADH^{-}$-$FMNH^{\bullet}$ to yield $FADH^{\bullet}$-$FMNH^{-}$. At high molar excess of NADPH, this process is reversible [63]. However, under in vivo conditions, the $FMNH^{-}$ entity acts as the major one-electron supplier to the ferric heme iron of P450s, thereby returning to the resting semiquinone form in the $FADH^{\bullet}$-$FMNH^{\bullet}$ duo [52, 64]. Electron cycling between the essentially equipotential members of this redox couple to regenerate $FMNH^{-}$ seems fairly unfavorable and, indeed, occurs as a single-exponential process at a modest rate of 55 s^{-1}, even dropping to a value of 11 s^{-1} when dithionite substitutes for NADPH as the reductant. This suggests cofactor binding to play a pivotal role in regulating internal electron flux [65]. Fully reduced FMN released in the gated electron transfer event serves in P450 reduction via a one-electron step. In summation, microsomal PORs usually cycle in a 1-3-2-1 sequence, denoting the total number of electrons carried by the flavins (Fig. 10.2) [64, 66]. Opposite to this, the microbial CYP102A1 fusion protein undergoes a reduction cycle of 0-2-1-0 lacking any priming reaction [67].

10.2.1.3 Structural Elements Governing Intramolecular Electron Transfer

A drastic step forward in the study of functional domains in POR proteins was made by comparison of the full-length amino acid sequences derived from a broad spectrum of species to unveil highly conserved signature motifs amenable to circumstantial analysis by genetic engineering [49, 50]. Moreover, availability of crystallographic data for human, rat and yeast PORs [68–70] enabled three-dimensional modeling of critical enzyme structures [71, 72]. Thus, investigation of the N-terminal α-helical signal anchor segments of mammalian oxidoreductases disclosed the carboxy termini to be located on the cytoplasmic side of the endoplasmic reticulum, with the first 55–56 amino acid residues being sufficient for stable membrane insertion/retention, proper orientation and maintenance of catalytic efficiency [73–75].

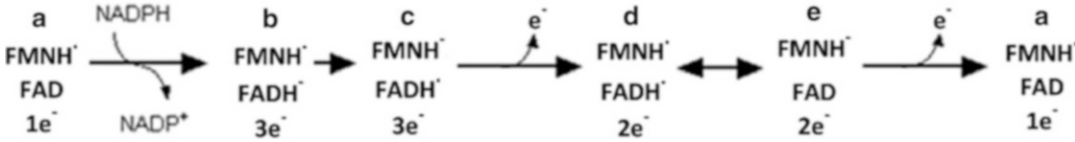

Fig. 10.2 POR-supported intra- and intermolecular electron conduction to P450s. Hydride transfer from NADPH to the stable semiquinone (**a**) elicits sequential formation of the fully reduced (**b**, **c**) intermediates to enable one-electron supply to ferric P450 associated with release of a resting semiquinone duo (**d**). Electron swapping between the latter redox couple regenerates a fully reduced cofactor (**e**) again permitting electron donation to P450s. The mammalian oxidoreductase thus cycles between the 1- and 3-electron reduced states

Despite the fairly low overall sequence identity (33–43 %) of POR enzymes from various organisms [49, 50], the FMN-binding domains exhibit a high degree of conservation [76]. Chain tracing in the scaffolds of human and rat proteins revealed an α-β-α architecture composed of a five-stranded parallel β-sheet in the core fold flanked by a variable number of α-helices, with the FMN cofactor positioned at the tip of the C-terminal side of the β-sheet [69, 71, 77]. Using the human enzyme (hPOR; NCBI reference sequence NP_000932.3) as a template, molecular docking and site-directed mutagenesis experiments suggested a set of residues such as Q90, T91, T142, H183 and N185 to be involved in FMN fixation, though Y143 and Y181 obviously act as key players [76, 78, 79]. The aromatic side chains of the two tyrosines, sitting on the *re*- and *si*-face, respectively, of the isoalloxazine ring, clasp the FMN unit at nearly the same distance of 3.5 Å [71, 77]. Both positions are conserved in the rat homolog [69] sharing 94 % sequence identity with the human counterpart [79], and Y→D exchange in the rodent protein was shown to indeed block efficient electron transfer [80]. Moreover, replacement in the human catalyst of F184, lying close to the pyrimidine tail of the cofactor, with leucine or glutamine caused a 40- to 50-fold increase in the K_d value for FMN association. This was interpreted to reflect a vital role of F184 in stabilization of the electron carrier [78]. Strikingly, L86 and L219, deeply buried in two hydrophobic cores of the FMN domain of POR from *Anopheles minimus*, aligns with F86 and F219 in the human analog. Experimental introduction into the insect enzyme of phenylalanine residues in place of the leucines proved to be beneficial to FMN docking and protein folding [75]. Of note, X-ray crystallography of oxidoreductase from the yeast *Saccharomyces cerevisiae* helped discover a second FMN-binding region at the interface of the linker and standard cofactor-bearing domain. The novel site displays low conservation throughout the gene family, with only two residues, namely, T71 and D187 corresponding to T93 and D211 in hPOR, being invariant [70]. It has been hypothesized that a single FMN molecule shuttles between the structural doublet associated with semiquinone transition from the neutral to the anionic state [70].

A fragment spanning about 40 amino acid residues of predominantly polar character bridges the gap between the FMN/FAD-harboring loci. This linker is speculated to serve in proper orientation of the flavins, the isoalloxazine rings of which make an angle of about 150° to each other and reside at a minimum distance of 3.5 Å [41, 69, 79]. In fact, mutations in the short random-coil hinge, preceding the FAD-connecting unit composed of residues G235 to R246 in the hPOR structure, induce drastic rearrangement of the FMN/FAD topology impacting intramolecular electron transfer [81]. Crystallographic analysis of the FAD-docking region in the rat protein showed the isoalloxazine entity to be hosted at the boundary between the cofactor- and NADPH-binding site, with the remainder of the molecule extending to the interface between the FAD-binding pocket and the connecting domain [69]. Site-directed mutagenesis was used to verify the functional importance of the various determinants. This demonstrated Y456 to make

van der Waals contact with the *si*-side of the FAD isoalloxazine structure and to hydrogen-bond to the ribityl 4′-hydroxyl, while amino groups in the side chains of R454 (equivalent to R457 in hPOR), G488 and T491 stabilize the negatively charged pyrophosphate. Moreover, the aromatic nucleus of Y478 stacks on one side of the adenine moiety [68, 69, 82]. Interestingly, the interplay of the S457/D675/C630 triad may have a dual role in the control of the flavin redox potential and stabilization of the transition state to facilitate hydride transfer [83, 84].

A set of homologous residues lining the NADPH-binding cavity, constituted of alternating α-helices and β-strands, operate in fixation and orientation of the cofactor in a bipartite mode. Thus, highly conserved amino acids encompassing C566, S596, R597, K602 and Y604 (rat POR numbering) make up a specific motif attracting the 2′-phosphate of NADPH via H-bonding or salt-bridging, such as to cause discrimination against NADH [79, 85–87]. In accord with this, introduction of hydrophobic elements in place of the positively charged arginine and lysine residues at positions 597 and 602 to create the triple mutant R597M/K602W/W677A resulted in a 170-fold increase in the apparent binding affinity for NADH compared to the wild-type enzyme, paralleled by an IC_{50} value for inhibition by $NADP^+$ that was 50-times higher than that of the parent enzyme [88]. Similarly, simple W676A exchange in hPOR allowed the NADH-dependent reductive potency to become equivalent to that of the NADPH-driven event [87]. On the other hand, this manipulation was found to compromise NADPH-promoted reduction beyond the two-electron level owing to slow release of $NADP^+$ from the active site upon first hydride transfer, suggestive of a vital function of the C-terminal tryptophan in electrochemical processes [89]. The mechanistic basis of such an action relies on the assumption that the π-stacking indole of W677, building a lid above the *re*-face of the FAD isoalloxazine, moves away to permit direct contact of the flavin moiety with the nicotinamide ring of NADPH required for efficient hydride transfer [69, 72]. Here, local movement of the short G631-N635 loop may be beneficial to NADPH/$NADP^+$ binding/release [90]. An overall diagram of the POR polypeptide fold disclosing the topology of the diverse cofactor-binding domains is presented in Fig. 10.3.

It should be pointed out that POR enzymes are highly polymorphic proteins. Currently, about 48 missense mutations have been identified in the human reductase (www.cypalleles.ki.se/por.

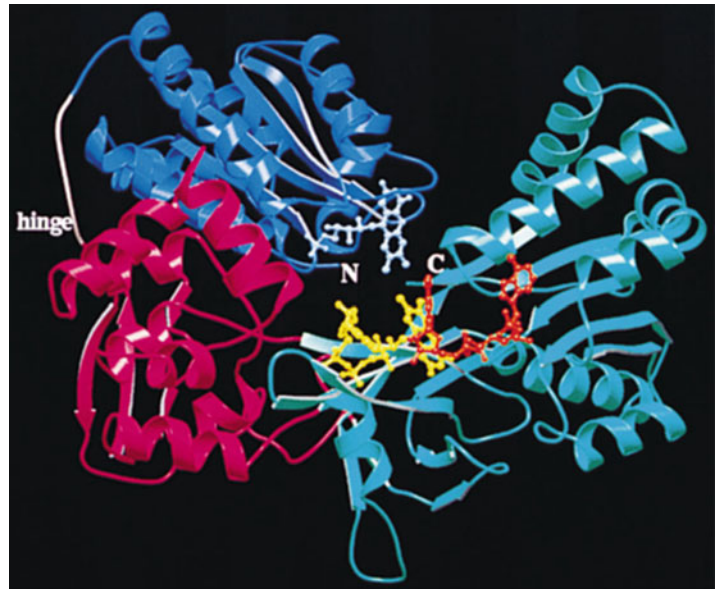

Fig. 10.3 Ribbon diagram illustrating the overall polypeptide fold and topology of POR. The FMN-binding domain is given in *blue*, while the NADP(H)- and FAD-docking sites are presented in *green*. The connecting interdomain fragment is depicted in *red*. Cofactors are presented in the ball and stick mode (PDB ID: 1AMO) (Reproduced from Ref. [69])

htm), part of which overlap with conserved residues critical for FMN/FAD/NADPH fixation [45, 79, 91]. Examples of this are found in the most important variants T142A, Y181D, R457H, Y459H, V492E, C569Y, R600W and Y607C [45, 79]. These amino acid substitutions have been recognized to be deleterious to electron transfer and, consequently, cause disordered steroidogenesis along with skeletal malformations when the allelic hPORs are to serve as obligatory donors to CYP17A1 and CYP19A1 [91, 92]. Moreover, the altered phenotypes may impact the P450-catalyzed metabolic biotransformation of both curative drugs/prodrugs and toxins [45, 46, 93]. Noteworthy, the Y181D-induced perturbation of electron flow/P450 activity has been reported to undergo restoration upon the addition of excess FMN to the assay media [76, 94]. In this case, the potential existence of a second FMN-binding site (see above) might permit the exogenous cofactor to act as a bypass.

10.2.1.4 Structural Features Steering Functional POR Docking to P450s

To bring about efficient electron shuttling from POR enzymes to P450s, a large-scale conformational rearrangement of the FMN domain is required. Available 3D structures of mammalian reductases display a closed conformation of the core region with the isoalloxazine ring of FMN being shielded by the FAD cofactor at a distance ranging from 4 to 5 Å [68, 69]. Hence, electron donation to P450s necessitates concerted movement of the domains leading to an open state associated with exposure of the FMN moiety to the solvent to enable contact with the hemoproteins. In this regard, the "closed-open" transition, as studied with free or membrane-anchored POR, was recognized to be conducted by the flexible hinge motif adjusting the distance between the FAD/FMN entities to 29–60 Å [81, 95, 96]. More detailed analysis by sophisticated spectroscopic techniques revealed the POR molecule to, indeed, toggle between a multiplicity of closed and open conformations in solution [97, 98]. Generally, opening is driven by flavin reduction, whereas closure predominates in the oxidized enzyme and is supported by NADPH binding to facilitate loading of reducing equivalents [99, 100]. These findings are in line with the "swinging" model of POR-mediated electron transfer from the nicotinamide coenzyme to the heme iron of P450s [101].

Based on the construction of model complexes between the redox partners, a docking area of ~870 $Å^2$ was calculated to guide productive encounter of the solvent-exposed FMN domain with P450s [81]. This patch, located on the surface of the extended reductase molecule, bears an electronegative profile arising from accommodation of three clusters of putative salt-bridging residues encompassing E92, E93, D113, E115, E116, E142, D144, D147 and D208 (rat POR numbering), speculated to provide a rationale for snuggly fit of the electropositive proximal face of the different P450s obviously binding in a very similar fashion [69, 71, 81, 102, 103]. The negatively charged elements surrounding the FMN moiety were predicted to form a cleft allowing a minimal distance of ~12 Å between the cofactor and the heme group [81]. The hypothetical acidic contact sites were substantiated by genetic engineering: Mutation of D113, E115 and E116 to alanine disclosed the residues to stabilize the CYP2B1/POR adduct on the one hand and open new avenues to more efficient electron transfer to the hemoprotein partner on the other [103]. Moreover, replacement of hPOR amino acids corresponding to E142, D144 and D147 in the rat homolog with the less bulky polar serine or glycine substitutes was found to moderately impinge on the catalytic efficiency (k_{cat}/K_m) of CYP2D6, while D208N exchange caused a drastic fall in P450-dependent activities [71, 104]. Two thirds of the determinants examined display 60–90 % conservation across the multitude of taxonomically diverse reductase species, the rest being invariant [76].

10.2.2 Cytochrome b_5

Cytochrome b_5 (b_5), occurring in a wide range of phyla, is a membrane-anchored amphipathic

hemoprotein operating in concert with POR or NADH-cytochrome b_5 oxidoreductase as electron donor to desaturating systems involved in fatty acid synthesis and plasmalogen-producing enzymes [105]. Of note, soluble forms of human b_5 and NADH-cytochrome b_5 oxidoreductase found in erythrocytes were shown to be capable of reducing methemoglobin [106, 107]; here, deletion of codon 298 in the gene of the flavoprotein component was detected to cause functional deficiency associated with hereditary methemoglobinemia [108]. Moreover, the ferrihemoglobin-coupled redox triad brought about O_2-dependent substrate turnover in a monooxygenase-type reaction [109]. In parallel, a considerable number of P450s were recognized to have substrate-specific obligatory requirement for electron supply by b_5 [110, 111].

10.2.2.1 Topology of the Membrane-Spanning and Heme-Binding Domains of Cytochrome b_5

Two mammalian b_5 isoforms were identified, one inserted into the endoplasmic reticulum and the other bound to the outer membrane of mitochondria. These proteins arise from different genes [112]. The hydrophobic membrane anchor of the microsomal homolog, functioning as a static retention signal, was shown to span the bilayer of the endoplasmic reticulum such that the carboxy-terminus extends to the lumen of the organelle [113, 114]. However, mutation of the C-terminal L124/M125/Y126 triad in rat b_5 to alanine was found to induce location of the engineered hemoprotein in both the cytosol and microsomal membrane, suggestive of the existence of loosely- and firmly-integrated forms differing by the overall content of α-helical structure [115, 116]. In fact, the membrane-interactive tail of b_5 has been detected to function as a stop-transfer sequence giving rise to inversion of protein orientation in the endoplasmic reticulum to permit versatile processing of nascent precytochrome b_5 during topogenesis, resulting in final positioning of the integral electron carrier in the N_{out}-C_{in} mode [117]. Another triad of potential interest embedded in the 43-amino-acid membrane-binding domain of b_5 refers to tryptophan residues at locations 108, 109 and 112. However, studies with the W108L/W112L double mutant failed to disclose any impact on electron transfer to CYP2B4 as a probe acceptor [118]. Finally, attention was drawn to P115, forming a 26° kink in a helix when occurring in the *trans* conformation. Surprisingly, P→A exchange resulted in normal insertion of the mutant into the membrane and a wild-type enzyme level of activity in a P450 test system [119].

Microsomal b_5, being 60 % α-helical, is a fairly small polypeptide composed of 134 amino acid residues, with the cytosolic heme-containing region showing ~92 % sequence identity throughout the different mammalian isoforms [105, 120]. Availability of the crystal and solution structure of the protein permitted insight into the architecture of the heme-binding pocket. Thus, the prosthetic group was shown to reside in a hydrophobic crevice, the iron atom being coordinated to histidines at positions 39 and 63; the latter reactant has some exposure to solvent via a water channel [121–123]. Dependence of the heme-holding stability on the histidine axial ligation was confirmed by H39S/C mutations, also affecting the spin state of the heme iron [124]. Apart from steric factors, changes in hydrophobicity of the heme microenvironment may modulate the electrochemical properties of the hemoprotein [125]. In accord with this, V45H/E substitutions were found to shift the redox potential of the wild-type protein ($E_0' = -10$ mV) to values of +8 mV and −26 mV, respectively [126]. Similarly, manipulation of hydrophobicity by replacement of V61 with histidine revealed to influence interaction of the heme with its pocket, resulting in broadening of the latter; this moved E_0' of the mutant by +21 mV [127]. Special interest focuses on the interplay of the F35/F58 duo, stabilizing heme docking through π-stacking overlap with the porphyrine macrocycle [128, 129]. Moreover, phenylalanine-35 is part of a hydrophobic patch of 350 $Å^2$ on the surface of b_5 [130] and member of a network that includes Y74 and the axial H39 being in direct van der Waals and electrostatic

contact with the heme [131, 132]. Apart from this, the conserved F35 is pivotal to fine tuning of the redox potential: F35Y exchange was discerned to make E_0' 66 mV more negative compared to the parent protein [133]. Finally, P40, another component of the surface patch producing a sharp γ-bend in the polypeptide chain, is believed to significantly contribute to a fixed folding pattern of the heme pocket due to its rotational restriction [134]. It should be kept in mind that, in contrast to the crystalline state, b_5 is heterogenous in solution due to the presence of two isomers, differing with respect to 180° rotation of the heme plane around the axis defined by α,γ-meso protons [135]. A diagram of key structural motifs in the b_5 backbone chain is given in Fig. 10.4.

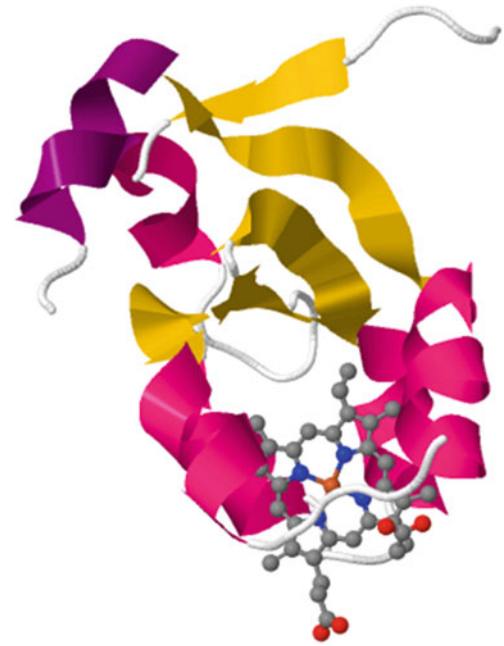

Fig. 10.4 Schematic structure of bovine cytochrome b_5. The approximately cylindrical molecule (PDB ID: 1CYO) houses α-helices 2–5 (*in red*) clustering around the prosthetic heme group given in *grey* balls and sticks. A five-stranded β-sheet (in *yellow*) in the center of the amphiphilic polypeptide separates the heme-binding pocket from a more peripheral helical segments 1 and 6 (in *violet*) (Data taken from Ref. [122])

10.2.2.2 Interaction of Cytochrome b_5 with Electron Donors

The microsomal FAD-containing NADH-cytochrome b_5 oxidoreductase acts as a physiological electron donor to the ferric b_5. Anaerobic photoreduction of the FAD moiety was observed to form the red anionic semiquinone being in equilibrium with the blue neutral species. The latter turned out to be the primary intermediate in the NADH-driven hydride transfer process [136, 137]. Here, the conserved T66 entity in the reductase structure was shown to participate in modulation of the rate-limiting interconversion of the semiquinone forms [137]. Furthermore, mutation experiments verified the importance of the specific arrangement of R63, Y65 and S99 in the β-sheet barrel core of the flavoprotein in maintenance of FAD docking by electrostatic and H-bonding attraction of the *si*-face of the isoalloxazine ring [138, 139]. Similarly, the backbone amide nitrogen of M126 forms a hydrogen bond to the phosphate oxygen of the cofactor [140]. In addition, a series of residues including K110, S127, G179 and P275 were predicted to participate in the anchoring and proper positioning of the NADH electron donor [140–145]. In this regard, the active-site C273 was considered to be critical for accurate orientation of the nicotinamide nucleus prior to hydride transfer [146]. Most interestingly, G179 and D239 were recognized to be required for efficient NADH/NADPH selectivity [144, 147].

Rapid electron transfer from NADH-cytochrome b_5 oxidoreductase to b_5 was shown to require N-terminal myristoylation of the flavoprotein to stabilize its orientation in the endoplasmic reticular membrane as a prerequisite for optimal productive encounter of the redox partners [148]. Here, circumstantial analysis implicated three reductase lysine residues hosted at positions 41, 125 and 163 in complementary charge pairing with the single exposed porphyrine propionate and a cluster of glutamate carboxyl groups at locations 43, 48, 49 and 53 (rat hemoprotein numbering) in the b_5 polypeptide, surrounding the heme edge at a distance of ~12 Å [149–152]. Qualitatively, the same b_5 carboxyls were recognized to be essential for electrostatic interaction with prospective cationic groups in the alternate POR electron donor

[153]. Employing the covalently cross-linked diflavoprotein/b_5 heterodimer as a model for a functional electron-transfer complex, FMN depletion unveiled the cofactor-binding POR domain to be the active center for responsiveness to the hemoprotein. Here, lysines at positions 72, 74 and 75 are likely candidates for charge pairing with the b_5 carboxyls [154]. As evidenced by the detrimental effect of removal of the N-terminus of POR on the functional coupling with b_5, the intact hydrophobic tails of both redox proteins are required for efficient cross-talk between the partners facilitated by free lateral movement in the plane of the membrane [155]. Here, the nature of the system utilized for reconstitution of the matrix may steer the kinetics of intra- and intermolecular electron transfer [156]. Noteworthy, flash-induced b_5 reduction by POR was found to proceed at a first-order rate about 10 % that measured with NADH-cytochrome b_5 oxidoreductase [157, 158].

10.2.2.3 Characteristics of the Catalytic Cytochrome b_5/Cytochrome P450 Redox Adduct

Cytochrome b_5 plays a supportive role as a modifier of NADPH/POR-driven monooxygenations depending on the type of substrate and P450 species involved. For example, the presence of b_5 invariably improves efficiency of product formation from methoxyflurane by CYP2B4 [159], fosters mephenytoin and chlorzoxazone turnover by CYP2C19 and CYP2E1 [160], and stimulates testosterone biotransformation by CYP3A4 [161].

The mechanism by which b_5 impacts P450 activity has been extensively studied. When bound to ferric P450, the intermediate carrier elicits a low-to-high spin transition in the iron coordination sphere of the heme chromophore of the terminal pigment [162, 163]. Owing to the unfavorable discrepancy in the midpoint potential between the Fe^{3+}/Fe^{2+} couples of b_5 (−2.6 to +5.1 mV) and substrate-free ferric P450 (~ −400 to −300 mV), acceptance by the latter species of the first electron from the presumed donor protein can be excluded [33, 125]. In contrast, E_0' for the labile oxyferrous P450 form is raised to 50 mV [164], permitting introduction of the second electron by ferrous b_5 [111, 165] at a rate faster than autoxidation of the Fe^{3+}-O_2^- intermediate associated with H_2O_2 release. This is expected to enhance economy of product formation at the expense of superoxide [166, 167]. It has to be noted that b_5 may also exert non-redox, conformational effects on P450s. Thus, the modifier was shown to increase the steady-state level of the substrate-bound iron-oxo complex through lowering the energy of activation [162, 168] and to influence the rate of regeneration of ferric P450 from the oxygenated precursor as an index of the velocity of oxidative substrate turnover [169]. Precedent to this kinetic behavior is given by the action of apocytochrome b_5 on the rate of productive decay of substrate-bound oxyferrous CYP101A1 [170]. Moreover, interaction of holo-/apo-b_5 with CYP17 triggers rearrangement of the iron-dioxygen ligand necessary to awaken lyase activity [171, 172] or promotes repositioning of substrate to favor 16-α-hydroxylation [173]. Generally, incorporation of heme-depleted b_5 into reconstituted systems containing members of the CYP2 and CYP3 families was found to enhance typical catalytic activities to differing extents [174, 175]. Specific studies with the CYP4A7 species suggested apo-b_5 to possibly alter the conformation of the substrate-binding pocket and/or accelerate product release [176]. In summation, these findings point at a dual role of b_5 as an electron donor on the one hand and an allosteric effector on the other [177, 178].

The hydrophobic α-helical, membrane-spanning domain of b_5 was demonstrated to play a dominant role in productive association with CYP2B4 [179]. However, introduction of alanines into the membrane anchor, expected to cause all amino acids distal to the insertion to undergo a 100° rotation, failed to disrupt any specific helix-helix interactions. This was interpreted to mean that b_5/P450 binding proceeds through a nonspecific mechanism [180]. In contrast, the S90-D104 fragment, linking the heme domain of b_5 with the C-terminal hydrophobic sequence, was postulated to restrict orientation of the donor/

acceptor heme regions, facilitating formation of a functional complex [181]. Stability of the latter was shown to be granted by electrostatic and H-bonding attraction of complementary P450 residues by the invariant b_5 amino acids Y30, E44, E48, D60 and T65, cooperating with the exposed heme propionate group [182–184].

10.2.3 Ferredoxins

Ferredoxins are small, soluble iron-sulfur proteins mediating electron transfer to P450s and other proteins such as nitrate and sulfite reductase. Classification of the intermediate carriers comprises different prototypes depending on the total number as well as Fe/S-proportion of the prosthetic clusters defining the active-site structure of the various electron shuttles [185]. In this regard, [Fe_2-S_2]-bearing ferredoxins, occurring in plants, bacteria and vertebrates, are of special interest [186]; the latter category includes both pro- and eukaryotic representatives [187]. Here, most extensive studies focus on the mammalian mitochondrial adrenodoxin (Adx) and the microbial putidaredoxin (Pdx) [188, 189], donating electrons to class I P450s [18]. Electron bridging requires prior transfer of reducing equivalents to ferredoxins by FAD-carrying NAD(P)H-ferredoxin reductases generally belonging to distinct types of unrelated protein families [40]. With respect to this, NADPH-adrenodoxin reductase (AdR) and NADH-putidaredoxin reductase (PdR) were uniformly assigned glutathione reductase-type redox proteins [190, 191].

10.2.3.1 Recognition of Adrenodoxin by Redox Partners

Site-directed mutagenesis experiments revealed the core domain of Adx, housing a single [Fe_2-S_2] cluster, to be mandatory for Adx/AdR association, while a second, acidic interaction site encompassing residues at positions 56–90 serves in docking of both AdR and P450s [192]. In accord with this, D72, D76 and D79 of Adx build up a tight H-bonding network with R211, R240 and R244 of AdR [193], but equally well operate in fixation of the steroidogenic CYP11A1 [194]. Noteworthy, the salt bridge between the invariant E74/R89 residues turned out to exert a principal stabilizing force impacting the orientation and redox properties of the iron-sulfur motif in parallel to AdR and CYP11A1 binding [195]. Genetic engineering of Y82 suggested the amino acid to be of importance in complex formation of Adx with CYP11A1 and CYP11B1, but to leave electron transfer unaffected [196]. In contrast, histidine at position 56 was recognized to control the integrity and ligand field of the protein region surrounding the [Fe_2-S_2] cluster [197]. Thus, H56T exchange was found to shift the redox potential of the wild-type Adx (−274 mV) to a value of −340 mV, causing a ~2.3-fold increase in the rate of CYP11A1 reduction [198]. Similarly, the vicinal T54 was recognized to modulate the protein's redox state: conservative T→S replacement lowered E_0' by ~60 mV as compared to the native ferredoxin without affecting AdR coupling and CYP11A1 reduction, though there was a marginal decrease in K_d for spectral binding of the hemoprotein [199, 200]. Of note, C-terminal truncation (Δ113–128) of Adx followed by S112W substitution was found to cause an 11-fold increase in the rate of CYP11A1 reduction associated with a 60-fold rise in the enzyme's catalytic efficiency [200]. Finally, sequential deletion of residues E47, G48, T49, L50 and A51, located in a surface loop covering the iron-sulfur center, disclosed the domain to be crucial to regulation of the redox potential and functional coupling of AdR and CYP11A1 [201, 202].

As can be readily seen, the extensive spacial overlap of the interaction sites of Adx for AdR and P450 makes formation of a ternary complex improbable [203]. This view is substantiated by results from carbodiimide-mediated covalent crosslinking of Adx carboxylates to lysines on either AdR or CYP11A1. Structure-based assessment of the individual crosslink positions excluded a cluster model, but unequivocally suggested the ferredoxin to act as a mobile electron shuttle [204, 205]. Here, transport of reducing equivalents was hypothesized to proceed via

both monomeric or dimeric Adx species [206]. The architecture of Adx-Adx assembly resulting in an asymmetric dimer was disclosed by crystal-based molecular modeling [207].

10.2.3.2 Molecular Recognition of Putidaredoxin by Redox Partners

Major driving forces in Pdx/PdR recognition were proven to encompass steric complementarity along with hydrophobicity and polarity. Thus, modeling studies combined with crystal-based mutagenesis experiments to modify both bulkiness of prospective key amino acids and their efficiency in charge pairing or van der Waals contacts identified the voluminous Y33 and R66 of Pdx, flanking the 365 $Å^2$ protein-protein interface, to bind to R65/T66 and E335, respectively, in PdR. Substitution of the two ferredoxin residues with amino acids of lower molecular mass significantly increased the binding affinity of mutated Pdx to PdR, but drastically diminished k_{cat} for electron transfer to the iron-sulfur cluster in view of moderate effects on E_0' [208, 209]. This was interpreted to mean that the bulky side chains of tyrosine and arginine prevent tight docking of Pdx, so that transfer of reducing equivalents may occur via alternate pathways. In fact, optimal orientation for swift electron flow from FAD to the [Fe_2-S_2] center was predicted to be provided by interaction of W310 of PdR with D38 of the intermediate carrier [208, 209]. Moreover, ion pairing of the two residues is expected to lower the activation free energy for reduction of the metal cluster [189]. Evaluation of mutation and crosslinking data suggested the α-helical E72 of Pdx to form a salt bridge with K409 of PdR serving to establish and stabilize the electron transfer complex [209, 210], while the adjacent C73 seems to not only modulate the ferredoxin's redox potential but to also define spacial approach of the subunits of the redox partners [208, 211]. Owing to flexibility of its aromatic ring, the C-terminal W106 of Pdx, oriented toward the center of the groove close to W330 of PdR [208], is thought to play a mediating and/or regulating role in the electron transfer process [212].

Importantly, the tryptophan at position 106 is of dominant importance in functional coupling of Pdx with the camphor-hydroxylating bacterial CYP101A1. Here, W106 is of higher relevance to transfer of the second electron to the oxyferrous hemoprotein than to donation of the first reducing equivalent to the ferric enzyme. This was argued to arise from the fact that the bulky, rigid indole ring of the tryptophan residue is apt to penetrate deep enough to approach the heme-binding loop of CYP101A1 [213] and induce structural changes required for acceleration of dioxygen activation, thus assisting the role of Pdx as an allosteric effector [189, 214]. It thus appears that the essential tryptophan exists in a conformational microheterogeneity [215]. In addition, D38 of the ferredoxin component was recognized to represent another hot spot in the two-step reductive event [214]. Starting from 3D modeling and molecular dynamics simulations, a series of amino acids such as D34 of the intermediate carrier were hypothesized to be likely candidates for intermolecular salt bridge formation, affording fixation of the Pdx/CYP101A1 complex [216]. In fact, D34N mutation was shown to depress catalytic efficiency (V_{max}/K_m) of the P450 system to a level 44 % of that found with the wild-type Pdx species [217]. Moreover, S42C exchange in the polypeptide clearly impacted donor/acceptor interaction [211].

Comparative evaluation of the general docking mode of the redox partners disclosed partial overlap of the proposed binding areas for PdR and CYP101A1 on the surface of the Pdx molecule, suggesting that the reductase and the hemoprotein cannot simultaneously interact with the ferredoxin [211]. This view seems to be in contrast to the competent function of a ternary PdR-Pdx-CYP101A1 fusion protein reported by others. Mobility of the fixed Pdx subunit of the latter construct appeared to be, nonetheless, high enough to pass electrons to exogenous native CYP101A1 introduced into the assay mixture [218]. In accord with this, analysis by optical biosensor techniques demonstrated the covalently immobilized three-component complex to exhibit only loose arrangement between Pdx and

the terminal acceptor [219]. Also, studies on the kinetic behavior in dependence on the molar proportion of the individual redox partners supported the notion that Pdx acts as an electron transfer shuttle between PdR and CYP101A1 in analogy to the Adx-promoted route [220]. This raises the question as to what extent the bacterial CYP101A1-dependent system might be comparable to the mitochondrial CYP11A1-steered redox chain. Thus, inspection of the superimposed Adx/Pdx 3D structures, no doubt, permits one to discern significant homology (Fig. 10.5). Despite this, the two ferredoxins cannot substitute for each other in the two catalytic pathways owing to pronounced discrepancies in a series of functional determinants: (1) none of the acidic residues of Pdx corresponding to those vital to Adx fixation to CYP11A1 participate in intermolecular interactions with CYP101A1; (2) while T49 of Adx controls the redox dynamics of the iron-sulfur cluster, the equivalent S44 in Pdx fails to play such a role; (3) whereas the C-terminal aromatic tryptophan of Pdx is pivotal to tight CYP101A1 docking, the extended analogous region of Adx is deficient in such a P450-binding element. The interplay of these shortcomings causes Pdx and Adx to be unable to donate the second electron to the oxyferrous forms of the heterologous hemoproteins [221].

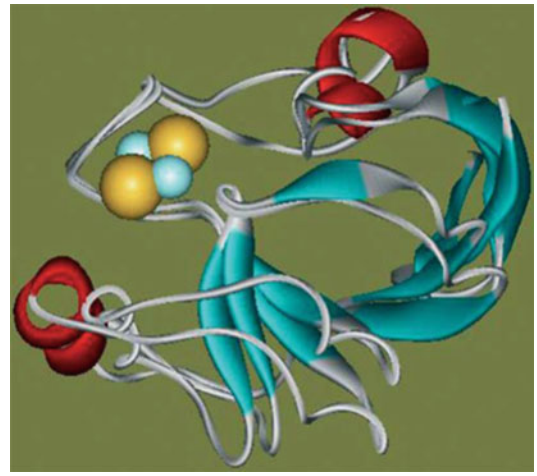

Fig. 10.5 Superposition of the three-dimensional structures of adrenodoxin (*top*) and putidaredoxin (*bottom*). The Adx (PDB ID: 1AYF) and Pdx (PDB ID: 1PUT) proteins, representing typical examples for vertebrate-type ferredoxins characterized by a sequence homology of ~35 %, display a similar planar geometry of the iron-sulfur cluster-containing region (spheres in *yellow* and *blue*). Generally, the overall folding topology of the α-helical and β-sheet elements shows a high degree of identity, with a 1.64 Å r.m.s. deviation between the two electron carriers (Reproduced from Ref. [221])

10.2.4 Unorthodox Electron Transfer Chains

Though P450s usually receive reducing equivalents from their dedicated redox partners, nonconventional electron transfer chains are frequently constructed to facilitate in vitro reconstitution of the donor/acceptor modules. For this purpose, the vertebrate-type ferredoxin/ferredoxin reductase components belong to the most frequently used surrogates of native intermediate carriers. Thus, the mitochondrial AdR/Adx couple turned out to interact with intact microsomal CYP1A1 such as to support erythromycin *N*-demethylation at higher efficiency compared to the inherent electron donor [222]. Similarly, Adx was demonstrated to cross-react with CYP2B enzymes, N-terminal hemoprotein truncation eliciting balanced reductive potency between the ferredoxin-promoted and P450 reductase-driven systems [223, 224]. Also, the truncated microsomal CYP17A1 and CYP21A2 proteins show higher steroid 17α-hydroxylase and 21-hydroxylase activity, respectively, with AdR/Adx compared to POR as the electron supplier [225]. Interestingly, CYP46A1, predominantly functional in cholesterol 24-hydroxylation in the brain, was found to interact with Adx as a redox component [226]. The mitochondrial carrier also sustains electron donation to the bacterial steroid 15β-hydroxylase CYP106A2 from *Bacillus megaterium* [227]. The system even operates at elevated catalytic capacity when AdR is replaced with NADPH-flavodoxin reductase from *Escherichia coli* to establish a novel robust redox chain [228]. Noteworthy, a mitochondrial ferredoxin

reductase/ferredoxin unit from the fission yeast *Schizosaccharomyces pombe* was found to have >50 % sequence similarity with the mammalian AdR/Adx counterpart. The redox pair supports CYP11A1-catalyzed biotransformation of 7-dehydrocholesterol [229].

In addition, [Fe_2-S_2] proteins from non-mitochondrial sources have been demonstrated to transfer electrons to heterologous P450s. For example, plant-type ferredoxin and NADPH-ferredoxin reductase from spinach chloroplasts promote oxidative substrate turnover by microsomal CYP1A2 and CYP3A4 [230, 231] as well as 25-hydroxylation of vitamin D_2 by CYP105A1 from *Streptomyces griseolus* [232]. Furthermore, bacterial electron transport systems such as the PdR/Pdx pair proved to foster β-carotene hydroxylation by the thermostable CYP175A1 species [233]. When working in concert with PdR, the microbial palustrisredoxin A factor readily feeds reducing equivalents to CYP199A2, preferentially metabolizing four-substituted benzoates [234]. Also, reconstitution of linredoxin and linredoxin reductase from a soil pseudomonad with CYP2B4 yields a collective efficiently metabolizing benzphetamine [235].

In some instances, *Escherichia coli* flavodoxin/flavodoxin reductase was detected to provide a basis for facile electron donation to microsomal P450s such as CYP1A2 [230], CYP3A4 [231] and CYP17A1 [236], but to equally-well pass electrons via a ping-pong mechanism to the microbial fatty acid oxidases CYP102A1 and CYP152A2 [237, 238]. Of note, a catalytically active system could also be established by employing flavodoxin reductase together with the unusual flavodoxin cindoxin from *Citrobacter braakii* as redox partners for CYP107H1 from *Bacillus subtilis*, having a role in biotin biosynthesis [19]. Finally, electron supply by POR from the yeast *Candida apicola* to the myristate-metabolizing CYP109B1 seems to be a unique case, where a eukaryotic diflavin reductase acts as a versatile electron donor to a bacterial hemoprotein [239]. In summation, cross-reactivity of electron carriers with a diversity of heterologous P450s can be reconciled with evolutionary conservation of a common functional domain architecture steering donor/acceptor interactions [32].

10.3 Topology of Critical Regions in P450s Dictating Interaction with Natural Redox Partners

10.3.1 Docking of NADPH-Cytochrome P450 Oxidoreductase

Data from chemical/immunochemical modification, molecular modeling and targeted mutagenesis were collated to generate an overall picture of key determinants in P450s responsible for POR fixation. Here, the N-terminal membrane-spanning signal anchor sequence of microsomal P450s seems to have a general role in protein-protein association: deletion of the membrane-immersed portion of CYP1A2 drastically decreases affinity for POR [230]. Genetic tailoring of a (Δ2–27)-variant of CYP2B4 proved to be detrimental to POR binding, resulting in a pronounced drop in the efficiency of electron transfer to the recipient [179, 240]. Chemical modification of the enzyme's N-terminal α-amino group through covalent attachment of fluorescein isothiocyanate was recognized to compromise reductase docking via motional perturbation of the fluorophore-labeled region, eliciting a long-range effect on some distant patch involved in productive POR complexation [241]. Similarly, truncation of CYP2D6 was found to increase the K_d value for reductase binding by a factor of 11 [242]. Surprisingly, analogous manipulation of CYP2C3 and CYP2E1 failed to impede fixation of the flavoprotein [243, 244]. In contrast, the N-terminus of CYP6B33 from the insect *Papilio multicaudatus* is likely to maintain a protein fold obviously instrumental to communication with POR [245]. Also, construction of the (Δ1–66)-derivative of CYP52A3 from the yeast *Candida maltosa* was found to diminish reactivity toward POR [246].

To assess critical residues in P450s involved in the functional coupling of POR, CYP1A1 was covalently modified through treatment with

acetic anhydride or an azido analog of benzphetamine. Selective blockage of four lysines at positions 97, 271, 279 and 407 was found to eliminate POR-dependent enzyme activity [247, 248]. This finding corresponds to results from studies with antibody targeted against a K271/K279-containing fragment of the hemoprotein, disclosing inhibition of metabolic turnover as the potential consequence of a rise in K_m for POR [249]. In addition, attachment of 4,4′-dithiodipyridine to C293 in the CYP1A1 polypeptide was shown to be reversible upon incorporation of POR into the assay media, suggesting the residue to be located close to the reductase-binding motif [250]. This view receives support from antibody-directed suppression of substrate turnover following blockage of a region in the CYP1A2 homolog aligning with positions C293 to N301 in CYP1A1 [251]. Moreover, nitration of Y243 and Y271 in the CYP1A2 molecule was found to slow down electron transfer from POR to the acceptor [252]. Finally, site-directed mutagenesis helped verify prospective key players: Replacement in CYP1A1 of lysine at positions 271 and 279 with isoleucine caused a severe loss of responsiveness to POR for the hemoprotein [253]. Similarly, there was a 2- to 4-fold increase in the K_d value for POR anchoring when the basic lysines occurring at positions 94, 99, 440 and 453 in CYP1A2 were exchanged for an acidic residue [254, 255].

Within the plethora of drug-metabolizing P450s, inhibition of CYP2B1-mediated substrate oxidation by immunoprecipitation of the enzyme's K122 to T231 sequence was shown to be less pronounced when antipeptide was added after reconstitution of the system with POR, proposing the epitope to be most likely engaged in POR association [256]. This concept is in line with R125 obviously having a critical role in this event [257]. Further lysine residues in CYP2B1, putatively serving as candidates for reductase recognition, reside at positions 251, 384, 422 and 433 [258]. Kinetic analysis of the chemically modified CYP2B4 analog in the absence and presence of protective amounts of POR disclosed lysines 139, 144, 251 and 384 to be in presumptive contact with the electron donor at a distance of about 3–4 Å [259]. Moreover, substitution of predominantly basic amino acids, hosted in the polypeptide fragment spanning residues R122 to K139, with the hydrophobic alanine entity drastically increased the K_d value for reductase binding to CYP2B4 [260]. Additional positively charged elements in the surface structure of the hemoprotein, identified by genetic engineering to promote electron flow from POR, include K225, H226, R232, R253 and H285 along with R422, K433 and R443 located in the vicinity of the heme edge [260–262]. On the other hand, a series of aromatic and hydrophobic amino acids such as F223, F227, F244, V267 and L270 were uncovered to participate in π-π-stacking and H-bonding interactions with POR [261, 263]. Of note, charge-reversal mutation K139E in the polymorphic CYP2B6.8 variant was found to impair functional complexation with POR [264]. This finding agrees with data from cross-linking experiments with the wild-type enzyme, disclosing competition of the latter with the synthetic D134-R140 peptide in reductase capture [265]. It should be mentioned that arginines at positions 139, 144 and 442, hypothesized to be beneficial to contacts with the electron donor in allelic CYP2C8 and CYP2C9 proteins as well as in CYP2C19, coincide with corresponding patches on CYP2B members [266–268]. Also, homology modeling of CYP2E1 in parallel with chemical inactivation by nitration of a series of tyrosines elucidated a close relationship between the FMN domain of POR and Y422 [269]. Noteworthy, C98W mutation in CYP3A4 was found to significantly hamper affinity to POR, associated with a 41 % diminution in the maximum rate of electron flow between the P450 and flavoprotein [270]. In addition, molecular modeling revealed the neighboring Y99 to be in close proximity to the cofactor-binding region of POR, while Y430 forms a hydrogen bond with an acidic reductase residue at a distance of 2.3 Å [271].

Inspection of microsomal P450s involved in the biosynthesis of natural products helped rescue further information about the architecture of donor/acceptor complexes. Thus, chemical and genetic modification of CYP17A1, lying at the

crossroad of androgen and corticoid formation, unveiled the positively charged amino acids K326, K327, R347 and K358 to constitute part of the POR-contacting area [272, 273]. Similarly, a set of missense mutations at K121, R339, R341 and R356 provided clues to better understanding of the mode of interaction of POR with the steroid 21-hydroxylase CYP21A2 [274–276]. Finally, construction of a molecular model of the lanosterol 14α-demethylase CYP51F1 from yeast allowed identification of unique residues such as H101, K358, R426 and K433, serving as prospective sites for reductase association [277]. A compilation of the topological data for POR docking to the diverse P450s is given in Table 10.1.

10.3.2 Docking of Cytochrome b_5

In cases where P450s exhibit an obligatory requirement for electron donation by b_5 to maintain optimal rates of substrate turnover, structural integrity of the hydrophobic tail portion of the oxidases seems to be pivotal to productive donor/acceptor coupling. For example, optical biosensor studies with CYP2B4 lacking amino acids 2–27 disclosed removal of the signal anchor to result in defective binding of the intermediate carrier accompanied by a pronounced drop in the reductive force [179, 240]. Apart from this, circumstantial exploration of a set of CYP2 members helped ascertain an array of critical b_5-docking entities sitting remote from the enzymes' N-terminus. Thus, strongly perturbed donor anchoring upon generation of the R129S derivative of CYP2A5 suggested the RRFS fragment in the polypeptide chain to be a key recognition motif [278]. This conclusion nicely coincides with the fact that the homologous CYP2A4, bearing a R129S point mutation, fails to stimulate substrate oxidation [279]. Interestingly, site-specific attack on K122, R125 and S128 in the CYP2B1 polypeptide by immunochemical manipulation or protein kinase-mediated phosphorylation was found to be competitively antagonized by the presence of b_5, suggesting these residues to be in contact with the electron donor [280, 281]. Moreover, elements R122, R126, R133, F135, M137, K139, H226 and K433, selected by computer docking of a CYP2B4 model, were substituted with alanine to evaluate the function of the amino acid side chain distal to the β-carbon. All the mutants tested displayed diminished ability to bind b_5 [260]. Genetic engineering was also employed to confirm the biological importance of K428 and K434 in CYP2E1/b_5 complexation [282].

Studies extended to other P450 families verified sites K127 and K421 on CYP3A4 to be essential for efficient b_5 coupling [283]. Moreover, impairment of the fundamental chemistry by introduction of mutations at positions 83, 88, 347, 358 and 449 in CYP17A1 was demonstrated to hamper propensity for 17,20-lyase activity by disrupting responsiveness to the b_5 component [171, 273, 284]. Table 10.1 provides a synopsis of key amino acids in P450s governing interaction with b_5.

10.3.3 Docking of Ferredoxins

Use of a specific fluorescence probe localized the heme group of the mitochondrial CYP11A1 protein ~26 Å remote from the binding surface for adrenodoxin (Adx) [285]. Here, basic residues K73, K109, K110, K126, K145, K267, K270, K338 and K342 on the mature hemoprotein form were substantiated to govern reactivity toward Adx by the ferredoxin's ability to act as an almost complete protector against the lysine-modifying agents, succinic anhydride or fluorescein isothiocyanate, employed for enzyme engineering [286, 287]. Two additional lysines corresponding to K377 and K381 in the precursor form of steroidogenic CYP11A1 were identified by site-directed mutagenesis as also being vital to Adx association. Estimated K_d values for donor docking increased about 150- to 600-fold compared to the wild-type enzyme depending on the particular lysine substitute [288]. This finding fits data from specific chemical labeling of lysines in the peptide comprising amino acids M369 to K381 in the CYP11A1 molecule, eliciting a

Table 10.1 Prospective key amino acids of P450 enzymes governing interactions with redox partners: representative results from molecular modeling, genomic analyses and site-directed mutagenesis

				Interacting redox partner			
CYP enzyme	Residue modified	Alignment position[a]	Location in 2° structure[b]	POR	b_5	Fdx[c]	Refs.
51F1	H101	57	αB	+			[277]
1A1	K97	59	αB	+			[247]
1A2	K94	59	αB	+			[254]
17A1	K83	59	αB		+		[171]
101A1	R72	59	αB		+	+	[298]
11A1	K73	63	αB			+	[286]
101D1	R77	63	αB			+	[304]
1A2	K99	64	αB	+			[254, 255]
17A1	K88	64	αB		+		[171]
2B1	K122	97	αC		+		[280]
2B4	R122	97	αC	+	+		[260]
11A1	K109	97	αC			+	[286]
101A1	R109	97	αC			+	[299]
119	R109	97	αC			+	[303]
3A4	K127	98	αC		+		[283]
11A1	K110	98	αC			+	[286]
2B1	R125	100	αC	+	+		[257]
101A1	R112	100	αC			+	[299–301]
101D1	R113	100	αC			+	[304]
2A5	R129	101	αC		+		[278, 279]
2B4	R126	101	αC	+	+		[260]
21A2	K121	101	αC	+			[274]
2B1	S128	103	αC		+		[281]
2B2	S128	103	αC		+		[281]
2B4	S128	103	αC		+		[281]
102A1	L104	104	αC	+			[354]
2B4	R133	108	αC1	+	+		[260]
2B4	F135	110	αC1	+	+		[260]
2B4	M137	112	αC1	+	+		[260]
2B4	K139	113	αC1	+	+		[259, 260]
2B6	K139	113	αC1	+			[264]
11A1	K126	114	αC1			+	[286]
2C9	R144	118	αD	+			[267]
11A1	K145	133	αD			+	[286]
2B4	H226	197	αG	+	+		[260, 261]
2B4	F227	198	αG	+			[261]
2B4	R232	203	αG	+			[261]
101A1	K197	209	αG			+	[302]
2B4	F244	215	αG	+			[261]
1A1	K271	221	αG	+			[247]
2B1	K251	222	αG	+			[258]
2B4	K251	222	αG	+			[259]
1A2	Y271	224	αG	+			[252]
2B4	R253	224	αG	+			[261]
1A1	K279	229	αG-αH	+			[253]
2B4	V267	236	αH	+			[263]
2B4	L270	239	αH	+			[263]
1A1	C292	241	αH-αI	+			[250]

(continued)

Table 10.1 (continued)

CYP enzyme	Residue modified	Alignment position[a]	Location in 2° structure[b]	Interacting redox partner			Refs.
				POR	b_5	Fdx[c]	
11A1	K267	245	αH-αI			+	[286]
11A1	K270	248	αH-αI			+	[286]
2B4	H285	250	αI	+			[262]
17A1	K326	288	αJ	+			[272]
17A1	R347	308	αJ‘	+	+		[273, 284]
21A2	R339	308	αJ‘	+			[276]
21A2	R341	310	αJ‘	+			[276]
51F1	K358	310	αJ‘	+			[277]
11A1	K338	315	αK			+	[286, 287]
27A1	K354	315	αK			+	[296]
199A2	R285	315	αK			+	[305]
11A1	K342	319	αK			+	[286]
17A1	R358	319	αK	+	+		[273, 284]
27A1	K358	319	αK			+	[296]
21A2	R356	325	αK	+			[276]
1A1	K407	349	β2(2)-β1(3)	+			[247]
2B1	K384	349	β2(2)-β1(3)	+			[258]
2B4	K384	349	β2(2)-β1(3)	+			[259]
51F1	R426	377	MR	+			[277]
3A4	K421	380	MR		+		[283]
27A1	R418	380	MR			+	[296]
11A1	K405	383	MR			+	[292]
101A1	K344	383	MR		+	+	[298]
51F1	K433	384	MR	+			[277]
2B1	K422	386	HBR	+			[258]
2B4	R422	386	HBR	+			[260]
2E1	Y422	386	HBR	+			[269]
102A1	Q387	387	HBR	+			[354]
1A2	K440	388	HBR	+			[254]
3A4	Y430	388	HBR	+			[271]
2E1	K428	391	HBR		+		[282]
1A2	K453	397	HBR	+			[255]
2B1	K433	397	HBR	+			[258]
2B4	K433	397	HBR	+	+		[260]
2E1	K434	397	HBR		+		[282]
1A2	R455	399	HBR	+			[254]
11A1	R426	404	αL			+	[292]
24A1	R466	404	αL			+	[294]
2B4	R443	407	αL	+			[260]
2C19	R442	407	αL	+			[268]
17A1	R449	407	αL		+		[284]
101D1	R371	407	αL			+	[304]
199A2	L369	408	αL			+	[305]

[a]Positions were determined by screening the sequences of the target P450 enzymes against the crystal structure of substrate-bound CYP102A1 (PDB ID: 1ZO9) as described previously [277, 307]

[b]Allocation of the alignment positions to definite domains of α-helical or β-sheet structure is based on the CYP102A1 architecture [314]. *MR* meander region, *HBR* heme-binding region

[c]The category of ferredoxins includes Adx, Arx, Pdx and Pux

drastic fall in responsiveness to the electron-supplying factor [289]. Of note, point mutation R→C at position 366 in CYP11B1, corresponding to K377 in the CYP11A1 congener, was detected to give rise to breakdown of the catalytic efficiency of 11β-hydroxylation to a level ~25 % that of the native protein. This has been interpreted to mean that a change to cysteine eliminates a positive charge and leaves a cove on the enzyme's surface, most likely impacting Adx fixation [290]. Interest also focused on residue C264 lying proximate to K267 in the so-called "hinge" region. Indeed, chemical blockage of the surface cysteine was found to hamper CYP11A1-promoted turnover through curtailing the catalyst's capacity to interact with Adx [291]. Moreover, biochemical and molecular modeling studies based on the crystal structure of the redox partner jointly supported the concept that K405 and R426 (numbering of the mature hemoprotein form) participate in electrostatic contacts with Adx [292]. There seems to exist an interplay between the latter amino acid and the conserved vicinal E429 residue responsible for fine tuning of the stability of the assembled complex [293]. Crystallographic analysis of the 24-hydroxylase CYP24A1 from rat again revealed structural elements K378 and K382, aligning with lysines at positions 377 and 381 in bovine CYP11A1, to operate as key players in Adx recognition. In addition, the invariant R466, located 8–10 Å remote from the conserved lysines, was assigned a dominant function in ferredoxin-driven electron transfer [294]. The critical arginine aligns with R426 in CYP11A1 and R458 in the murine CYP27B1. In fact, R458Q substitution was detected to induce a 36-fold rise in the apparent K_m value for Adx associated with a drastic decrease in electron pressure [295]. Finally, introduction of the K354A/K358A/R418S triad into CYP27A1 involved in bile acid biosynthesis was shown to be destructive to ferredoxin binding [296].

Epitope mapping, carried out with bacterial CYP101A1 from *Pseudomonas putida* in the presence of a set of antigenic peptides directed against areas presumed to be of functional relevance, suggested regions spanning residues 63–72 and 108–117, respectively, to potentially participate in putidaredoxin docking [297]. This view was underpinned by the severe loss of reactivity toward Pdx upon creation of hemoprotein variants bearing non-ionic amino acids in place of the positively charged arginine at positions 72, 109 and 112 [217, 298, 299]. It should be emphasized that ferredoxin binding to R112 has been recognized to also be beneficial to intracomplex electron transfer to the ferric heme iron-oxo species [300, 301]. Moreover, the ability of the intermediate carrier to shield K197 in the P450 molecule from attack by chemical modifiers qualifies the lysine residue as part of the Pdx recognition site [302]. Similarly, reversal of the cationic charge by K344E mutation was demonstrated to cause perturbation of donor docking [298]. Interestingly, CYP119A1 from thermophilic *Sulfolobus acidocaldarius* utilizes Pdx as the electron supplier. Here, D77R mutation of the hemoprotein was detected to markedly enhance fixation of the redox partner and stimulate electron flow by a factor of about 5 compared to the parent enzyme, obviously eliminating a potentially repulsive protein-protein interaction [303]. The repellent effect of D77 thus might serve in proper Pdx orientation.

Other bacterial P450s receive electrons via $[Fe_2\text{-}S_2]$-type ferredoxins genomically associated with the individual oxidases. For example, evaluation of the electrostatic surface profile of CYP101D1 from the oligotrophic *Novosphingobium aromaticivorans* suggested amino acids such as R77, R113 and R371 to contribute to specificity in [2Fe-2S]-type ferredoxin (Arx) recognition [304]. Furthermore, the benzoic acid-oxidizing CYP199A2 from *Rhodopseudomonas palustris* was recognized to carry two surface hot spots presumed to be significant factors in steering cross-reactivity of ferredoxins. Thus, the presence of R285 as well as charge reversal at L369 were hypothesized to be responsible for preferential functional coupling of the physiological redox partner palustrisredoxin compared to the heterologous Pdx [305, 306]. A summary of data for ferredoxin docking to vertebrate-type P450s is presented in Table 10.1.

10.3.4 Overall Architecture of Redox Domains and Mechanism of Electron Donor Docking

Increasing interest in elucidation of the molecular mechanism of electron transfer in P450 systems creates fundamental demand for visualization of the architecture of donor-binding sites ruling catalytic potency of the enzymes. To accomplish this goal, homology modeling has to be carried out using sophisticated strategies for construct building. Judging from data for root mean square (r.m.s.) deviation of critical C_α atoms and φ/ψ-angle distribution, comparative alignment by knowledge-based techniques of P450s from different phyla with the bacterial CYP102A1, having its 3D structure determined, suggested the microbial enzyme to be a robust template for elucidation of structure-function relationships [277, 307]. Thus, mapping of key amino acid residues from microsomal, mitochondrial and bacterial hemoprotein species recognized to contribute to redox partner interactions (Table 10.1) onto the CYP102A1 scaffold yielded a scenario (Fig. 10.6) describing the general spatial distribution of contact sites [32].

As can be seen, the majority of points presumed to dictate contact with redox proteins cluster close to the center of the proximal face of the hemoprotein model. Highest density of binding sites, amounting to 47 % of the total number of key players, is found in the triad formed by α-helical structures C/C1, bordering the core fold on the top, the G-helical fragment, located more in the periphery of the P450 molecule, and the heme-binding region. The remaining interaction sites appear to be of minor importance, each housing but 5–8 % of the overall volume of anchoring elements (Table 10.1). Surprisingly, the population of functional determinants in the various target P450s, residing in the three preeminent donor-docking epitopes, displays a very low to moderate extent of conservation ranging from 9 % to 27 %. This might arise from the need for conformational flexibility to enable encounter with heterologous redox proteins. Indeed, ~38 % of the contact sites harbored in helices C/C1/G and the heme-binding domain have overlap of POR fixation with b_5 recognition. This behavior agrees with the ability of increasing amounts of b_5, integrated into assay media containing a constant level of POR, to gradually transform the biphasic kinetic tracings, prototypic of NADPH-driven P450 reduction, to a sluggish monophasic reaction as is characteristic of electron donation by b_5 [308, 309]. This lends support to the notion of a functional antagonism between the two redox proteins. On the other hand, b_5 fails to interfere with nonproductive physical anchoring of reductase to P450, as evidenced by visible difference spectrometry [308]. This seems to hint at functional diversification of the POR-docking loci [310] potentially acting in substrate-induced cooperativity [241]. Though overlap of regions involved in POR and ferredoxin association is lacking, the redox domain architecture (Fig. 10.6) displays epitopes fostering binding of the two carrier species to cluster in close proximity to each other in helices B/C and the H-I interhelical loop, possibly caused by certain analogy in the structural organization of the electron transfer proteins [185]. Similarly, evolutionary commonality induces joint contact points for b_5 and ferredoxins on the proximal face of P450s constituted by portions of helices B, C, K and the meander stretch (Table 10.1). It should be mentioned that the crystal structure of an archetypal b_5 homolog isolated from a bacterial strain has been identified [311]. This prompts one to speculate that b_5-type proteins may act as natural electron donors also to certain microbial P450s.

Evaluation of the array of data summarized in Table 10.1 disclosed 81 % of the overall population of amino acids predicted to operate in redox partner binding in the various target P450s to belong to the category of positively charged entities, about two thirds of the reactants being represented by lysine residues and one third by arginines. Indeed, calculation of the electrostatic surface potential for a series of P450s showed the dipole moment of the hemoproteins to be oriented such as to help direct the intermediate

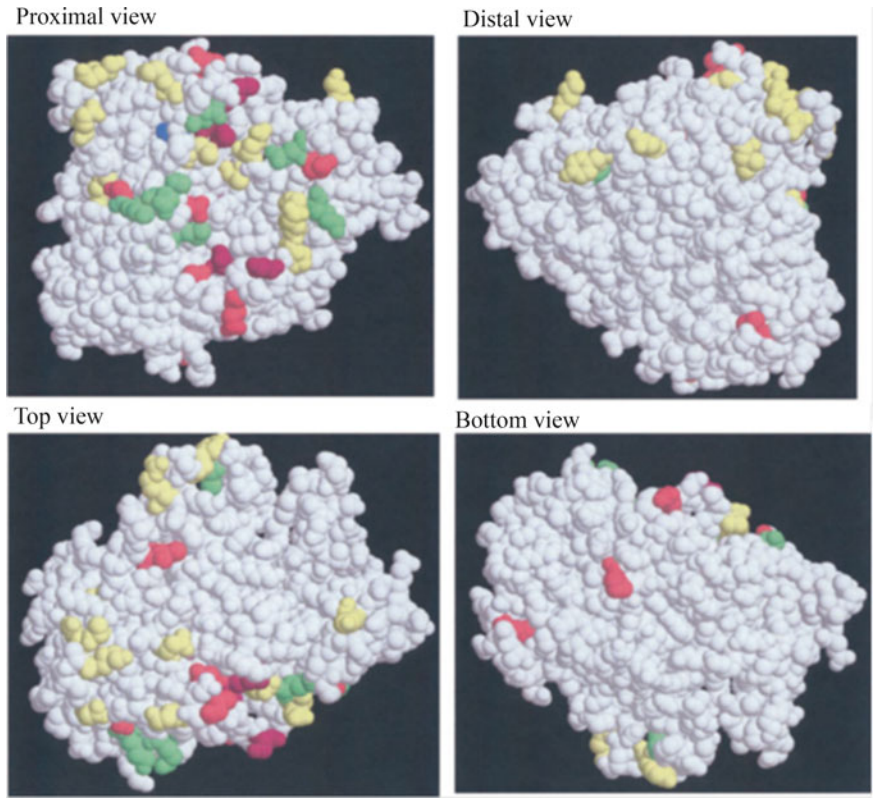

Fig. 10.6 Generalized molecular model featuring critical surface sites in P450s operating in recognition and binding of redox proteins. The composite profile was built by mapping the topological data of key determinants steering electron donor fixation onto the substrate-bound CYP102A1 template. The color code denotes: *yellow spheres*, POR-binding sites; *blue spheres*, b_5-binding sites; *green spheres*, sites common to POR and b_5; *red spheres*, Fdx-binding sites; *purple spheres*, sites common to Fdx and b_5. For *top* and *bottom* views, the coordinates of the images were rotated by 90° in the *x*-axis (Data taken from Ref. [32])

carriers toward a patch of positively charged elements on the proximal face [312–314]. This behavior underpins salt-bridge formation with carboxylates in the donor proteins (see Sect. 10.2) to be the most salient driving force in complexation, as exemplified by the allocation of interfacial residues involved in the CYP3A4-b_5 encounter [283] depicted in Fig. 10.7. In agreement with this principle, charge shielding by high concentrations of mobile ions was shown to elicit disintegration of donor/acceptor anchoring associated with a drop in electron flow [255, 293, 298]. Moreover, ~10 % of the key players bear a polar side group serving in generation of a flexible H-bonding link to some basic group(s) in the intermediate carriers, with tyrosines presumably being favored mediators of weakly polar inter-residue contacts [252, 269, 271].

Since electrostatic phenomena, no doubt, prevail in functional coupling of redox partners, it does not seem surprising that only a minority (~9 %) of the total of sites attracting electron donors can be assigned to the class of lipophilic amino acids largely accommodated in helices C1 and G. Here, aromatic and aliphatic representatives cooperate in π-π-stacking and van der Waals interactions with reactants in the diverse redox proteins [260, 261, 263, 305].

10.3.5 Factors Impacting Organization of Protein-Protein Association

10.3.5.1 The Role of Phospholipids

The phospholipid matrix serving in insertion and assembly of the components of the P450-

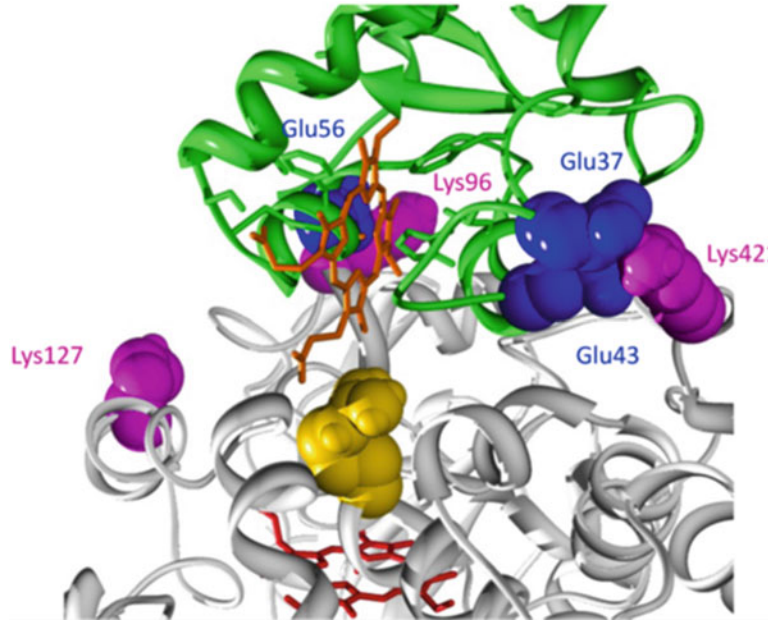

Fig. 10.7 Functional importance of electrostatic interactions between the protein surfaces of cytochrome b_5 and CYP3A4. The monooxygenase and the electron carrier are presented in *white* and *green*, with their heme groups being shown in *red* and *orange*, respectively. The interacting residues on the redox partners are depicted in *magenta* and *blue*, while the critical R446 is colored *golden*. As is evident, b_5 approaches the B-B′ loop region and helix C of CYP3A4 via helices α4 and α5. Protein domains on the oxygenase far from the docking surface are truncated (Reproduced from Ref. [283])

dependent redox machinery was detected to strongly impact efficiency of electron transport in microsomal and mitochondrial systems by providing structural features permitting improved recognition, ordering and alignment of redox partners [315]. In this respect, the synthetic dilauroyl phosphatidylcholine as well as natural phospholipids were shown to decrease the apparent dissociation constant for P450/POR complexes to an extent depending on both the chain length of the lipids and the mode of reconstitution, yielding either micellar or vesicular systems [316–318]. Owing to predominance of positive charges on the proximal profile of P450s (see above), mixtures containing anionic lipids such as phosphatidylserine were found to favor P450/POR association by forcing the proteins into correct orientation toward each other [319–321]. Facilitated donor/acceptor binding appears to generally require prior phospholipid-induced relaxation of the tight multimeric P450 aggregates [322]. Indeed, displacement of the P450 oligomerization equilibrium toward monomers by use of a nanoscale construct bearing a palmitoyl-oleoyl phosphatidylcholine bilayer drastically improved flavoprotein-promoted P450 reducibility [323]. Collectively, phospholipids were recognized to act as allosteric effectors eliciting conformational alterations in P450s associated with an increase in α-helical content of the hemoproteins. This fosters functional coupling of different types of electron carriers [324, 325]. Thus, lipid was demonstrated to also modulate affinity of b_5 for CYP2B4 [326]. Conversely, b_5 binding to the enzyme caused a ~2-fold rise in reactivity of phosphatidylcholine to CYP2B4 [327]. Similarly, cholesterol lowers K_d for Adx docking to cardiolipin-saturated CYP11A1 by a factor of up to 20, while the ferredoxin, in its turn, improves cholesterol binding to steroidogenic CYP11A1 [328].

10.3.5.2 The Role of P450-P450 Aggregation

Formation of hetero-oligomers of P450 is well documented and may play a decisive role in regulatory mechanisms of electron transfer [329]. In fact, the combined presence of CYP1A2 and CYP2B4 reconstituted with POR in the same phosphatidylcholine vesicles provides conclusive evidence from changes in the enzyme-specific monooxygenase activities that the CYP1A2 moiety of the heteromeric P450 complex generates a high-affinity reductase adduct more effectively competing for the redox protein than CYP2B4 [330]. Comparable results were obtained when the CYP2E1/CYP2B4 pair was embedded into a phospholipid matrix in the presence of POR to probe competition for the reductant. Here, low levels of CYP2E1 turned out to cause a 23-fold increase in the apparent K_m value of CYP2B4 for the donor protein, while the analogous K_m of CYP2E1 for POR decreased significantly, allowing CYP2E1 to outact CYP2B4 [331]. Of note, CYP2A6/CYP2E1/POR co-expression in microsomal membranes disclosed the presence of a prototypic CYP2A6 substrate to impair electron flow to CYP2E1, suggestive of a regulatory function of substrate in P450 aggregation [332]. This view is substantiated by drug-drug interactions occurring as the output of competition for the ancillary POR enzyme of co-reconstituted P450 couples such as CYP2C9/CYP2C19 or CYP2D6/CYP3A4 [333, 334]. Furthermore, the formation in liposomal membranes of an equimolar complex between the mitochondrial CYP11A1 and CYP11B1 enzymes was found to have a stimulatory effect on the CYP11B1-dependent 11β-hydroxylase activity as the consequence of a conformational alteration, corresponding to changes in the K_m value for Adx [335]. A mathematical model taking account of the possible existence of multiple types of P450-based dimer formations was developed to explore the most probable mechanism(s) of such interactions in more detail [336].

One would be remiss without mentioning that a fraction of P450s integrated into membranous systems may also exist as homo-oligomers. Here, formation of large aggregates causes P450 immobilization to an extent depending on the lipid-to-protein ratio [337, 338]. Interestingly, incorporation of POR or b_5 was shown to readily disrupt the aggregation state of P450s, when in a membrane, via transient complexation with the monooxygenases. This might influence the amount of productive donor/acceptor adducts determining catalytic activity [339, 340]. Again, substrate may interfere with the docking events to modulate reactivity of the redox partners [33, 177].

10.4 P450/Redox Partner Fusion Enzymes

10.4.1 Natural Fusion Proteins

Among fusion enzymes, the cytosolic CYP102A1 from *Bacillus megaterium* represents a unique self-sufficient flavohemoprotein catalyzing (ω–n)-hydroxylation of medium- to long-chain saturated fatty acids [341]. Owing to its soluble nature and applicability as an excellent paradigm for the understanding of structure/function relationships in class II-type P450s, CYP102A1 represents the most extensively studied member of the CYP102A subfamily consisting of a large number of relatives, though only four additional homologs, namely CYP102A2/A3/A5 and A7 from diverse *Bacillus* strains, have so far been characterized. Here, comparison of the polypeptide structures revealed some deviations in active-site architecture [342–344].

The CYP102A1 enzyme is composed of an N-terminal heme domain connected via a short protein linker with a eukaryotic-like diflavin reductase module bearing one equivalent each of FAD and FMN [345]. Availability of the crystal structure of the FAD/NADPH-binding domain helped identify sites involved in NADPH fixation such as S965, R966, K972 and Y974 [346]. Noteworthy, the side chain of W1046 shields the FAD isoalloxazine ring from

NADPH, and motion of this residue drives pyridine nucleotide specificity to the formation of an $FADH_2$-$NAD(P)^+$ charge-transfer intermediate [347]. Aromatic stacking with W854 and Y860 was shown to stabilize the FAD cofactor, while amino acids at positions 729–743 have the potential to make contacts with the cognate FMN domain [346]. Due to the dimeric nature of CYP102A1, the obligatory electron tunneling route traverses both constituents of the dimer during a single turnover by switching from the FAD-binding site of one monomer to the FMN domain of the other one prior to passing on to the terminal acceptor [348]. Interestingly, modulation of the electrostatic microenvironment of the FMN-docking pocket, housing critical residues Y536 and G570 [349], by unusual integration of positively charged lysines at positions 572 and 580 as well as decreased flexibility of the short cofactor-binding loop were presumed to be jointly responsible for the observed repression of the neutral, blue FMN semiquinone radical paralleled by stabilization of the red, anionic hydroquinone species. This was shown to be coupled with a change in the E_0' values of the redox pairs securing electron flow to the heme unit [350–352]. In this regard, W574, located in the FMN domain, was demonstrated to provide a direct through-bond electron transfer pathway including P382 and C400 in the heme-binding peptide [349, 350], while the highly conserved W96 turned out to have a function in heme association and control of the spin state of the iron [353]. Moreover, the area around L104 and Q387 in the intact heme/FMN-binding fragment (Fig. 10.8) revealed to be vital to efficient functional association of the partners [354]. It has to be mentioned that a soluble form of microsomal b_5 was found to also undergo tight binding to CYP102A1, eliciting a low-to-high spin transition in the enzyme's heme iron. This suggested the electron donor to occupy a contact site on the proximal face of the P450 heme that overlaps with that for the FMN domain of the diflavin reductase [355].

Genetic exploration of the fungus *Fusarium oxysporum* revealed the existence of a loosely membrane-associated, self-sufficient flavocytochrome termed CYP505A1, sharing ~41 % sequence identity with the P450 moiety of the bacterial CYP102A1 counterpart [356]. The enzyme catalyzes pyridine nucleotide-driven (ω-1)- to (ω-3)-hydroxylation of saturated C9 to C16 fatty acids [357]. The reductase unit in the primary CYP505A1 structure, having 35 % sequence identity with that of CYP102A1, was shown to be fixed to the heme region via a linker consisting of 20 amino acids of mainly hydrophilic character [356]. Noteworthy, 28 % of the residues hosted in fractions forming the NADPH/FAD- and FMN-binding domains disclosed to be invariant, with hydrophilicity clearly prevailing in the bond-making events [356]. Here, electron transfer was shown to be strongly stimulated by the presence of substrate [358]. Another self-sufficient member of the CYP505 family, classified CYP505B1,

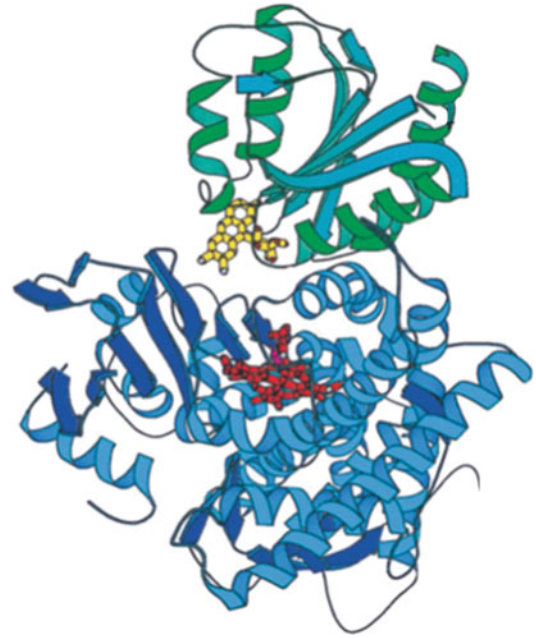

Fig. 10.8 View of the 3D structure of the complex between the heme- and FMN-binding domains of bacterial CYP102A1. The flavin-binding domain (*green*) hosting the FMN cofactor (*yellow*) is physically linked on the same polypeptide to the region (*blue*) surrounding the iron-porphyrin macrocycle (*red*). In this complex, the dimethylbenzene ring of FMN is oriented perpendicular to the heme plane at a distance of ~18 Å (Data taken from Ref. [350])

was isolated from the ascomycete *Fusarium verticillioides* and found to participate in the biosynthesis of the polyketide mycotoxin fumonisin. The flavohemoprotein displays 41 % sequence identity to CYP505A1 and 33 % identity to CYP102A1, with the putative cofactor-docking regions being arranged in the same order as in the homologs cited [359].

In addition, new types of P450-redox partner fusions have been unveiled. An example is bacterial P450 XplA (CYP177A1) from the *Rhodococcus rhodochrous* strain 11Y, catalyzing reductive denitration of the military explosive hexahydro-1,3,5-trinitro-1,3,5-triazine (RDX) [360]. The enzyme has an unusual structural organization comprising the N-terminal P450 heme domain fused to a flavodoxin unit [361, 362]. The latter was shown to contain most of the elements of a signature typical for FMN binding [360]. Unexpected features include the low affinity of the non-covalently bound FMN to its docking site (K_d = 1.09 μM) compared to reactivity of the cofactor toward flavodoxins from other bacterial sources and the strong positive shift of the redox potential of the FMN semiquinone/hydroquinone couple $\left(E_0' = -172\ \text{mV}\right)$, being the likely electron donor to the XplA heme [363].

Efficient RDX degradation was shown to require expression of the partnering reductase XplB. The FAD-containing carrier transfers reducing equivalents to the XplA-FMN in a 1:1 complex with high specificity for NADPH as the electron source [362, 363]. Here, collision of the two subunits represents a rate-limiting step. Of note, the deduced amino acid sequence of XplB has 42 % similarity to bovine mitochondrial AdR [360]. In accord with this, the XplA flavodoxin domain is capable of receiving electrons also from ferredoxin reductase before transferring them to the P450 heme [364].

Circumstantial exploration of the bacterial genome sequence library uncovered a completely novel class of self-sufficient P450 systems, representing a distinctive community of enzymes C-terminally fused to a phthalate dioxygenase reductase (PDR) module as the redox partner. The latter is folded into three domains involved in NADH/FMN binding and docking of the [Fe_2-S_2] cluster [365]. Thus, CYP116B1 from *Cupriavidus metallidurans*, a thiocarbamate herbicide-oxygenating fusion protein, displays stoichiometric binding of both FMN and the iron-sulfur center, electron transfer being supported by NAD(P)H with clear dominance of the triphosphopyridine nucleotide [366]. Similarly, CYP116B2 from a *Rhodococcus* species was demonstrated to be composed of an N-terminal P450 moiety separated by a short segment of about 16 amino acids from the reductase-like fragment, sharing 34 % sequence identity with the PDR family [367]. Closer investigation of the electron-supplying subunit predicted P578 to contact pyridine nucleotides, with NADPH having a ~500-fold preference over NADH in terms of the estimated K_d values [367, 368]. Moreover, the stretch spanning residues S532 to S536 was found to conform to the consensus motif for binding of the phosphate group of FMN, while a cluster of four highly conserved cysteines at positions 722, 727, 730 and 760 constitutes a [Fe_2-S_2] ferredoxin-type center [367]. The reduction potentials of the FMN semiquinone/hydroquinone and FeS entities were calculated to be approximately −270 mV and −214 mV, respectively [369]. Substrate screening for CYP116B2 revealed the enzyme to mediate dealkylation of substituted aromatic alkyl ethers, catalytic efficiency being higher with compounds bearing a shorter alkyl chain [370]. In addition, a new self-sufficient member of the CYP116 family was identified in *Rhodococcus ruber*. The fusion protein was recognized to have >90 % amino acid sequence identity to CYP116B2 and to consist of a heme domain, an FMN-hosting region and an iron-sulfur unit. In the presence of NADPH, the enzyme shows hydroxylase activity toward polycyclic aromatic hydrocarbons such as naphthalene or fluorene [371].

10.4.2 Artificial Self-Sufficient Fusion Proteins

The catalytic diversity of P450s has high potential for biotechnological exploitation. However,

industrial application is frustrated by the need of costly NAD(P)H cofactors, cumbersome reconstitution of auxiliary electron donor systems and fairly low metabolic turnover. To simplify the procedure and improve the catalytic outcome, the natural P450/redox partner fusion proteins addressed above may represent excellent paradigms for the sculpturing of man-made chimeric analogs of desired autonomic electron transport [372]. This requires cDNA shuffling to design assembly of redox chain building blocks on a "molecular Lego" principle [373]. Also, a versatile "drop-in" vector for rapid creation of self-sufficient P450s has been developed [374].

10.4.2.1 P450/Diflavin Reductase Fusion Enzymes

A useful tool for the generation of simplistic P450 redox systems is featured by covalent fixation of the hemoprotein portion to a POR-like unit with the aim to construct the most suitable fusion [375]. In this way, the (Δ1–41)-truncated reductase moiety from yeast was genetically attached to rat CYP1A1. The construct displayed rotational mobility of the P450 fragment higher than that of CYP1A1 alone [376]. In the presence of NADPH, the rate of reduction of the substrate-bound fusion enzyme was found to be $>50\ s^{-1}$, suggesting that electrons were rapidly transferred from the cofactor through FAD and FMN to the heme iron [377]. Similarly, human CYP1A1 was connected to N-terminally truncated rat POR via a Ser-Thr dipeptide linker. Activity toward resorufins was shown to be 11- to 22-fold higher compared to the control [378]. Of note, human CYP1A2 genetically engineered with yeast reductase proved to be about twice as efficient in oxidative ethoxyresorufin biotransformation relative to the CYP1A1 fusion system [379]. Moreover, a fused construct derived from the cDNA for canine CYP2B11 in tandem with the code for the modified rat oxidoreductase exhibited an androstenedione metabolite profile very similar to that found with the reconstituted components [380]. The same approach was adapted to arrange chimeras produced by joining the C-terminus of mammalian CYP2C11 or CYP2D6 to the cytoplasmic domain of the cognate flavoproteins via a dipeptide linker. In either case, molecular organization seemed to be suboptimal, as judged from comparison of the k_{cat} values for substrate turnover with those of the non-fused systems [381, 382]. Similar observations were made upon linkage of human CYP3A4 to rat POR. Addition of excess exogenous POR and b_5 to the reaction mixtures were found to drastically enhance the rate of testosterone 6β-hydroxylation [161]. Deficiency in catalytic capacity of the fused construct may arise from the fairly short linker region restricting flexibility in orientation toward each other of the functional interfaces of the CYP3A4 and POR modules required to permit swift electron transfer. Optimization was achieved by engineering a number of triple adducts, among which the CYP3A4/reductase/b_5 product turned out to reflect the most appropriate ordering for high activity compared to the reconstitution premixes [383]. Though fusion of rat CYP4A1 with the native reductase unit gave a biocatalyst mediating lauric acid ω-hydroxylation at a rate threefold higher than that determined in reconstitution assays, metabolic capacity was not fully exhausted: supplementation with purified flavoprotein/b_5 strongly stimulated fatty acid consumption by potentially increasing collision frequency of the redox partners [384, 385].

The fusion strategy was also extended to microsomal steroidogenic P450s. Thus, the multifunctional CYP17A1 domain of different mammalian species was connected to a truncated form of yeast or rat reductase to yield a self-contained unit characterized by 17α-hydroxylase and 17,20-lyase activity, promoting biotransformation of progesterone and pregnenolone to the corresponding C19-derivatives [386, 387]. Here, the length and amino acid sequence of the hinge region between the redox components was demonstrated to play a decisive role in efficient intramolecular electron transfer [388]. Of interest, donation to the fused adduct of reducing equivalents by exogenous b_5 was shown to boost the lyase pathway to an extent depending on the genetic ancestry of the CYP17A1 moiety examined [389]. Similarly, linkage of bovine

CYP21A2 to N-terminally modified yeast POR gave a flavohemoprotein driving conversion of 17α-hydroxyprogesterone to 11-deoxycortisol at a catalytic efficiency two- to four-times greater than that found with the reconstituted CYP21A2 redox chain [390]. Surprisingly, a mitochondrial form of rat CYP27A1, when fixed to a heterologous POR motif, displayed notable potency for 27-hydroxylation of 5β-cholestanetriol in the absence of its native electron suppliers [391].

A suit of vectors for the expression of fungal and plant P450s as non-natural genetic fusions with various reductase isoforms have been developed. Thus, engineering of CYP51 from *Saccharomyces cerevisiae* to allow connection with its cognate redox partner resulted in swift 3-hydroxylanostenol demethylation [392]. Also, chimeric plant P450s CYP71B1, CYP73A and CYP76B1 were shown to work with higher overall capacity when plant reductases were permitted to act as fusion partners. Here, cinnamate 4-hydroxylation, a key reaction in phenylpropanoid biosynthesis, induces swift production of relevant secondary metabolites steering plant development, while catabolism of recalcitrant herbicides such as chlortoluron is of major importance in defense reactions [393–396].

Efforts were also undertaken to evaluate exploitation of the *Bacillus megaterium* (CYP102A1) reductase component (BMR) as a surrogate of POR, having 35 % sequence identity with the microbial analog [397]. In this way, a series of soluble self-sufficient CYP2C chimeras, generated by gene-fused assembly of the N-terminally modified P450s with BMR via a Pro-Ser-Arg linker, displayed activities toward prototypic marker substrates comparing favorably with those reported for the wild-type enzymes [381, 398, 399]. Similar observations were made with the CYP2E1/BMR and CYP3A4/BMR constructs, though coupling levels between product formation and NADPH consumption did not exceed 8–15 % [398, 400, 401]. Furthermore, swapping of the oxidoreductase module of the P450-like self-sufficient neuronal nitric oxide synthase for BMR was found to give rise to a manipulated multi-domain construct of low stability, nevertheless displaying appreciable oxygenase activity prone to the regulatory action of the calmodulin messenger protein [402]. Finally, fusion-mediated development of a reaction host for efficient 3′-hydroxylation of 4′,7-dihydroxyisoflavone (daidzein) was carried out by cross-linking CYP105D7 via a 20 amino acid peptide to the BMR-like reductase fragment of the self-contained CYP102D1 from *Streptomyces avermitilis*. The engineered enzyme metabolized daidzein at a k_{cat}/K_m value 24-fold higher than that measured with CYP105D7 reconstituted with Pdx/PdR [403].

10.4.2.2 P450/Ferredoxin/Ferredoxin Reductase Fusion Enzymes

A novel type of architecture was tested for utility in simplifying the P450-dependent redox machinery. Thus, microsomal rat CYP1A1 was manipulated by gene fusion to obtain a triple adduct encompassing Fdx and FdR from plant chloroplasts. Here, the CYP1A1/Fdx/FdR order revealed to permit the most efficient oxidative turnover of 7-ethoxycoumarin and the herbicide chlortoluron [404]. Similarly, mammalian mitochondrial CYP11A1, CYP11B1 and CYP27A1 enzymes were tethered to their native accessory redox partners via the production of a series of expression cassettes. Again, arrangement of the ligated modules was recognized to have a pivotal impact on the catalytic potency of the individual constructs, with the P450/AdR/Adx congener being superior to other species. This suggested Adx to be a key factor in determining the reaction rate [405–407].

Moreover, bacterial CYP101A1 from *Pseudomonas putida* was fixed to its dedicated electron donors to yield a tandem linear fusion enzyme. Of note, highest NADH-promoted camphor turnover was attained with an assembly, where the PdR/Pdx duo, linked by peptides of variable length, preceded the P450 domain, though activity as such was but 30 % that of the reconstituted wild-type system [218]. In contrast to this, a novel site-specific, branched CYP101A1 fusion protein with spatially equal geometry of the three-redox-component adduct was created to minimize structural constraints. To this end, the P450 module cross-linked with PdR via a

peptide, including a reactive glutamine residue and Pdx attached to a lysine-bearing tag at the C-terminus, were associated with each other by the help of transglutaminase. This product displayed tenfold higher activity compared to the simple chimera described above [408]. Using PCNA, a DNA sliding clamp, as a scaffold in the engineering of a ring-shaped heterotrimeric complex of CYP101A1 tightly juxtaposed to its attendant electron donors, catalytic activity of the resulting construct could be raised to a level two orders of magnitude higher than that of the P450 alone [409]. Notably, a thermostable system was modeled by linkage of CYP175A1 from *Thermus thermophilus* to a new type of FdR and Fdx, with five small amino acids being inserted as a hinge between each component to increase flexibility. The fused protein displayed full NADPH-driven reactivity toward *β*-carotene even at 70 °C [410].

10.4.2.3 P450/Dioxygenase Reductase-Like Fusion Enzymes

Stimulus was given by the CYP116B2 precedent to mimicking the fusion organization of the enzyme's redox center. Thus, a plant-bacterial chimera was created by ligating the P450 domain of CYP93C1 from the soybean *Glycine max* to the PDR-like reductase module of the rhodococcal monooxygenase, catalyzing naringenin-to-genistein transformation at improved efficiency compared to hemoprotein mated with a usual plant reductase [395]. The same procedure was employed to engender genetically engineered merging of the FMN/Fe_2S_2-containing carrier moiety with the C-terminal heme unit of CYP101A1, CYP153A or CYP203A, yielding biocatalysts avidly attacking a diversity of compounds such as *d*-camphor, alkanes and 4-hydroxybenzoate [374, 411–413]. Also, interest focused on harnessing improved catalytic potency and broadening of substrate spectra upon fusion of the native or mutated, macrolide biosynthetic CYP107L1 protein with the PDR-type building block [414, 415]. Moreover, strategies were developed to attach the isolated heme domain of the explosive-degrading CYP177A1(XplA) via a 16-amino-acid-linker to the modified C-terminal reductase partner of CYP116B2. The artificial adduct revealed substrate specificities comparable to those of the wild-type enzyme with a K_d value for RDX docking of ~5 μM [362, 374]. It should be noted that a rare bacterial reductase has been purified from *Nocardia farcinica* bearing some resemblance to the molecular organization of PDR, though carrying an NADPH/FAD-binding module and an Fe_4S_4 cluster. Fusion of the electron donor with CYP51 gave a chimera that demethylated lanosterol at a 35-fold higher efficiency relative to the P450 unit alone [416].

10.5 Procedures to Evade Requirements for Supporting Redox Proteins and Cofactor Utilization

10.5.1 The Peroxide Shunt Pathway

The peroxide shunt serves in driving P450-catalyzed monooxygenations in the absence of an NADPH-dependent redox partner by reacting ferric hemoprotein with H_2O_2 or organic peroxides to generate the Fe^{3+}-OOH^- intermediate, protonation of which leads to release of water and formation of the high-energy iron-oxene species [417]. In this regard, the single-component bacterial peroxygenases CYP152B1 from *Sphingomonas paucimobilis*, CYP152A1 from *Bacillus subtilis* and CYP152A2 from *Clostridium acetobutylicum*, primarily catalyzing α- and β-hydroxylation of long-chain fatty acids, may be ideal model systems [28, 238, 418]; here, salt bridge formation between the fatty acid's carboxylate and an arginine located near the heme was shown to be essential to H_2O_2 ligation and proton delivery to initiate facile O-O bond cleavage [419]. More recently, a new member of the CYP152 family was purified from a *Jeotgalicoccus* species, operating in the peroxide-dependent biosynthesis of 1-alkenes via fatty acid decarboxylation [420]. Moreover, the microbial CYP107AJ1 from *Streptomyces peuceticus* has been ascribed to a putative peroxygenase class of P450s owing to lack of reactivity toward NADPH-driven redox partners, contrasting with the high catalytic efficiency in

H_2O_2-supported 7-ethoxycoumarin dealkylation [421]. Similarly, human CYP2S1 was found to be resistant to reduction by POR, while mediating swift oxidative metabolism of a series of environmental carcinogens in the presence of hydrogen peroxide, cumene hydroperoxide or fatty acid hydroperoxides [26, 27]. In analogy, mammalian brain CYP2D18 was detected to support conversion of dopamine to aminochrome exclusively in a peroxygenase mode [422].

Apart from this specific behavior, P450s usually accepting reducing equivalents from a natural redox partner may, nevertheless, exploit peroxides as alternative oxygen donors in substrate biotransformations. For instance, CYP2B4 was demonstrated to utilize cumene hydroperoxide or fatty acid hydroperoxides to bring about N-oxidation of 4-chloroaniline. Albeit, turnover was found to occur at a rate not exceeding 25 % of that observed with the pyridine nucleotide-driven process [423, 424]. Notably, exchange of the enzyme's highly conserved T302 for alanine was recognized to accelerate inactivation of the mutant through peroxide-induced denaturation of the apoprotein matrix and degradation of the heme macrocycle, pointing at a function of the threonine residue in P450 stabilization or diminution of the level of free reactive oxidant [425]. Employing CYP2D6 and CYP3A4 as probe catalysts because of their high substrate promiscuity, efficiency of the peroxygenase-like metabolic route relative to that determined by the action of natural cofactors was shown to largely rely on the type of "oxygen surrogate" employed [231, 426]. To maximize productive interactions of P450s with peroxides and minimize oxidative hemoprotein damage, substantial work was done by genetic enzyme engineering. Thus, CYP3A4 was subjected to random and site-directed mutagenesis to engender formation of a F228I/T309A variant characterized by a V_{max}/K_m for cumene hydroperoxide-supported 7-benzyloxyquinoline debenzylation 11-fold higher than the value observed with the wild-type enzyme. However, k_{cat} as such only amounted to ~18 % the level measured with CYP3A4 fortified with NADPH [427]. Among bacterial P450s, three random mutants that showed improved capacity for H_2O_2-dependent naphthalene oxidation were generated from CYP101A1. Here, DNA sequencing revealed that amino acid substitutions C242F, R280L and E331K potentially interfered with peroxide binding [428]. Kinetic analysis of the F87A mutant of full-length CYP102A1 unveiled the modified enzyme to be a somewhat more efficient utilizer of H_2O_2 in medium-chain fatty acid hydroxylation compared to the parental species, where peroxide-supported activity is hardly detectable, but to shift C-H bond functionalization away from the terminal position [429]. Applying sequential rounds of random mutagenesis, peroxidative catalyst performance of the F87A-modified heme domain of CYP102A1 was drastically improved by evolution of an allelic variant carrying nine additional amino acid substitutions dispersed throughout the protein scaffold, with exception of the active-site cavity and substrate access channel [430]. Enhanced H_2O_2-driven peroxygenase activity was shown to extend to fatty acid substrates and styrene, although major limitations of this system are rapid suicide inactivation as the result of peroxide-mediated heme destruction and significant decrease in thermostability [430]. Here, quantum mechanical and molecular mechanical calculations allowed rational identification of key oxidizable targets, permitting replacement of the latter with less sensitive entities. In fact, the double mutant W96A/F405L gave a more stable construct [431]. Moreover, thermostabilization of the laboratory-evolved heme-domain peroxygenase variant was achieved by further directed evolution, leading to the introduction of eight new amino acid substitutions [432].

10.5.2 Photo- and Electrochemical Manipulation of the P450 System

Innovative approaches to supersede the obligatory proteinaceous redox chains in the P450 toolbox include light-induced electron transfer to the heme iron via photoactivatable mediators or direct delivery of reducing equivalents from

electrodes to promote substrate metabolism [34, 433]. In this way, light-induced reductive dehalogenation of environmental pollutants such as pentachloroethane was brought about in reaction mixtures containing EDTA/proflavin and CYP101A1. Activity remained unaffected upon the addition of exogenous Pdx [434]. Great promise was also shown by the construction of hybrid CYP102A1 heme domains consisting of Ru(II)-diimine photosensitizers attached to the single cysteine residues of the K97C, Q109C, Q397C and L407C mutants, strategically positioned in close proximity to the heme. Continuous irradiation of the systems with visible light permitted hydroxylation of lauric acid with variable total turnover numbers, with the L407C variant being the most efficient catalyst despite some degradation due to oxidative damage [435]. Similarly, cadmium sulfide semiconductor nanoparticles, frequently referred to as quantum dots (QDs), have attracted interest due to their unique size-tunable properties and high photostability during the light-dependent generation of free superoxide and hydroxyl radical species [436]. Adsorption of the positively charged hexahistidine-tagged CYP152A1 on the mercaptoacetic acid-capped QD surface was recognized to yield nanohybrids of differential spatial conformation [437]. UV light-induced triggering of the hemoprotein's peroxygenase activity was shown to cause α- and β-hydroxylation of myristic acid as well as conversion of *N*-acetyl-3,7-dihydroxyphenoxazine to resorufin at a rate 50 % of that found with H_2O_2 as the oxidant [438, 439].

Interfacing of P450s to viable amperometric devices to obtain highly efficient catalysis through direct mediator-free transfer of reducing equivalents requires modification of electrodes with agents that facilitate electron flow, prevent protein denaturation and cause appropriate orientation of the enzymes. To attain this goal, different types of bioelectrocatalysts have been developed [440]. Thus, riboflavin-bearing CYP1A2, CYP2B4 and CYP11A1 enzymes entrapped in a phospholipid vesicular system were cross-linked via glutaraldehyde to screen-printed (SP) thick film rhodium-graphite working electrodes, poised at −500 mV vs. Ag/AgCl reference electrodes. Rates of biosensor-driven *p*-hydroxylation of aniline, *N*-demethylation of aminopyrine and cholesterol side-chain cleavage were close to those obtained with NAD(P)H as the electron source [441]. Alternatively, CYP2B4 was adsorbed onto SP electrodes coated with colloidal gold nanoparticles stabilized with didodecyldimethylammonium bromide (DDAB) in the presence of the Nafion ionomer to improve film permeability. The construct adequately mediated benzphetamine *N*-dealkylation [442]. Modifying the immobilization scheme, studies were carried out with monomerized CYP2B4 incorporated into thin layers of non-ionic detergent and montmorillonite, a member of the mineral group of clays, on glassy carbon (GC) electrodes. Here, k_{cat} for aminopyrine turnover was shown to be comparable to the value of the microsomal system [443]. Moreover, a biocompatible film containing colloidal gold nanoparticles and chitosan was used to encapsulate CYP2B6 on GC sensors. Product analysis confirmed C-hydroxylation and heteroatom release from bupropion, lidocaine and cyclophosphamide to be the main pathways of drug oxidation [444]. Studies were also conducted with carbon cloth (CC) electrodes coated by immersion into DDAB dispersions embedding bacterial CYP101A1. Electrolyses performed under aerobic conditions in the presence of styrene and *cis*-*β*-methylstyrene as the probe substrates revealed styrene oxide and *trans*-*β*-methylstyrene oxide to be the major products resulting from oxidative attack by the P450, while some byproducts were speculated to rather arise from H_2O_2-driven reactions [445].

Substantial progress was achieved by construction of enzyme films of predesigned architecture via layer-by-layer self-assembly of hemoproteins and oppositely charged polyions on the surface of electrodes. Applying this regimen, CC sensors elaborated by casting CYP1A2/poly(styrenesulfonate) (PSS) microemulsions onto the solid supporters displayed good electrocatalytic performance of O_2 reduction to hydrogen peroxide, mediating epoxidation of styrene faster than CYP101A1 [446].

Electrochemical exploration was extended to assembly of enzyme films on the surface of derivatized gold electrodes by alternate adsorption of a P450 layer on top of a poly (diallyldimethyl-ammonium) (PDDA) layer. In this way, immobilization of CYP2E1 and CYP3A4 resulted in sensor devices mediating oxidative turnover of *p*-nitrophenol and midazolam, respectively, at fairly low catalytic rates [447, 448]. Here, covalent enzyme linkage to gold electrodes via flexible spacer molecules, bearing both thiol and disulfide groups as well as anchors to the proteins, was shown to increase metabolic efficiency. Making use of this strategy, the exposed C261 and C268 residues of CYP2E1 were intimately connected with cystamine-maleimide on gold biosensors. This procedure stimulated conversion of *p*-nitrophenol to *p*-nitrocatechol by a factor of 22 relative to the Au/PDDA array [447]. Similarly, human CYP2C9 was bonded to a gold electrode by the aid of its N-terminal lysine fixed to an 11-mercaptoundecanoic acid and octanethiol self-assembled monolayer. Electron transfer was calculated to proceed at a rate ranging from 6 to 31 s^{-1}, with warfarin being metabolized to the 7-hydroxy derivative at an apparent K_m of 3 μM [449].

10.6 Conclusions and Future Prospects

The present review focuses on the description of electron transfer events with emphasis on topological and functional features in the P450-dependent redox chain to gain a more detailed, structure-based insight into fundamental molecular principles steering donor-acceptor interactions. Improved comprehension may permit engineering to introduce more efficient electrochemical properties into the system such as facilitated redox partner association and intermolecular electron flow [200, 303], but equally-well may pave the way for the development of technologically viable hemoprotein species for extensive exploitation as versatile biocatalysts [35]. Here, directed evolution and DNA shuffling may be useful in the sculpturing of self-sufficient fusion proteins for preselected metabolic implementation [376, 395, 404] or in the development of peroxygenase-like P450s with upgraded resistance toward oxidative destruction [430, 431] to obviate the tedious reconstitution procedure. Also, artificial photo- and electrocatalytic devices might help avoid costly NAD(P)H utilization [434, 442].

Despite conspicuous biotechnological advances [450], industrial large-scale production of fine chemicals is presently limited to a fairly low number of processes making preferential use of microbial whole-cell catalysts harboring recombinant P450s co-expressed with an appropriate electron donor [451]. Relevant examples include hydrocortisone production via $P450_{lun}$-mediated 11β-hydroxylation of 11-deoxycortisol in a fungal bioreactor [452] or manufacture of the cholesterol-lowering drug pravastatin by CYP105A3-driven attack on compactin, employing the *Streptomyces* sp. Y-110 as the host [453]. Moreover, CYP71AV1-promoted three-step oxidation of amorphadiene to artemisinic acid, the immediate precursor of the antimalarial drug artemisinin, permitted industrial scale-up due to high productivity of the engineered *Saccharomyces cerevisiae* factory [454]. Similarly, long-chain α,ω-dicarboxylic acids, widely used as raw materials for the synthesis of products such as perfumes, hot-melting adhesives, engineering plastics or high quality lubricants, have been generated on a commercial scale from *n*-alkanes by fungal fermentation catalyzed by *Candida tropicalis*, housing CYP52A1 in conjunction with POR as the redox machinery [455].

Specialized exploitation of manipulated hemoproteins was recognized to be of high interest in gene-directed enzyme prodrug therapy (GDEPT) of cancer. Here, introduction of tumor-selective retroviral vectors, encoding P450s characterized by high metabolic potency in the reductase-supported intratumoral conversion of anticarcinogenic compounds such as cyclophosphamide or ifosfamide to their active intermediates, displayed a substantial therapeutic progress [456]. This has given an impetus to

improvement of reactivity of CYP2B enzymes toward the oxazaphosphorines [457, 458]. In this regard, creation of the 114V/477W double mutant of human CYP2B6 increased the catalytic efficiency of cyclophosphamide oxidation by a factor of 4 [459]. Also, there is clear opportunity to expedite therapeutic efficacy by utilization of the fusion gene of the self-sufficient CYP2B6/POR chimera for infection of tumor cells [460]. The current advances lend confidence that this novel strategy may be promoted by the development of more sophisticated vector and promotor systems.

The engineered P450 redox machinery may also be exploited in phyto- and bioremediation processes. Thus, expression in tobacco plants of human CYP1A proteins or CYP76B1 from *Helianthus tuberosus* as hybrid enzymes fused with POR increased herbicide resistance toward a series of phenylureas such as chlortoluron due to swift detoxification [379, 396]. Similarly, transduction of rice plants with human CYP2B6 or CYP2C19 enhanced the ability to remove atrazine and metolachlor herbicides from soil [461]. Interest has also arisen in transgenic *Arabidopsis* plants producing the bizarre fusion protein CYP177A1(XplA) for targeted degradation of the widespread military explosive RDX, a priority pollutant contaminating liquid culture and soil leachate [462]. One factor complicating introduction of such technologies for environmental clean-up may be concerns about field application of genetically modified organisms, possibly entailing certain risks. Nevertheless, remediation of the biotope needs a robust catalytic apparatus capable of killing off hazardous anthropogenic toxicants via more flexible, pollutant-specific oxyfunctionalization. Here, polycyclic aromatic hydrocarbons such as phenanthrene, naphthalene, fluorene or benzo[*a*]pyrene proved to be targets for optimized biotransformation by chimeric CYP1A1/POR, mutated CYP102A1, fused CYP116B3 or modified CYP5136A3, expressed in microbial recombinant cells [371, 463–465]. However, inoculation and efficient maintenance of the population density of the engineered microbial biomass in terrestrial habitats still need improvement [466].

Finally, exploitation of P450-based electroanalytical techniques may become of increasing interest to enable more practical applications. Given appreciable sensitivity and recognition selectivity, miniaturized amperometric biosensors might be utilized for the determination of compounds important in pharmaceutical industry, clinical practice and environmental monitoring [467, 468]. Also, microfluidic devices were developed to improve analytical performance by decreasing analysis time and increasing reliability through automation [440]. This may foster high-throughput screening during the search for structural features of dynamic molecules having potential for therapeutic implementation [469].

Collectively, catalytic versatility, no doubt, adds the P450 redox system to the enzymatic armory for large-scale exploitation in a vast array of biotechnological areas. Despite huge progress in recent years, members of the hemoprotein family are, nevertheless, thought of as relatively fragile biocatalysts prone to spontaneous structural disruption or rapid inactivation at temperatures >40 °C [430]. Hence, future engineering strategies will have to focus on erasure of these shortcomings and evolution of novel activities to allow widespread application in metabolic processes.

Reviews *Abbreviations*: *AdR* NADPH-adrenodoxin reductase, *Adx* adrenodoxin, *Arx* [2Fe-2S]-type ferredoxin, b_5 cytochrome b_5, *BMR Bacillus megaterium* (CYP102A1) reductase component, *CC* carbon cloth electrode, *CYP or P450* cytochrome P450, *FdR* NAD(P)H-ferredoxin reductase, *Fdx* ferredoxin, *GC* glassy carbon electrode, *PCNA* proliferating cell nuclear antigen, *PdR* NADH-putidaredoxin reductase, *PDR* phthalate dioxygenase reductase, *Pdx* putidaredoxin, *POR* NADPH-P450 oxidoreductase, *Pux* palustrisredoxin, *r.m.s.* root mean square deviation, *SP* screen-printed electrode.

References

1. Nelson DR (2006) Cytochrome P450 nomenclature, 2004. Methods Mol Biol 320:1–10
2. Hlavica P (2011) Insect cytochromes P450: topology of structural elements predicted to govern catalytic versatility. J Inorg Biochem 105:1354–1364
3. Bak S, Beisson F, Bishop G, Hamberger B, Höfer R, Paquette S, Werck-Reichhart D (2011) Cytochromes p450. Arabidopsis Book 9:e0144

4. Hlavica P (2013) Evaluation of structural features in fungal cytochromes P450 predicted to rule catalytic diversification. Biochim Biophys Acta 1834:205–220
5. Lewis DFV, Wiseman A (2005) A selective review of bacterial forms of cytochrome P450 enzymes. Enzyme Microb Technol 36:377–384
6. Omura T, Sato R (1964) The carbon monoxide-binding pigment of liver microsomes. I. Evidence for its hemoprotein nature. J Biol Chem 239:2370–2378
7. Bernhardt R, Waterman MR (2007) Cytochrome P450 and steroid hormone biosynthesis. Met Ions Life Sci 3:361–396
8. Hlavica P, Lehnerer M (2010) Oxidative biotransformation of fatty acids by cytochromes P450: predicted key structural elements orchestrating substrate specificity, regioselectivity and catalytic efficiency. Curr Drug Metab 11:85–104
9. Hlavica P (2006) Functional interaction of nitrogenous organic bases with cytochrome P450: a critical assessment and update of substrate features and predicted key active-site elements steering the access, binding, and orientation of amines. Biochim Biophys Acta 1764:645–670
10. Brown CM, Reisfeld B, Mayeno AN (2008) Cytochrome P450: a structure-based summary of biotransformations using representative substrates. Drug Metab Rev 40:1–100
11. Meunier B, de Visser SP, Shaik S (2004) Mechanism of oxidation reactions catalyzed by cytochrome P450 enzymes. Chem Rev 104:3947–3980
12. Denisov IG, Makris TM, Sligar SG, Schlichting I (2005) Structure and chemistry of cytochrome P450. Chem Rev 105:2253–2277
13. Newcomb M, Hollenberg PF, Coon MJ (2003) Multiple mechanisms and multiple oxidants in P450-catalyzed hydroxylations. Arch Biochem Biophys 409:72–79
14. Hlavica P (2004) Models and mechanisms of O-O bond activation by cytochrome P450. A critical assessment of the potential role of multiple active intermediates in oxidative catalysis. Eur J Biochem 271:4335–4360
15. Hrycay EG, Bandiera SM (2012) The monooxygenase, peroxidase, and peroxygenase properties of cytochrome P450. Arch Biochem Biophys 522:71–89
16. Lewis DFV, Watson E, Lake BG (1998) Evolution of the cytochrome P450 superfamily: sequence alignments and pharmacogenetics. Mutat Res 410:245–270
17. Hannemann F, Bichet A, Ewen KM, Bernhardt R (2007) Cytochrome P450 systems – biological variations of electron transport chains. Biochim Biophys Acta 1770:330–344
18. Paine MJI, Scrutton NS, Munro AW, Gutierrez A, Roberts GCK, Wolf CR (2005) Electron transfer partners of cytochrome P450. In: Ortiz de Montellano PR (ed) Cytochrome P450: structure, mechanism, and biochemistry, 3rd edn. Kluwer Academic/Plenum Publishers, New York, pp 115–148
19. Stok JE, De Voss JJ (2000) Expression, purification, and characterization of BioI: a carbon-carbon bond cleaving cytochrome P450 involved in biotin biosynthesis in *Bacillus subtilis*. Arch Biochem Biophys 384:351–360
20. Lawson RJ, von Wachenfeldt C, Haq I, Perkins J, Munro AW (2004) Expression and characterization of the two flavodoxin proteins of *Bacillus subtilis*, YkuN and YkuP: biophysical properties and interactions with cytochrome P450 BioI. Biochemistry 43:12390–12409
21. Hawkes DB, Adams GW, Burlingame AL, Ortiz de Montellano PR, De Voss JJ (2002) Cytochrome $P450_{cin}$ (CYP176A), isolation, expression, and characterization. J Biol Chem 277:27725–27732
22. Hawkes DB, Slessor KE, Bernhardt PV, De Voss JJ (2010) Cloning, expression and purification of cindoxin, an unusual FMN-containing cytochrome P450 redox partner. Chembiochem 11:1107–1114
23. Kimmich N, Das A, Sevrioukova I, Meharenna Y, Sligar SG, Poulos TL (2007) Electron transfer between cytochrome $P450_{cin}$ and its FMN-containing redox partner, cinredoxin. J Biol Chem 282:27006–27011
24. Yeom J, Park W (2012) Biochemical characterization of ferredoxin-$NADP^+$ reductase interaction with flavodoxin in *Pseudomonas putida*. BMB Rep 45:476–481
25. Oshima R, Fushinobu S, Su F, Zhang L, Takaya N, Shoun H (2004) Structural evidence for direct hydride transfer from NADH to cytochrome $P450_{nor}$. J Mol Biol 342:207–217
26. Bui PH, Hankinson O (2009) Functional characterization of human cytochrome P450 2S1 using a synthetic gene-expressed protein in *Escherichia coli*. Mol Pharmacol 76:1031–1043
27. Bui PH, Hsu EL, Hankinson O (2009) Fatty acid hydroperoxides support cytochrome P450 2S1-mediated bioactivation of benzo[*a*]pyrene-7,8-dihydrodiol. Mol Pharmacol 76:1044–1052
28. Lee DS, Yamada A, Sugimoto H, Matsunaga I, Ogura H, Ichihara K, Adachi S, Park SY, Shiro Y (2003) Substrate recognition and molecular mechanism of fatty acid hydroxylation by cytochrome P450 from *Bacillus subtilis*. J Biol Chem 278:9761–9767
29. Chen CYK, Poole EM, Ulrich CM, Kulmacz RJ, Wang LH (2012) Functional analysis of human thromboxane synthase polymorphic variants. Pharmacogenet Genomics 22:653–658
30. Song WV, Funk CD, Brash AR (1993) Molecular cloning of an allene oxide synthase: a cytochrome P450 specialized for the metabolism of fatty acid hydroperoxides. Proc Natl Acad Sci U S A 90:8519–8523
31. Lewis DFV, Hlavica P (2000) Interactions between redox partners in various cytochrome P450 systems:

functional and structural aspects. Biochim Biophys Acta 1460:353–374
32. Hlavica P, Schulze J, Lewis DFV (2003) Functional interaction of cytochrome P450 with its redox partners: a critical assessment and update of the topology and predicted contact regions. J Inorg Biochem 96:279–297
33. Hlavica P (2007) Control by substrate of the cytochrome P450-dependent redox machinery: mechanistic insights. Curr Drug Metab 8:594–611
34. Hlavica P (2009) Assembly of non-natural electron transfer conduits in the cytochrome P450 system: a critical assessment and update of artificial redox constructs amenable to exploitation in biotechnological areas. Biotechnol Adv 27:103–121
35. Bernhardt R (2006) Cytochromes P450 as versatile biocatalysts. J Biotechnol 124:128–145
36. Kumar S (2010) Engineering P450 biocatalysts for biotechnology, medicine, and bioremediation. Expert Opin Drug Metab Toxicol 6:115–131
37. Murataliev MB, Feyereisen R, Walker FA (2004) Electron transfer by diflavin reductases. Biochim Biophys Acta 1698:1–26
38. Iyanagi T, Xia C, Kim JJP (2012) NADPH-cytochrome P450 oxidoreductase: prototypic member of the diflavin reductase family. Arch Biochem Biophys 528:72–89
39. Jenkins CM, Waterman MR (1999) Flavodoxin as a model for the P450-interacting domain of NADPH-cytochrome P450 reductase. Drug Metab Rev 31:195–203
40. Aliverti A, Pandini V, Pennati A, de Rosa M, Zanetti G (2008) Structural and functional diversity of ferredoxin-$NADP^+$ reductase. Arch Biochem Biophys 474:283–291
41. Porter TD, Kasper CB (1986) NADPH-cytochrome P-450 oxidoreductase: flavin mononucleotide and flavin adenine dinucleotide domains evolved from different flavoproteins. Biochemistry 25:1682–1687
42. Sancho J (2006) Flavodoxins: sequence, folding, binding, function and beyond. Cell Mol Life Sci 63:855–864
43. Ceccarelli EA, Arakaki AK, Cortez N, Carrillo N (2004) Functional plasticity and catalytic efficiency in plant and bacterial ferredoxin-NADP(H) reductases. Biochim Biophys Acta 1698:155–165
44. Yamano S, Aoyama T, McBride OW, Hardwick JP, Gelboin HV, Gonzalez FJ (1989) Human NADPH-P450 oxidoreductase: complementary DNA cloning, sequence and Vaccinia virus-mediated expression and localization of the *CYPOR* gene to chromosome 7. Mol Pharmacol 36:83–88
45. Hart SN, Zhong X (2008) P450-oxidoreductase: genetic polymorphism and implications for drug metabolism and toxicity. Expert Opin Metab Toxicol 4:439–452
46. Hu L, Zhuo W, He YJ, Zhou HH, Fan L (2012) Pharmacogenetics of P450 oxidoreductase: implications in drug metabolism and therapy. Pharmacogenet Genomics 22:812–819
47. Porter TD, Beck TW, Kasper CB (1990) NADPH-cytochrome P-450 oxidoreductase gene organization correlates with structural domains of the proteins. Biochemistry 29:9814–9818
48. Hovemann BT, Sehlmeyer F, Malz J (1997) *Drosophila melanogaster* NADPH-cytochrome P450 oxidoreductase: pronounced expression in antennae may be related to odorant clearance. Gene 189:213–219
49. Yadav JS, Loper JC (2000) Cytochrome P450 oxidoreductase gene and its differentially terminated cDNAs from the white rot fungus *Phanerochaete chrysosporium*. Curr Genet 37:65–73
50. Durst F, Nelson DR (1995) Diversity and evolution of plant P450 and P450-reductases. Drug Metabol Drug Interact 12:189–206
51. Jensen KL, Møller B (2010) Plant NADPH-cytochrome P450 oxidoreductases. Phytochemistry 71:132–141
52. Iyanagi T, Makino N, Mason HS (1974) Redox properties of the reduced nicotinamide adenine dinucleotide phosphate-cytochrome P450 and reduced nicotinamide adenine dinucleotide-cytochrome b_5 reductases. Biochemistry 13:1701–1710
53. Oprian DD, Coon MJ (1982) Oxidation-reduction states of FMN and FAD in NADPH-cytochrome P-450 reductase during reduction by NADPH. J Biol Chem 257:8935–8944
54. Massey V, Palmer G (1966) On the existence of spectrally distinct classes of flavoprotein semiquinones. A new method for quantitative production of flavoprotein semiquinones. Biochemistry 5:3181–3189
55. Müller F, Brüstlein M, Hemmerich P, Massey V, Walker WH (1972) Light-absorption studies on neutral flavin radicals. Eur J Biochem 25:573–580
56. Brenner S, Hay S, Munro AW, Scrutton NS (2008) Inter-flavin electron transfer in cytochrome P450 reductase – effects of solvent and pH identify hidden complexity in mechanism. FEBS J 275:4540–4557
57. Das A, Sligar SG (2009) Modulation of the cytochrome P450 reductase redox potential by the phospholipid bilayer. Biochemistry 48:12104–12112
58. Louerat-Oriou B, Perret A, Pompon D (1998) Differential redox and electron-transfer properties of purified yeast, plant and human NADPH-cytochrome P-450 reductases highly modulate cytochrome P-450 activities. Eur J Biochem 258:1040–1049
59. Daff SN, Chapman SK, Turner KL, Holt RA, Govindaraj S, Poulos TL, Munro AW (1997) Redox control of the catalytic cycle of flavocytochrome P-450BM3. Biochemistry 36:13816–13823
60. Hefti MH, Vervoort J, van Berkel WJH (2003) Deflavination and reconstitution of flavoproteins. Tackling fold and function. Eur J Biochem 270:4227–4242
61. Wolthers KR, Basran J, Munro AW, Scrutton NS (2003) Molecular dissection of human synthase reductase: determination of the flavin redox

potentials in full-length enzyme and isolated flavin-binding domains. Biochemistry 42:3911–3920
62. Iyanagi T (2007) Molecular mechanism of phase I and phase II drug-metabolizing enzymes: implications for detoxification. Int Rev Cytol 260:35–112
63. Gutierrez A, Paine M, Wolf CR, Scrutton NS, Roberts GCK (2002) Relaxation kinetics of cytochrome P450 reductase: internal electron transfer is limited by conformational changes and regulated by coenzyme binding. Biochemistry 41:4626–4637
64. Munro AW, Noble MA, Robledo L, Daff SN, Chapman SK (2001) Determination of the redox properties of human NADPH-cytochrome P450 reductase. Biochemistry 40:1956–1963
65. Gutierrez A, Munro AW, Grunau A, Wolf CR, Scrutton NS, Roberts GCK (2003) Interflavin electron transfer in human cytochrome P450 reductase is enhanced by coenzyme binding. Eur J Biochem 270:2612–2621
66. Vermilion JL, Ballou DP, Massey V, Coon MJ (1981) Separate roles of FMN and FAD in catalysis by liver microsomal NADPH-cytochrome P-450 reductase. J Biol Chem 256:266–277
67. Murataliev MB, Klein M, Fulco A, Feyereisen R (1997) Functional interactions in cytochrome P450BM3: flavin semiquinone intermediates, role of NADP(H), and mechanism of electron transfer by the flavoprotein domain. Biochemistry 36:8401–8412
68. Xia C, Panda SP, Marohnic CC, Martasek P, Masters BS, Kim JJP (2011) Structural basis for human NADPH-cytochrome P450 oxidoreductase deficiency. Proc Natl Acad Sci U S A 108:13486–13491
69. Wang M, Roberts DL, Paschke R, Shea TM, Masters BSS, Kim JJP (1997) Three-dimensional structure of NADPH-cytochrome P450 reductase: prototype for FMN- and FAD-containing enzymes. Proc Natl Acad Sci U S A 94:8411–8416
70. Lamb DC, Kim Y, Yermalitskaya LV, Yermalitsky VN, Lepesheva GI, Kelly SL, Waterman MR, Podust LM (2006) A second FMN binding site in yeast NADPH-cytochrome P450 reductase suggests a mechanism of electron transfer by diflavin reductases. Structure 14:51–61
71. Zhao Q, Modi S, Smith G, Paine M, McDonagh PD, Wolf CR, Tew D, Lian LY, Roberts GCK, Driessen HPC (1999) Crystal structure of the FMN-binding domain of human cytochrome P450 reductase at 1.93 Å resolution. Protein Sci 8:298–306
72. Hubbard PA, Shen AL, Paschke R, Kasper CB, Kim JJP (2001) NADPH-cytochrome P450 oxidoreductase. Structural basis for hydride and electron transfer. J Biol Chem 276:29163–29170
73. Kida Y, Ohgiya S, Mihara K, Sakaguchi M (1998) Membrane topology of NADPH-cytochrome P450 reductase on the endoplasmic reticulum. Arch Biochem Biophys 351:175–179
74. Bonina TA, Gilep AA, Estabrook RW, Usanov SA (2005) Engineering of proteolytically stable NADPH-cytochrome P450 reductase. Biochemistry (Mosc) 70:357–365
75. Sarapusit S, Xia C, Misra I, Rongnoparut P, Kim JJP (2008) NADPH-cytochrome P450 oxidoreductase from the mosquito *Anopheles minimus*: kinetic studies and the influence of Leu86 and Leu219 on cofactor binding and protein stability. Arch Biochem Biophys 477:53–59
76. Nicolo C, Flück CE, Mullis PE, Pandey AV (2010) Restoration of mutant cytochrome P450 reductase activity by external flavin. Mol Cell Endocrinol 321:245–252
77. Barsukov I, Modi S, Lian LY, Sze KH, Paine MJI, Wolf CR, Roberts GCK (1997) ^{1}H, ^{15}N and ^{13}C NMR resonance assignment, secondary structure and global fold of the FMN-binding domain of human cytochrome P450 reductase. J Biomol NMR 10:63–75
78. Paine MJI, Ayivor S, Munro A, Tsan P, Lian LY, Roberts GCK, Wolf CR (2001) Role of the conserved phenylalanine 181 of NADPH-cytochrome P450 oxidoreductase in FMN binding and catalytic activity. Biochemistry 40:13439–13447
79. Flück CE, Mullis PE, Pandey AV (2009) Modeling of human P450 oxidoreductase structure by in silico mutagenesis and MD simulation. Mol Cell Endocrinol 313:17–22
80. Shen AL, Porter TD, Wilson TE, Kasper CB (1989) Structural analysis of the FMN- binding domain of NADPH-cytochrome P-450 oxidoreductase by site-directed mutagenesis. J Biol Chem 264:7584–7589
81. Hamdane D, Xia C, Im SC, Zhang H, Kim JJP, Waskell L (2009) Structure and function of an NADPH-cytochrome P450 oxidoreductase in an open conformation capable of reducing cytochrome P450. J Biol Chem 284:11374–11384
82. Shen AL, Kasper CB (2000) Differential contributions of NADPH-cytochrome P450 oxidoreductase FAD binding site residues to flavin binding and catalysis. J Biol Chem 275:41087–41091
83. Shen AL, Kasper CB (1996) Role of Ser457 of NADPH-cytochrome P450 oxidoreductase in catalysis and control of FAD oxidation-reduction potential. Biochemistry 35:9451–9459
84. Shen AL, Sem DS, Kasper CB (1999) Mechanistic studies on the reductive half-reaction of NADPH-cytochrome P450 oxidoreductase. J Biol Chem 274:5391–5398
85. Shen AL, Christensen MJ, Kasper CB (1991) NADPH-cytochrome P-450 oxidoreductase. The role of cysteine 566 in catalysis and cofactor binding. J Biol Chem 266:19976–19980
86. Sem DS, Kasper CB (1993) Interaction with arginine 597 of NADPH-cytochrome P-450 oxidoreductase is

a primary source of the uniform binding energy used to discriminate between NADPH and NADH. Biochemistry 32:11548–11558
87. Döhr O, Paine MJI, Friedberg T, Roberts GCK, Wolf CR (2001) Engineering of a functional human NADH-dependent cytochrome P450 system. Proc Natl Acad Sci U S A 98:81–86
88. Elmore CL, Porter TD (2002) Modification of the nucleotide cofactor-binding site of cytochrome P-450 reductase to enhance turnover with NADH in vivo. J Biol Chem 277:48960–48964
89. Gutierrez A, Doehr O, Paine M, Wolf R, Scrutton NS, Roberts GCK (2000) Trp-676 facilitates nicotinamide coenzyme exchange in the reductive half-reaction of human cytochrome P450 reductase: properties of the soluble W676H and W676A mutant reductases. Biochemistry 39:15990–15999
90. Xia C, Hamdane D, Shen AL, Choi V, Kasper CB, Pearl NM, Zhang H, Im SC, Waskell L, Kim JJP (2011) Conformational changes of NADPH-cytochrome P450 oxidoreductase are essential for catalysis and cofactor binding. J Biol Chem 286:16246–16260
91. Huang N, Pandey AV, Agrawal V, Reardon W, Lapunzina PD, Mowat D, Jabs EW, Van Vliet G, Sack J, Flück CE, Miller WL (2005) Diversity and function of mutations in P450 oxidoreductase in patients with Antley-Bixler syndrome and disordered steroidogenesis. Am J Hum Genet 76:729–749
92. Pandey AV, Kempna P, Hofer G, Mullis PE, Flück CE (2007) Modulation of human CYP19A1 activity by mutant NADPH-P450 oxidoreductase. Mol Endocrinol 21:2579–2595
93. Chen X, Pan LQ, Naranmandura H, Zeng S, Chen SQ (2012) Influence of various polymorphic variants of cytochrome P450 oxidoreductase (POR) on drug metabolic activity of CYP3A4 and CYP2B6. PLoS One 7:e38495
94. Marohnic CC, Panda SP, McCammon K, Rueff J, Masters BSS, Kranendonk M (2010) Human cytochrome P450 oxidoreductase deficiency caused by the Y181D mutation: molecular consequences and rescue of defect. Drug Metab Dispos 38:332–340
95. Aigrain L, Pompon D, Morera S, Truan G (2009) Structure of the open conformation of a functional chimeric NADPH-cytochrome P450 reductase. EMBO Rep 10:742–747
96. Wadsäter M, Laursen T, Singha A, Hatzakis NS, Stamou D, Barker R, Mortensen K, Feidenhans R, Lindberg Møller B, Cardenas M (2012) Monitoring shifts in the conformation equilibrium of the membrane protein cytochrome P450 reductase (POR) in nanodiscs. J Biol Chem 287:34596–34603
97. Hay S, Brenner S, Khara B, Quinn AM, Rigby SEJ, Scrutton NS (2010) Nature of the energy landscape for gated electron transfer in a dynamic redox protein. J Am Chem Soc 132:9738–9745
98. Pudney CR, Heyes DJ, Khara B, Hay S, Rigby SEJ, Scrutton NS (2012) Kinetic and spectroscopic probes of motions and catalysis in the cytochrome P450 reductase family of enzymes. FEBS J 279:1534–1544
99. Pudney CR, Khara B, Johannissen LO, Scrutton NS (2011) Coupled motions direct electrons along human microsomal P450 chains. PLoS Biol 9: e1001222
100. Vincent B, Morellet N, Fatemi F, Aigrain L, Truan G, Guittet E, Lescop E (2012) The closed and compact domain organization of the 70-kDa human cytochrome P450 reductase in its oxidized state as revealed by NMR. J Mol Biol 420:296–309
101. Laursen T, Jensen K, Lindberg Møller B (2011) Conformational changes of the NADPH-dependent cytochrome P450 reductase in the course of electron transfer to cytochromes P450. Biochim Biophys Acta 1814:132–138
102. Hong Y, Li H, Yuan YC, Chen S (2010) Sequence-function correlation of aromatase and its interaction with reductase. J Steroid Biochem Mol Biol 118:203–206
103. Jang HH, Jamakhandi AP, Sullivan SZ, Yun CH, Hollenberg PF, Miller GP (2010) Beta sheet 2-alpha helix C loop of cytochrome P450 reductase serves as a docking site for redox partners. Biochim Biophys Acta 1804:1285–1293
104. Shen AL, Kasper CB (1995) Role of acidic residues in the interaction of NADPH- cytochrome P450 oxidoreductase with cytochrome P450 and cytochrome *c*. J Biol Chem 270:27475–27480
105. Schenkman JB, Jansson I (2003) The many roles of cytochrome b_5. Pharmacol Ther 97:139–152
106. Hultquist DE, Dean RT, Douglas RH (1974) Homogenous cytochrome b_5 from human erythrocytes. Biochem Biophys Res Commun 60:28–34
107. Bando S, Takano T, Yubisui T, Shirabe K, Takeshita M, Nakagawa A (2004) Structure of human erythrocyte NADH-cytochrome b_5 reductase. Biol Crystallogr 60:1929–1934
108. Shirabe K, Fujimoto Y, Yubisui T, Takeshita M (1994) An in-frame deletion of codon 298 in the NADH-cytochrome b_5 reductase gene results in hereditary methemoglobinemia type II (generalized type). A functional implication for the role of the COOH-terminal region of the enzyme. J Biol Chem 269:5952–5957
109. Golly I, Hlavica P (1983) The role of hemoglobin in the N-oxidation of 4-chloroaniline. Biochim Biophys Acta 760:69–76
110. Imai Y (1981) The roles of cytochrome b_5 in reconstituted monooxygenase systems containing various forms of hepatic microsomal cytochrome P-450. J Biochem 89:351–362
111. Pompon D, Coon MJ (1984) On the mechanism of action of cytochrome P-450. Oxidation and reduction of the ferrous dioxygen complex of liver microsomal cytochrome P-450 by cytochrome b_5. J Biol Chem 259:15377–15385

112. Lederer F, Ghrir R, Guiard B, Cortial S, Ito A (1983) Two homologous cytochromes b_5 in a single cell. Eur J Biochem 132:95–102
113. Vergeres G, Ramsden J, Waskell L (1995) The carboxyl-terminus of the membrane binding domain of cytochrome b_5 spans the bilayer of the endoplasmic reticulum. J Biol Chem 270:3414–3422
114. Honsho M, Mitoma J, Ito A (1998) Retention of cytochrome b_5 in the endoplasmic reticulum is transmembrane and luminal domain-dependent. J Biol Chem 273:20860–20866
115. Tanaka S, Kinoshita J, Kuroda R, Ito A (2003) Integration of cytochrome b_5 into endo- plasmic reticulum membrane: participation of carboxy-terminal portion of the transmembrane domain. J Biochem 133:247–251
116. Hanlon MR, Begum RR, Newbold RJ, Whitford D, Wallace BA (2000) *In vitro* membrane-inserted conformation of the cytochrome b_5 tail. Biochem J 352:117–124
117. Kaderbhai MA, Morgan R, Kaderbhai NN (2003) The membrane-interactive tail of cytochrome b_5 can function as a stop-transfer sequence in concert with a signal sequence to give inversion of protein topology in the endoplasmic reticulum. Arch Biochem Biophys 412:259–266
118. Vergeres G, Waskell L (1995) Cytochrome b_5, its functions, structure and membrane topology. Biochimie 77:604–620
119. Vergeres G, Waskell L (1992) Expression of cytochrome b_5 in yeast and characterization of mutants of the membrane-anchoring domain. J Biol Chem 267:12583–12591
120. Cowley AB, Altuve A, Kuchment O, Terzyan S, Zhang X, Rivera M, Benson DR (2002) Toward engineering the stability and hemin-binding properties of microsomal cytochrome b_5 into rat outer mitochondrial membrane cytochrome b_5: examining the influence of residues 25 and 71. Biochemistry 41:11566–11581
121. Mathews FS, Levine M, Argos P (1972) Three-dimensional fourier synthesis of calf liver cytochrome b_5 at 2.8 Å resolution. J Mol Biol 64:449–464
122. Durley RCE, Mathews FS (1996) Refinement and structural analysis of bovine cytochrome b_5 at 1.5 Å resolution. Acta Cryst D52:65–76
123. Konopka K, Waskell L (1988) Modification of trypsin-solubilized cytochrome b_5, apo-cytochrome b_5, and liposome-bound cytochrome b_5 by diethylpyrocarbonate. Arch Biochem Biophys 261:55–63
124. Wang WH, Lu J, Yao P, Xie Y, Huang ZX (2003) The distinct heme coordination environments and heme-binding stabilities of His39Ser and His39Cys mutants of cytochrome b_5. Protein Eng 16:1047–1054
125. Aono T, Sakamoto Y, Miura M, Takeuchi F, Hori H, Tsubaki M (2010) Direct electrochemical analysis of human cytochromes b_5 with a mutated heme pocket showed a good correlation between their midpoint and half wave potentials. J Biomed Sci 17:90–104
126. Cao C, Zhang Q, Wang ZQ, Wang YF, Wang YH, Wu H, Huang ZX (2003) ^{1}H NMR studies of the effect of mutation at valine 45 on heme microenvironment of cytochrome b_5. Biochimie 85:1007–1016
127. Cao C, Zhang Q, Xue LL, Ma J, Wang YH, Wu H, Huang ZX (2003) The solution structure of the oxidized bovine microsomal cytochrome b_5 mutant V61H. Biochem Biophys Res Commun 307:600–609
128. Dangi B, Sarma S, Yan C, Banville DL, Guiles RD (1998) The origin of differences in the physical properties of the equilibrium forms of cytochrome b_5 revealed through high-resolution NMR structures and backbone dynamic analyses. Biochemistry 37:8289–8302
129. Shan L, Lu JX, Gan JH, Wang YH, Huang ZX, Xia ZX (2005) Structure of the F58W mutant of cytochrome b_5: the mutation leads to multiple conformations and weakens stacking interactions. Acta Cryst D61:180–189
130. Mathews FS, Czerwinski EW (1985) Cytochrome b_5 and cytochrome b_5 reductase from the chemical and X-ray diffraction viewpoint. In: Martonosi AN (ed) The enzymes of biological membranes, 4th edn. Springer, New York, pp 235–300
131. Vergeres G, Chen DY, Wu FF, Waskell L (1993) The function of tyrosine 74 of cytochrome b_5. Arch Biochem Biophys 305:231–241
132. Yao P, Wu J, Wang YH, Sun BY, Xia ZX, Huang ZX (2002) X-ray crystallography, CD and kinetic studies revealed the essence of the abnormal behaviors of the cytochrome b_5 Phe35→Tyr mutant. Eur J Biochem 269:4287–4296
133. Yao P, Xie Y, Wang YH, Sun YL, Huang ZX, Xiao GT, Wang SD (1997) Importance of the conserved phenylalanine-35 of cytochrome b_5 to the protein's stability and redox potential. Protein Eng 10:575–581
134. Wang ZQ, Wang YH, Qian W, Wang HH, Chunyu LJ, Xie Y, Huang ZX (1999) Methanol-induced unfolding and refolding of cytochrome b_5 and its P40V mutant monitored by UV-visible, CD, and fluorescence spectra. J Protein Chem 18:547–555
135. Banci L, Bertini I, Rosato A, Scacchieri S (2000) Solution structure of oxidized microsomal rabbit cytochrome b_5. Factors determining the heterologous binding of the heme. Eur J Biochem 267:755–766
136. Kobayashi K, Iyanagi T, Ohara H, Hayashi K (1988) One-electron reduction of hepatic NADH-cytochrome b_5 reductase as studied by pulse radiolysis. J Biol Chem 263:7493–7499
137. Kimura S, Kawamura M, Iyanagi T (2003) Role of Thr66 in porcine NADH-cytochrome b_5 reductase in catalysis and control of the rate-limiting step in electron transfer. J Biol Chem 278:3580–3589

138. Nishida H, Inaka K, Miki K (1995) Specific arrangement of three amino acid residues for flavin-binding barrel structures in NADH-cytochrome b_5 reductase and the other flavin-dependent reductases. FEBS Lett 361:97–100
139. Kimura S, Nishida H, Iyanagi T (2001) Effects of flavin-binding motif amino acid mutations in the NADH-cytochrome b_5 reductase catalytic domain on protein stability and catalysis. J Biochem 130:481–490
140. Bewley MC, Marohnic CC, Barber MJ (2001) The structure and biochemistry of NADH-dependent cytochrome b_5 reductase are now consistent. Biochemistry 40:13574–13582
141. Strittmatter P, Kittler JM, Coghill JE (1992) Characterization of the role of lysine 110 of NADH-cytochrome b_5 reductase in the binding and oxidation of NADH by site-directed mutagenesis. J Biol Chem 267:20164–20167
142. Fujimoto Y, Shirabe K, Nagai T, Yubisui T, Takehita M (1993) Role of Lys-110 of human NADH-cytochrome b_5 reductase in NADH binding as probed by site-directed mutagenesis. FEBS Lett 322:30–32
143. Yubisui T, Shirabe K, Takeshita M, Kobayashi Y, Fukumaki Y, Sakaki Y, Takano T (1991) Structural role of serine 127 in the NADH-binding site of human NADH-cytochrome b_5 reductase. J Biol Chem 266:66–70
144. Roma GW, Crowley LJ, Davis CA, Barber MJ (2005) Mutagenesis of glycine 179 modulates both catalytic efficiency and reduced pyridine nucleotide specificity in cytochrome b_5 reductase. Biochemistry 44:13467–13476
145. Percy MJ, Crowley LJ, Boudreaux J, Barber MJ (2006) Expression of a novel P275L variant of NADH-cytochrome b_5 reductase gives functional insight into the conserved motif important for pyridine nucleotide binding. Arch Biochem Biophys 447:59–67
146. Shirabe K, Yubisui T, Nishino T, Takeshita M (1991) Role of cysteine residues in human NADH-cytochrome b_5 reductase studied by site-directed mutagenesis. CYS-273 and CYS-283 are located close to the NADH-binding site but are not catalytically essential. J Biol Chem 266:7531–7536
147. Marohnic CC, Bewley MC, Barber MJ (2003) Engineering and characterization of a NADPH-utilizing cytochrome b_5 reductase. Biochemistry 42:11170–11182
148. Ozols J, Carr SA, Strittmatter P (1984) Identification of the NH_2-terminal blocking group of NADH-cytochrome b_5 reductase as myristic acid and the complete amino acid sequence of the membrane-binding domain. J Biol Chem 259:13349–13354
149. Strittmatter P, Hackett CS, Korza G, Ozols J (1990) Characterization of the covalent cross-links of the active sites of amidinated cytochrome b_5 and NADH-cytochrome b_5 reductase. J Biol Chem 265:21709–21713
150. Strittmatter P, Kittler J, Goghill JE, Ozols J (1992) Characterization of lysyl residues of NADH-cytochrome b_5 reductase implicated in charge-pairing with active-site carboxyl residues of cytochrome b_5 by site-directed mutagenesis of an expression vector for the flavoprotein. J Biol Chem 267:2519–2523
151. Dailey HA, Strittmatter P (1979) Modification and identification of cytochrome b_5 carboxyl groups involved in protein-protein interaction with cytochrome b_5 reductase. J Biol Chem 254:5388–5396
152. Kawano M, Shirabe K, Nagai T, Takeshita M (1998) Role of carboxyl residues surrounding heme of human cytochrome b_5 in electrostatic interaction with NADH-cytochrome b_5 reductase. Biochem Biophys Res Commun 245:666–669
153. Dailey HA, Strittmatter P (1980) Characterization of the interaction of amphipathic cytochrome b_5 with stearyl coenzyme A desaturase and NADPH-cytochrome P450 reductase. J Biol Chem 255:5184–5189
154. Nisimoto Y, Otsuka-Murakami H (1988) Cytochrome b_5, cytochrome *c*, and cytochrome P-450 interactions with NADPH-cytochrome P-450 reductase in phospholipid vesicles. Biochemistry 27:5869–5876
155. Enoch HG, Strittmatter P (1979) Cytochrome b_5 reduction by NADPH-cytochrome P-450 reductase. J Biol Chem 254:8976–8981
156. Guengerich FP (2005) Reduction of cytochrome b_5 by NADPH-cytochrome P450 reductase. Arch Biochem Biophys 440:204–211
157. Bhattacharyya AK, Hurley JK, Tollin G, Waskell L (1994) Investigation of the rate limiting step for electron transfer from NADPH-cytochrome P450 reductase to cytochrome b_5: laser flash-photolysis study. Arch Biochem Biophys 310:318–324
158. Meyer TE, Shirabe K, Yubisui T, Takeshita M, Bes MT, Cusanovich MA, Tollin G (1995) Transient kinetics of intracomplex electron transfer in the human cytochrome b_5 reductase-cytochrome b_5 system: NAD^+ modulates protein-protein binding and electron transfer. Arch Biochem Biophys 318:457–464
159. Gruenke L, Konopka K, Cadieu M, Waskell L (1995) The stoichiometry of the cyto- chrome P-450-catalyzed metabolism of methoxyfurane and benzphetamine in the presence and absence of cytochrome b_5. J Biol Chem 270:24707–24718
160. Peng HM, Auchus RJ (2013) The action of cytochrome b_5 on CYP2E1 and CYP2C19 activities requires anionic residues D58 and D65. Biochemistry 52:210–220
161. Shet MS, Faulkner KM, Holmans PL, Fisher CW, Estabrook RW (1995) The effects of cytochrome b_5, NADPH-P450 reductase, and lipid on the rate of 6β-hydroxylation of testosterone as catalyzed by a

human P450 3A4 fusion protein. Arch Biochem Biophys 318:314–321
162. Hlavica P (1984) On the function of cytochrome b_5 in the cytochrome P-450-dependent oxygenase system. Arch Biochem Biophys 228:600–608
163. Tamburini PP, Gibson GG (1983) Thermodynamic studies on the protein-protein interactions between cytochrome P-450 and cytochrome b_5. Evidence for a central role of the cytochrome P-450 spin state in the coupling of substrate and cytochrome b_5 binding to the terminal hemoprotein. J Biol Chem 258:13444–13452
164. Guengerich FP (1983) Oxidation-reduction properties of rat liver cytochromes P-450 and NADPH-cytochrome P-450 reductase related to catalysis in reconstituted systems. Biochemistry 22:2811–2820
165. Noshiro M, Ullrich V, Omura T (1981) Cytochrome b_5 as electron donor for oxycytochrome P-450. Eur J Biochem 116:521–526
166. Ingelman-Sundberg M, Johansson I (1980) Cytochrome b_5 as electron donor to rabbit liver cytochrome P-450LM2 in reconstituted phospholipid vesicles. Biochem Biophys Res Commun 97:582–589
167. Gorsky LD, Coon MJ (1986) Effects of conditions for reconstitution with cytochrome b_5 on the formation of products in cytochrome P-450-catalyzed reactions. Drug Metab Dispos 14:89–96
168. Golly I, Hlavica P (1987) Regulative mechanisms in NADH- and NADPH-supported N-oxidation of 4-chloroaniline catalyzed by cytochrome b_5-enriched rabbit liver microsomal fractions. Biochim Biophys Acta 913:219–227
169. Guengerich FP, Ballou DP, Coon MJ (1976) Spectral intermediates in the reaction of oxygen with purified liver microsomal cytochrome P-450. Biochem Biophys Res Commun 70:951–956
170. Lipscomb JD, Sligar SG, Namtvedt MJ, Gunsalus IC (1976) Autoxidation and hydroxylation reactions of oxygenated cytochrome P-450_{cam}. J Biol Chem 251:1116–1124
171. Lee-Robichaud P, Akhtar ME, Akhtar M (1998) Control of androgen biosynthesis in the human through the interaction of Arg347 and Arg358 of CYP17 with cytochrome b_5. Biochem J 332:293–296
172. Auchus RJ, Lee TC, Miller WL (1998) Cytochrome b_5 augments the 17,20-lyase activity of human P450c17 without direct electron transfer. J Biol Chem 273:3158–3165
173. Storbeck KH, Swart AC, Goosen P, Swart P (2013) Cytochrome b_5: novel roles in steroidogenesis. Mol Cell Endocrinol 371:87–99
174. Yamazaki H, Shimada T, Martin MV, Guengerich FP (2001) Stimulation of cytochrome P450 reactions by apo-cytochrome b_5. Evidence against transfer of heme from cytochrome P450 3A4 to apo-cytochrome b_5 or heme oxygenase. J Biol Chem 276:30885–30891
175. Yamazaki H, Nakamura M, Komatsu T, Ohyama K, Hatanaka N, Asahi S, Shimada N, Guengerich FP, Shimada T, Nakajima M, Yokoi T (2002) Roles of NADPH-cytochrome P450 reductase and apo- and holo-cytochrome b_5 on xenobiotic oxidations catalyzed by 12 recombinant human cytochrome P450s expressed in membranes of *Escherichia coli*. Protein Expr Purif 24:329–337
176. Loughran PA, Roman LJ, Miller T, Masters BSS (2001) The kinetic and spectral characterization of the *E. coli*-expressed mammalian CYP4A7: cytochrome b_5 effects vary with substrate. Arch Biochem Biophys 385:311–321
177. Hlavica P, Lewis DFV (2001) Allosteric phenomena in cytochrome P450-catalyzed monooxygenations. Eur J Biochem 268:4817–4832
178. Porter TD (2002) The roles of cytochrome b_5 in cytochrome P450 reactions. J Biochem Mol Toxicol 16:311–316
179. Ivanov YD, Kanaeva IP, Kuznetsov VY, Lehnerer M, Schulze J, Hlavica P, Archakov AI (1999) The optical biosensor studies on the role of hydrophobic tails of NADPH-cytochrome P450 reductase and cytochromes P450 2B4 and b_5 upon productive complex formation with a monomeric reconstituted system. Arch Biochem Biophys 362:87–93
180. Mulrooney SB, Meinhardt DR, Waskell L (2004) The α-helical membrane spanning domain of cytochrome b_5 interacts with cytochrome P450 via nonspecific interactions. Biochim Biophys Acta 1674:319–326
181. Clarke TA, Im SC, Bidwai A, Waskell L (2004) The role of the length and sequence of the linker domain of cytochrome b_5 in stimulating cytochrome P450 2B4 catalysis. J Biol Chem 279:36809–36818
182. Hlavica P, Kellermann J, Golly I, Lehnerer M (1994) Chemical modification of Tyr34 and Tyr129 in rabbit liver microsomal cytochrome b_5 affects interaction with cytochrome P-450 2B4. Eur J Biochem 224:1039–1046
183. Stayton PS, Poulos TL, Sligar SG (1989) Putidaredoxin competitively inhibits cytochrome b_5-cytochrome P450_{cam} association: a proposed molecular model for a cytochrome P450_{cam} electron-transfer complex. Biochemistry 28:8201–8205
184. Stayton PS, Fisher MT, Sligar SG (1988) Determination of cytochrome b_5 association reactions. Characterization of metmyoglobin and cytochrome P-450_{cam} binding to genetically engineered cytochrome b_5. J Biol Chem 263:13544–13548
185. Degtyarenko KN, Kulikova TA (2001) Evolution of bioinorganic motifs in P450- containing systems. Biochem Soc Trans 29:139–147
186. Grindberg AV, Hannemann F, Schiffler B, Müller J, Heinemann U, Bernhardt R (2000) Adrenodoxin: structure, stability, and electron transfer properties. Proteins 40:590–612
187. Kostic M, Pochapsky SS, Obenauer J, Mo H, Pagani GM, Pejchal R, Pochapsky TC (2002) Comparison

of functional domains in vertebrate-type ferredoxins. Biochemistry 41:5978–5989
188. Ewen KM, Kleser M, Bernhardt R (2011) Adrenodoxin: the archetype of vertebrate-type [2Fe-2S] cluster ferredoxins. Biochim Biophys Acta 1814:111–125
189. Sevrioukova IF, Poulos TL (2011) Structural biology of redox partner interactions in $P450_{cam}$ monooxygenase: a fresh look at an old system. Arch Biochem Biophys 507:66–74
190. Ziegler GA, Vonrhein C, Hanukoglu I, Schulz GE (1999) The structure of adrenodoxin reductase of mitochondrial P450 systems: electron transfer for steroid biosynthesis. J Mol Biol 289:981–990
191. Sevrioukova IF, Poulos TL (2002) Putidaredoxin reductase, a new function for an old protein. J Biol Chem 277:25831–25839
192. Heinz A, Hannemann F, Müller JJ, Heinemann U, Bernhardt R (2005) The interaction domain of the redox protein adrenodoxin is mandatory for binding of the electron acceptor CYP11A1, but is not required for binding of the electron donor adrenodoxin reductase. Biochem Biophys Res Commun 228:491–498
193. Müller JJ, Lapko A, Bourenkov G, Ruckpaul K, Heinemann U (2001) Adrenodoxin reductase-adrenodoxin complex structure suggests electron transfer path in steroid biosynthesis. J Biol Chem 276:2786–2789
194. Coghlan VM, Vickery LE (1991) Site-specific mutations in human ferredoxin that affect binding to ferredoxin reductase and cytochrome $P450_{scc}$. J Biol Chem 266:18606–18612
195. Grindberg AV, Bernhardt R (2001) Contribution of a salt bridge to the thermostability of adrenodoxin determined by site-directed mutagenesis. Arch Biochem Biophys 396:25–34
196. Beckert V, Dettmer R, Bernhardt R (1994) Mutations of tyrosine 82 in bovine adrenodoxin that affect binding to cytochromes P450 11A1 and P450 11B1 but not electron transfer. J Biol Chem 269:2568–2573
197. Beckert V, Schrauber H, Bernhardt R, van Dijk AA, Kakoschke C, Wray V (1995) Mutational effects on the spectroscopic properties and biological activities of oxidized bovine adrenodoxin, and their structural implications. Eur J Biochem 231:226–235
198. Beckert V, Bernhardt R (1997) Specific aspects of electron transfer from adrenodoxin to cytochromes $P450_{scc}$ and $P450_{11\beta}$. J Biol Chem 272:4883–4888
199. Uhlmann H, Bernhardt R (1995) The role of threonine 54 in adrenodoxin for the properties of its iron-sulfur cluster and its electron function. J Biol Chem 270:29959–29966
200. Schiffler B, Kiefer M, Wilken A, Hannemann F, Adolph HW, Bernhardt R (2001) The interaction of bovine adrenodoxin with CYP11A1 (cytochrome $P450_{scc}$) and CYP11B1 (cytochrome $P450_{11\beta}$). Acceleration of reduction and substrate conversion by site-directed mutagenesis of adrenodoxin. J Biol Chem 276:36225–36232
201. Hannemann F, Rottmann M, Schiffler B, Zapp J, Bernhardt R (2001) The loop region covering the iron-sulfur cluster in bovine adrenodoxin comprises a new interaction site for redox partners. J Biol Chem 276:1369–1375
202. Zöllner A, Hannemann F, Lisurek M, Bernhardt R (2002) Deletions in the loop surrounding the iron-sulfur cluster of adrenodoxin severely affect the interactions with its native redox partners adrenodoxin reductase and cytochrome $P450_{scc}$ (CYP11A1). J Inorg Biochem 91:644–654
203. Vickery LE (1997) Molecular recognition and electron transfer in mitochondrial steroid hydroxylase systems. Steroids 62:124–127
204. Lambeth JD, Geren LM, Millett F (1984) Adrenodoxin interaction with adrenodoxin reductase and cytochrome $P\text{-}450_{scc.}$ Cross-linking of protein complexes and effects of adrenodoxin modification by 1-ethyl-3-(3-dimethylaminopropyl)carbodiimide. J Biol Chem 259:10025–10029
205. Müller EC, Lapko A, Otto A, Müller JJ, Ruckpaul K, Heinemann U (2001) Covalently crosslinked complexes of bovine adrenodoxin with adrenodoxin reductase and cytochrome $P450_{scc}$. Mass spectrometry and Edman degradation of complexes of the steroidogenic hydroxylase system. Eur J Biochem 268:1837–1843
206. Beilke D, Weiss R, Löhr F, Pristovsek P, Hannemann F, Bernhardt R, Rüterjans H (2002) A new electron transport mechanism in mitochondrial steroid hydroxylase systems based on structural changes upon the reduction of adrenodoxin. Biochemistry 41:7969–7978
207. Müller A, Müller JJ, Muller YA, Uhlmann H, Bernhardt R, Heinemann U (1998) New aspects of electron transfer revealed by the crystal structure of a truncated bovine adrenodoxin, Adx(4-108). Structure 6:269–280
208. Kuznetsov VY, Blair E, Farmer PJ, Poulos TL, Pifferitti A, Sevrioukova IF (2005) The putidaredoxin reductase-putidaredoxin electron transfer complex. Theoretical and experimental studies. J Biol Chem 280:16135–16142
209. Sevrioukova IF, Poulos TL, Churbanova IY (2010) Crystal structure of the putidaredoxin reductase-putidaredoxin electron transfer complex. J Biol Chem 285:13616–13620
210. Aoki M, Ishimori K, Morishima I (1998) Roles of negatively charged surface residues of putidaredoxin in interactions with redox partners in $P450_{cam}$ monooxygenase system. Biochim Biophys Acta 1386:157–167
211. Holden M, Mayhew M, Bunk D, Roitberg A, Vilker V (1997) Probing the interactions of putidaredoxin

with redox partners in camphor P450 5-monooxygenase by mutagenesis of surface residues. J Biol Chem 272:21720–21725
212. Sevrioukova IF, Garcia C, Li H, Bhaskar B, Poulos TL (2003) Crystal structure of putidaredoxin, the [2Fe-2S] component of the $P450_{cam}$ monooxygenase system from *Pseudomonas putida*. J Mol Biol 333:377–392
213. Zhang W, Pochapsky SS, Pochapsky TC, Jain NU (2008) Solution NMR structure of putidaredoxin-cytochrome $P450_{cam}$ complex via a combined residual dipolar coupling-spin labeling approach suggests a role for Trp106 of putidaredoxin in complex formation. J Mol Biol 384:349–363
214. Kuznetsov VY, Poulos TL, Sevrioukova IF (2006) Putidaredoxin-to-cytochrome $P450_{cam}$ electron transfer: differences between the two reductive steps required for catalysis. Biochemistry 45:11934–11944
215. Stayton PS, Sligar SG (1991) Structural microheterogeneity of a tryptophan residue required for efficient biological electron transfer between putidaredoxin and cytochrome P-450_{cam}. Biochemistry 30:1845–1851
216. Pochapsky TC, Lyons TA, Kazanis S, Arakaki T, Ratnaswamy G (1996) A structure-based model for cytochrome $P450_{cam}$-putidaredoxin interactions. Biochimie 78:723–733
217. Roitberg AE, Holden MJ, Mayhew MP, Kurnikov IV, Beratan DN, Vilker VL (1998) Binding and electron transfer between putidaredoxin and cytochrome $P450_{cam}$. Theory and experiments. J Am Chem Soc 120:8927–8932
218. Sibbesen O, De Voss JJ, Ortiz de Montellano PR (1996) Putidaredoxin reductase-putidaredoxin-cytochrome $P450_{cam}$ triple fusion protein. Construction of a self-sufficient *Escherichia coli* catalytic system. J Biol Chem 271:22462–22469
219. Ivanov YD, Kanaeva IP, Karuzina II, Archakov AI, Hui Bon Hoa G, Sligar SG (2001) Molecular recognition in the $P450_{cam}$ monooxygenase system: direct monitoring of protein-protein interactions by using optical biosensor. Arch Biochem Biophys 391:255–264
220. Purdy MM, Koo LS, Ortiz de Montellano PR, Klinman JP (2004) Steady-state kinetic investigation of cytochrome $P450_{cam}$: interaction with redox partners and reaction with molecular oxygen. Biochemistry 43:271–281
221. Schiffler B, Bernhardt R (2003) Bacterial (CYP101) and mitochondrial P450 systems – how comparable are they? Biochem Biophys Res Commun 312:223–228
222. Anandatheerthavarada HK, Addya S, Mullick J, Avadhani NG (1998) Interaction of adrenodoxin with P450 1A1 and its truncated form P450MT2 through different domains: differential modulation of enzyme activities. Biochemistry 37:1150–1160
223. Lehnerer M, Schulze J, Bernhardt R, Hlavica P (1999) Some properties of mitochondrial adrenodoxin associated with its nonconventional electron donor function toward rabbit liver microsomal P450 2B4. Biochem Biophys Res Commun 254:83–87
224. Lehnerer M, Schulze J, Petzold A, Bernhardt R, Hlavica P (1995) Rabbit liver cytochrome P-450 2B5: high-level expression of the full-length protein in *Escherichia coli*, purification, and catalytic activity. Biochim Biophys Acta 1245:107–115
225. Pechurskaya T, Harnastai IN, Grabovec IP, Gilep AA, Usanov SA (2007) Adrenodoxin supports reactions catalyzed by microsomal steroidogenic cytochrome P450s. Biochem Biophys Res Commun 353:598–604
226. Liao WL, Dodder NG, Mast N, Pikuleva IA, Turko IV (2009) Steroid and protein ligand binding to cytochrome P450 46A1 as assessed by hydrogen-deuterium exchange and mass spectrometry. Biochemistry 48:4150–4158
227. Hannemann F, Virus C, Bernhardt R (2006) Design of an *Escherichia coli* system for whole cell mediated steroid synthesis and molecular evolution of steroid hydroxylases. J Biotechnol 124:172–181
228. Ringle M, Khatri Y, Zapp J, Hannemann F, Bernhardt R (2012) Application of a new versatile electron transfer system for cytochrome P450-based *Escherichia coli* whole-cell bioconversions. Appl Microbiol Biotechnol 97:7741–7754
229. Ewen KM, Schiffler B, Uhlmann-Schiffler H, Bernhardt R, Hannemann F (2008) The endogenous adrenodoxin reductase-like flavoprotein arh1 supports heterologous cytochrome P450-dependent substrate conversions in *Schizosaccharomyces pombe*. FEMS Yeast Res 8:432–441
230. Dong MS, Yamazaki H, Guo Z, Guengerich FP (1996) Recombinant human cytochrome P450 1A2 and an N-terminal-truncated form: construction, purification, aggregation properties, and interactions with flavodoxin, ferredoxin, and NADPH-cytochrome P450 reductase. Arch Biochem Biophys 327:11–19
231. Yamazaki H, Ueng YF, Shimada T, Guengerich FP (1995) Roles of divalent metal ions in oxidations catalyzed by recombinant cytochrome P450 3A4 and replacement of NADPH-cytochrome P450 reductase with other flavoproteins, ferredoxin, and oxygen surrogates. Biochemistry 34:8380–8389
232. Sawada N, Sakaki T, Yoneda S, Kusudo T, Shinkyo R, Ohta M, Inouye K (2004) Conversion of vitamin D_3 to 1α,25-dihydroxyvitamin D_3 by *Streptomyces griseolus* cytochrome P450SU-1. Biochem Biophys Res Commun 320:156–164
233. Momoi K, Hofmann U, Schmid RD, Urlacher VB (2006) Reconstitution of β-carotene hydroxylase activity of thermostable CYP175A1 monooxygenase. Biochem Biophys Res Commun 339:331–336
234. Bell SG, Hoskins N, Xu F, Caprotti D, Rao Z, Wong LL (2006) Cytochrome P450 enzymes from the

metabolically diverse bacterium *Rhodopseudomonas palustris*. Biochem Biophys Res Commun 342:191–196
235. Bernhardt R, Gunsalus IC (1992) Reconstitution of cytochrome P450 2B4 (LM2) activity with camphor and linalool monooxygenase electron donors. Biochem Biophys Res Commun 187:310–317
236. Jenkins CM, Waterman MR (1994) Flavodoxin and NADPH-flavodoxin reductase from *Escherichia coli* support bovine cytochrome P450c17 hydroxylase activities. J Biol Chem 269:27401–27408
237. McIver L, Leadbeater C, Campopiano DJ, Baxter RL, Daff SN, Chapman SK, Munro AW (1998) Characterization of flavodoxin $NADP^+$ oxidoreductase and flavodoxin; key components of electron transfer in *Escherichia coli*. Eur J Biochem 257:577–585
238. Girhard M, Schuster S, Dietrich M, Dürre P, Urlacher VB (2007) Cytochrome P450 monooxygenase from *Clostridium acetobutylicum*: a new α-fatty acid hydroxylase. Biochem Biophys Res Commun 362:114–119
239. Girhard M, Tieves F, Weber E, Smit MS, Urlacher VB (2013) Cytochrome P450 reductase from *Candida apicola*: versatile redox partner of bacterial P450s. Appl Microbiol Biotechnol 97:1625–1635
240. Lehnerer M, Schulze J, Pernecky SJ, Lewis DFV, Eulitz M, Hlavica P (1998) Influence of mutation of the amino-terminal signal anchor sequence of cytochrome P450 2B4 on the enzyme structure and electron transfer processes. J Biochem 124:396–403
241. Hlavica P, Golly I, Wolf J (1987) Influence of N, N-dimethylaniline on the association of phenobarbital-induced cytochrome P450 and NADPH-cytochrome c (P450) reductase in a reconstituted rabbit liver microsomal enzyme system. Biochim Biophys Acta 915:28–36
242. Hanna IH, Kim MS, Guengerich FP (2001) Heterologous expression of cytochrome P450 2D6 mutants, electron transfer, and catalysis of bufuralol hydroxylation: the role of aspartate 30 in structural integrity. Arch Biochem Biophys 393:255–261
243. von Wachenfeldt C, Richardson TH, Cosme J, Johnson EF (1997) Microsomal P450 2C3 is expressed as a soluble dimer in *Escherichia coli* following modifications of its N-terminus. Arch Biochem Biophys 339:107–114
244. Voznesensky AI, Schenkman JB, Pernecky SJ, Coon MJ (1994) The NH_2-terminal region of rabbit CYP2E1 is not essential for interaction with NADPH-cytochrome P450 reductase. Biochem Biophys Res Commun 203:156–161
245. Mao W, Berenbaum MR, Schuler MA (2008) Modifications in the N-terminus of an insect cytochrome P450 enhance production of catalytically active protein in baculovirus-Sf9 cell expression systems. Insect Biochem Mol Biol 38:66–75
246. Scheller U, Kraft R, Schröder KL, Schunck WH (1994) Generation of a soluble and functional cytosolic domain of microsomal cytochrome P450 52A3. J Biol Chem 269:12779–12783
247. Shen S, Strobel HW (1992) The role of cytochrome P450 lysine residues in the interaction between cytochrome P450 1A1 and NADPH-cytochrome P450 reductase. Arch Biochem Biophys 294:83–90
248. Cvrk T, Hodek P, Strobel HW (1996) Identification and characterization of cytochrome P450 1A1 amino acid residues interacting with a radiolabeled photoaffinity diazido-benzphetamine analogue. Arch Biochem Biophys 330:142–152
249. Shen S, Strobel HW (1995) Functional assessment of specific amino acid residues of cytochrome P450 1A1 using anti-peptide antibodies. Arch Biochem Biophys 320:162–169
250. Parkinson A, Ryan DE, Thomas PE, Jerina DM, Sayer JM, van Bladeren PJ, Haniu M, Shively JE, Levin W (1986) Chemical modification and inactivation of rabbit liver microsomal cytochrome P-450c by 2-bromo-4′-nitroacetophenone. J Biol Chem 261:11478–11486
251. Edwards RJ, Singleton AM, Murray BP, Sesardic D, Rich KJ, Davies DS, Boobis AR (1990) An anti-peptide antibody targeted to a specific region of rat cytochrome P-450 1A2 inhibits enzyme activity. Biochem J 266:497–504
252. Jänig GR, Kraft R, Blanck J, Ristau O, Rabe H, Ruckpaul K (1987) Chemical modification of cytochrome P-450LM4. Identification of functionally linked tyrosine residues. Biochim Biophys Acta 916:512–523
253. Cvrk T, Strobel HW (2001) Role of Lys271 and Lys279 residues in the interaction of cytochrome P450 1A1 with NADPH-cytochrome P450 reductase. Arch Biochem Biophys 385:290–300
254. Shimizu T, Tateishi T, Hatano M, Fuji-Kuriyama Y (1991) Probing the role of lysines and arginines in the catalytic function of cytochrome P450d by site-directed mutagenesis. J Biol Chem 266:3372–3375
255. Mayuzumi H, Sambongi C, Hiroya K, Shimizu T, Tateishi T, Hatano M (1993) Effect of mutations of ionic amino acids of cytochrome P450 1A2 on catalytic activities toward 7-ethoxycoumarin and methanol. Biochemistry 32:5622–5628
256. Frey AB, Waxman DJ, Kreibich G (1985) The structure of phenobarbital-inducible rat liver cytochrome P-450 isozyme PB-4. J Biol Chem 260:15253–15265
257. Omata Y, Dai R, Smith SV, Robinson RC, Friedman FK (2000) Synthetic peptide mimics of a predicted topographical interaction surface: the cytochrome P450 2B1 recognition domain for NADPH-cytochrome P450 reductase. J Protein Chem 19:23–32
258. Shen S, Strobel HW (1993) Role of lysine and arginine residues of cytochrome P450 in the interaction between cytochrome P450 2B1 and NADPH-

cytochrome P450 reductase. Arch Biochem Biophys 304:257–265
259. Bernhardt R, Kraft R, Otto A, Ruckpaul K (1988) Electrostatic interaction between cytochrome P-450LM2 and NADPH-cytochrome P-450 reductase. Biomed Biochim Acta 47:581–592
260. Bridges A, Gruenke L, Chang YT, Vakser IA, Loew G, Waskell L (1998) Identification of the binding site on cytochrome P450 2B4 for cytochrome b_5 and cytochrome P450 reductase. J Biol Chem 273:17036–17049
261. Lehnerer M, Schulze J, Achterhold K, Lewis DFV, Hlavica P (2000) Identification of key residues in rabbit liver microsomal cytochrome P450 2B4: importance in interactions with NADPH-cytochrome P450 reductase. J Biochem 127:163–169
262. Schulze J, Tschöp K, Lehnerer M, Hlavica P (2000) Residue 285 in cytochrome P450 2B4 lacking the NH_2-terminal hydrophobic sequence has a role in the functional association of NADPH-cytochrome P450 reductase. Biochem Biophys Res Commun 270:777–781
263. Kenaan C, Zhang H, Shea EV, Hollenberg PF (2011) Uncovering the role of hydrophobic residues in cytochrome P450-cytochrome P450 reductase interactions. Biochemistry 50:3957–3967
264. Zhang H, Sridar C, Kenaan C, Amunugama H, Ballou DP, Hollenberg PF (2011) Polymorphic variants of cytochrome P450 2B6 (CYP2B6.4-CYP2B6.9) exhibit altered rates of metabolism for bupropion and efavirenz: a charge-reversal mutation in the K139E variant (CYP2B6.8) impairs formation of a functional cytochrome P450-reductase complex. J Pharmacol Exp Ther 338:803–809
265. Bumpus NN, Hollenberg PF (2010) Cross-linking of human cytochrome P450 2B6 to NADPH-cytochrome P450 reductase: identification of a potential site of interaction. J Inorg Biochem 104:485–488
266. Kaspera R, Naraharisetti SB, Evangelista EA, Marciante KD, Psaty BM, Totah RA (2011) Drug metabolism by CYP2C8.3 is determined by substrate dependent interactions with cytochrome P450 reductase and cytochrome b_5. Biochem Pharmacol 82:681–691
267. Crespi CI, Miller VP (1997) The R144C change in the CYP2C9.2 allele alters interaction of the cytochrome P450 with NADPH:cytochrome P450 oxidoreductase. Pharmacogenetics 7:203–210
268. Wada Y, Mitsuda M, Ishihara Y, Watanabe M, Iwasaki M, Asahi S (2008) Important amino acid residues that confer CYP2C19 selective activity to CYP2C9. J Biochem 144:323–333
269. Lin H, Myshkin E, Waskell L, Hollenberg PF (2007) Peroxynitrite inactivation of human cytochrome P450s 2B6 and 2E1: heme modification and site-specific nitrotyrosine formation. Chem Res Toxicol 20:1612–1622
270. Wen B, Lampe JN, Roberts AG, Atkins WM, Rodrigues AD, Nelson SD (2006) Cysteine 98 in CYP3A4 contributes to conformational integrity required for P450 interaction with CYP reductase. Arch Biochem Biophys 454:42–54
271. Lin H, Kenaan C, Zhang H, Hollenberg PF (2012) Reaction of human cytochrome P450 3A4 with peroxinitrite: nitrotyrosine formation on the proximal side impairs its interaction with NADPH-cytochrome P450 reductase. Chem Res Toxicol 25:2642–2653
272. Nikfarjam L, Izumi S, Yamazaki T, Kominami S (2006) The interaction of cytochrome P450 17α with NADPH-cytochrome P450 reductase, investigated using chemical modification and MALDI-TOF mass spectrometry. Biochim Biophys Acta 1764:1126–1131
273. Geller DH, Auchus RJ, Miller WL (1999) P450c17 mutations R347H and R358Q selectively disrupt 17,20-lyase ctivity by disrupting interactions with P450 oxidoreductase and cytochrome b_5. Mol Endocrinol 13:167–175
274. Riepe FG, Hiort O, Grötzinger J, Sippell WG, Krone N, Holterhus PM (2008) Functional and structural consequences of a novel point mutation in the *CYP21A2* gene causing congenital adrenal hyperplasia: potential relevance of helix C for P450 oxidoreductase-21-hydroxylase interaction. J Clin Endocrinol Metab 93:2891–2895
275. Lajic S, Levo A, Nikoshkov A, Lundberg Y, Partanen J, Wedell A (1997) A cluster of missense mutations at Arg356 of human steroid 21-hydroxylase may impair redox partner interaction. Hum Genet 99:704–709
276. Robins T, Carlsson J, Sunnerhagen M, Wedell A, Person B (2006) Molecular model of human CYP21 based on mammalian CYP2C5: structural features correlate with clinical severity of mutations causing congenital adrenal hyperplasia. Mol Endocrinol 20:2946–2964
277. Ji H, Zhang W, Zhou Y, Zhang M, Zhu J, Song Y, Lü J, Zhu J (2000) A three-dimesional model of lanosterol 14α-demethylase of *Candida albicans* and its interaction with azole antifungals. J Med Chem 43:2493–2505
278. Juvonen RO, Iwasaki M, Negishi M (1992) Roles of residues 129 and 209 in the alteration by cytochrome b_5 of hydroxylase activities in mouse 2A P450S. Biochemistry 31:11519–11523
279. Honkakoski P, Linnala-Kankkunen A, Usanov SA, Lang MA (1992) Highly homologous cytochromes P-450 and b_5: a model to study protein-protein interactions in a reconstituted monooxygenase system. Biochim Biophys Acta 1122:6–14
280. Omata Y, Sakamoto H, Robinson RC, Pincus MR, Friedman FK (1994) Interaction between cytochrome P450 2B1 and cytochrome b_5: inhibition by synthetic peptides indicates a role for P450 residues

Lys-122 and Arg-125. Biochem Biophys Res Commun 201:1090–1095
281. Epstein PM, Curti M, Jansson I, Huang CK, Schenkman JB (1989) Phosphorylation of cytochrome P450: regulation by cytochrome b_5. Arch Biochem Biophys 271:424–432
282. Gao Q, Doneanu CE, Shaffer SA, Adman ET, Goodlett DR, Nelson SD (2006) Identification of the interactions between cytochrome P450 2E1 and cytochrome b_5 by mass spectrometry and site-directed mutagenesis. J Biol Chem 281:20404–20417
283. Zhao C, Gao Q, Roberts AG, Shaffer SA, Doneanu CE, Xue S, Goodlett DR, Nelson SD, Atkins WM (2012) Cross-linking mass spectrometry and mutagenesis confirm the functional importance of surface interactions between CYP3A4 and holo/apo cytochrome b_5. Biochemistry 51:9488–9500
284. Lee-Robichaud P, Akhtar ME, Akhtar M (1999) Lysine mutagenesis identifies cationic charges of human CYP17 that interact with cytochrome b_5 to promote male sex-hormone biosynthesis. Biochem J 342:309–312
285. Tuls J, Geren L, Lambeth JD, Millett F (1987) The use of a specific fluorescence probe to study the interaction of adrenodoxin with adrenodoxin reductase and cytochrome P-450_{scc}. J Biol Chem 262:10020–10025
286. Adamovich TB, Pikuleva IA, Chashchin VL, Usanov SA (1989) Selective chemical modification of cytochrome P-450_{scc} lysine residues. Identification of lysines involved in the interaction with adrenodoxin. Biochim Biophys Acta 996:247–253
287. Tuls J, Geren L, Millett F (1989) Fluorescein isothiocyanate specifically modifies lysine 338 of cytochrome P-450_{scc} and inhibits adrenodoxin binding. J Biol Chem 264:16421–16425
288. Wada A, Waterman MR (1992) Identification by site-directed mutagenesis of two lysine residues in cholesterol side chain cleavage cytochrome P450 that are essential for adrenodoxin binding. J Biol Chem 267:22877–22882
289. Tsubaki M, Iwamoto Y, Hiwatashi A, Ichikawa Y (1989) Inhibition of electron transfer from adrenodoxin to cytochrome P-450_{scc} by chemical modification with pyridoxal 5′-phosphate: identification of adrenodoxin-binding site of cytochrome P-450_{scc}. Biochemistry 28:6899–6907
290. Parajes S, Loidi L, Reisch N, Dhir V, Rose IT, Hampel R, Quinkler M, Conway GS, Castro-Feijoo-L, Araujo-Vilar D, Pornbo M, Dominguez F, Williams EL, Cole TR, Kirk JM, Kaminsky E, Rumsby G, Arlt W, Krone N (2010) Functional consequences of seven novel mutations in the *CYP11B1* gene: four mutations associated with nonclassic and three mutations causing classic 11β-hydroxylase deficiency. J Clin Endocrinol Metab 95:779–788
291. Chernogolov A, Usanov S, Kraft R, Schwarz D (1994) Selective chemical modification of Cys 264 with diiodofluorescein iodacetamide as a tool to study the membrane topology of cytochrome $P450_{scc}$ (CYP11A1). FEBS Lett 340:83–88
292. Usanov SA, Graham SE, Lepesheva GI, Azeva TN, Strushkevich NV, Gilep AA, Estabrook RW, Peterson JA (2002) Probing the interaction of bovine cytochrome $P450_{scc}$ (CYP11A1) with adrenodoxin: evaluating site-directed mutations by molecular modeling. Biochemistry 41:8310–8320
293. Strushkevich NV, Harnastai IN, Usanov SA (2010) Mechanism of steroidogenic electron transport: role of conserved Glu 429 in destabilization of CYP11A1-adrenodoxin complex. Biochemistry (Mosc) 75:570–578
294. Annalora AJ, Goodin DB, Hong WX, Zhang Q, Johnson EF, Stout CD (2010) Crystal structure of CYP24A1, a mitochondrial cytochrome P450 involved in vitamin D metabolism. J Mol Biol 396:441–451
295. Urushino N, Yamamoto K, Kagawa N, Ikushiro S, Kamakura M, Yamada S, Kato S, Inouye K, Sakaki T (2006) Interaction between mitochondrial CYP27B1 and adrenodoxin: role of arginine 458 of mouse CYP27B1. Biochemistry 45:4405–4412
296. Pikuleva IA, Cao C, Waterman MR (1999) An additional electrostatic interaction between adrenodoxin and P450c27 (CYP27A1) results in tighter binding than between adrenodoxin and $P450_{scc}$ (CYP11A1). J Biol Chem 274:2045–2052
297. Kolesanova EF, Kozin SA, Rumyantsev AB, Jung C, Hui Bon Hoa G, Archakov AI (1997) Epitope mapping of cytochrome $P450_{cam}$ (CYP101). Arch Biochem Biophys 341:229–237
298. Stayton PS, Sligar SG (1990) The cytochrome P-450_{cam} binding surface as defined by site-directed mutagenesis and electrostatic modeling. Biochemistry 29:7381–7386
299. Shimada H, Nagano S, Hori H, Ishimura Y (2001) Putidaredoxin-cytochrome $P450_{cam}$ interaction. J Inorg Biochem 83:255–260
300. Unno M, Shimada H, Toba Y, Makino R, Ishimura Y (1996) Role of Arg 112 of cytochrome $P450_{cam}$ in the electron transfer from reduced putidaredoxin. J Biol Chem 271:17869–17874
301. Nagano S, Shimada H, Tarumi A, Hishiki T, Kimata-Ariga Y, Egawa T, Suematsu M, Park SY, Adachi S, Shiro Y, Ishimura Y (2003) Infrared spectroscopic and mutational studies on putidaredoxin-induced conformational changes in ferrous CO-$P450_{cam}$. Biochemistry 42:14507–14514
302. Bernhardt R, Kraft R, Alterman M, Otto A, Schrauber H, Gunsalus IC, Ruckpaul K (1992) Common mechanism of interaction between cytochrome P-450 and electron donors in different monooxygenase systems. In: Archakov AI, Bachmanova GI (eds) Cytochrome P-450:

biochemistry and biophysics. INCO-TNC, Moscow, pp 204–209
303. Koo LS, Immoos CE, Cohen MS, Farmer PJ, Ortiz de Montellano PR (2002) Enhanced electron transfer and lauric acid hydroxylation by site-directed mutagenesis of CYP119. J Am Chem Soc 124:5684–5691
304. Yang W, Bell SG, Wang H, Zhou W, Hoskins N, Dale A, Bartlam M, Wong LL, Rao Z (2010) Molecular characterization of a class I P450 electron transfer system from *Novosphingobium aromaticivorans* DSM 12444. J Biol Chem 285:27372–27384
305. Bell SG, Xu F, Forward I, Bartlam M, Rao Z, Wong LL (2008) Crystal structure of CYP199A2, a *para*-substituted benzoic acid oxidizing cytochrome P450 from *Rhodopseudomonas palustris*. J Mol Biol 383:561–574
306. Bell SG, Xu F, Johnson EOD, Forward IM, Bartlam M, Rao Z, Wong LL (2010) Protein recognition in ferredoxin-P450 electron transfer in the class I CYP199A2 system from *Rhodopseudomonas palustris*. J Biol Inorg Chem 15:315–328
307. Williams PA, Cosme J, Sridhar V, Johnson EF, McRee DE (2000) Microsomal cytochrome P450 2C5: comparison to microbial P450s and unique features. J Inorg Biochem 81:183–190
308. Golly I, Hlavica P, Schartau W (1988) The functional role of cytochrome b_5 reincorporated into hepatic microsomal fractions. Arch Biochem Biophys 260:232–240
309. Fisher GJ, Gaylor JL (1982) Kinetic investigation of rat liver microsomal electron transport from NADH to cytochrome P450. J Biol Chem 257:7449–7455
310. Golly I, Hlavica P (1993) Inactivation of phenobarbital-inducible rabbit-liver microsomal cytochrome P-450 by allylisopropylacetamide: impact on electron transfer. Biochim Biophys Acta 1142:74–82
311. Kostanjevecki V, Leys D, Van Driessche G, Meyer TE, Cusanovich MA, Fischer U, Guisez Y, Van Beeumen J (1999) Structure and characterization of *Ectothiorhodospira vacuolata* cytochrome b_{558}, a prokaryotic homologue of cytochrome b_5. J Biol Chem 274:35614–35620
312. Williams PA, Cosme J, Sridhar V, Johnson EF, McRee DE (2000) Mammalian microsomal cytochrome P450 monooxygenase: structural adaptations for membrane binding and functional diversity. Mol Cell 5:121–131
313. Geller DH, Auchus RJ, Mendonca BB, Miller WL (1997) The genetic and functional basis of isolated 17,20-lyase deficiency. Nat Genet 17:201–205
314. Hasemann CA, Kurumbail RG, Boddupalli SS, Peterson JA, Deisenhofer J (1995) Structure and function of cytochromes P450: a comparative analysis of three crystal structures. Structure 2:41–62
315. Ingelman-Sundberg M (1986) Cytochrome P450 organization and membrane interactions. In: Ortiz de Montellano PR (ed) Cytochrome P450: structure, mechanism, and biochemistry. Plenum Press, New York, pp 119–160
316. Müller-Enoch D, Churchill P, Fleischer S, Guengerich FP (1984) Interaction of liver microsomal cytochrome P-450 and NADPH-cytochrome P-450 reductase in the presence and absence of lipid. J Biol Chem 259:8174–8182
317. Balvers WG, Boersma MG, Veeger C, Rietjens MCM (1993) Kinetics of cytochromes P-450 IA1 and IIB1 in reconstituted systems with dilauroyl- and distearoyl-glycerophosphocholine. Eur J Biochem 215:373–381
318. Blanck J, Jänig GR, Schwarz D, Ruckpaul K (1989) Role of lipid in the electron transfer between NADPH-cytochrome P-450 reductase and cytochrome P-450 from mammalian liver cells. Xenobiotica 19:1231–1246
319. Balvers WG, Boersma MG, Vervoort J, Ouwehand A, Rietjens MCM (1993) A specific interaction between NADPH-cytochrome reductase and phosphatidyl serine and phosphatidyl inositol. Eur J Biochem 218:1021–1029
320. Ingelman-Sundberg M, Blanck J, Smettan G, Ruckpaul K (1983) Reduction of cytochrome P-450LM_2 by NADPH in reconstituted phospholipid vesicles is dependent on membrane charge. Eur J Biochem 134:157–162
321. Imaoka S, Imai Y, Shimada T, Funae Y (1992) Role of phospholipids in reconstituted cytochrome P450 3A form and mechanism of their activation of catalytic activity. Biochemistry 31:6063–6069
322. Causey KM, Eyer CS, Backes WL (1990) Dual role of phospholipid in the reconstitution of cytochrome P-450LM_2-dependent activities. Mol Pharmacol 38:134–142
323. Davydov DR, Sineva EV, Sistla S, Davydova NY, Frank DJ, Sligar SG, Halpert JR (2010) Electron transfer in the complex of membrane-bound human cytochrome P450 3A4 with the flavin domain of P450BM-3: the effect of oligomerization of the heme protein and intermittent modulation of the spin equilibrium. Biochim Biophys Acta 1797:378–390
324. Ingelman-Sundberg M (1977) Phospholipids and detergents as effectors in the liver microsomal hydroxylase system. Biochim Biophys Acta 488:225–234
325. Yun CH, Ahn T, Guengerich FP (1998) Conformational change and activation of cytochrome P450 2B1 induced by salt and phospholipid. Arch Biochem Biophys 356:229–238
326. Bendzko P, Usanov SA, Pfeil W, Ruckpaul K (1982) Role of the hydrophobic tail of cytochrome b_5 in the interaction with cytochrome P450LM_2. Acta Biol Med Ger 41:K1–K8
327. Golly I, Hlavica P (1987) Influence of cytochrome b_5 on electron flow from NADPH-cytochrome *c* (P-450) reductase to cytochrome P450. In: Benford DJ, Bridges JW, Gibson GG (eds) Drug metabolism

– from molecules to man. Taylor & Francis, London, pp 468–472
328. Pember SO, Powell GL, Lambeth JD (1983) Cytochrome P-450$_{scc}$-phospholipid interactions. Evidence for a cardiolipin binding site and thermodynamics of enzyme interactions with cardiolipin, cholesterol, and adrenodoxin. J Biol Chem 258:3198–3206
329. Reed JR, Backes WL (2012) Formation of P450-P450 complexes and their effect on P450 function. Pharmacol Ther 133:299–310
330. Reed JR, Eyer M, Backes WL (2010) Functional interactions between cytochromes P450 1A2 and 2B4 require both enzymes to reside in the same phospholipid vesicle. Evidence for physical complex formation. J Biol Chem 285:8942–8952
331. Kenaan C, Shea EV, Lin H, Zhang H, Pratt-Hyatt MJ, Hollenberg PF (2013) Interactions between CYP2E1 and CYP2B4: effects on affinity for NADPH-cytochrome P450 reductase and substrate metabolism. Drug Metab Dispos 41:101–110
332. Tan Y, Patten CJ, Smith T, Yang CS (1997) Competitive interactions between cytochromes P450 2A6 and 2E1 for NADPH-cytochrome P450 oxidoreductase in the microsomal membranes produced by a baculovirus expression system. Arch Biochem Biophys 342:82–91
333. Hazai E, Kupfer D (2005) Interactions between CYP2C9 and CYP2C19 in reconstituted binary systems influence their catalytic activity: possible rationale for the inability of CYP2C19 to catalyze methoxychlor demethylation in human liver microsomes. Drug Metab Dispos 33:157–164
334. Li DN, Pritchard MP, Hanlon SP, Burchell B, Wolf CR, Friedberg T (1999) Competition between cytochrome P-450 isozymes for NADPH-cytochrome P-450 oxidoreductase affects drug metabolism. J Pharmacol Exp Ther 289:661–667
335. Ikushiro S, Kominami S, Tekemori S (1992) Adrenal P-450$_{scc}$ modulates activity of P-450$_{11\beta}$ in liposomal and mitochondrial membranes. J Biol Chem 267:1464–1469
336. Hazai E, Bikadi Z, Simonyi M, Kupfer D (2005) Association of cytochrome P450 enzymes is a determining factor in their catalytic activity. J Comput Aided Mol Des 19:271–285
337. Kawato S, Gut J, Cherry RJ, Winterhalter KH, Richter C (1982) Rotation of cytochrome P-450. I. Investigations of protein-protein interactions of cytochrome P-450 in phospholipid vesicles and liver microsomes. J Biol Chem 257:7023–7029
338. Gut J, Richter C, Cherry RJ, Winterhalter KH, Kawato S (1982) Rotation of cytochrome P-450. II. Specific interactions of cytochrome P-450 with NADPH-cytochrome P-450 reductase in phospholipid vesicles. J Biol Chem 257:7030–7036
339. Gut J, Richter C, Cherry RJ, Winterhalter KH, Kawato S (1983) Rotation of cytochrome P-450. Complex formation of cytochrome P-450 with NADPH-cytochrome P-450 reductase in liposomes demonstrated by combining protein rotation with antibody-induced cross-linking. J Biol Chem 258:8588–8594
340. Yamada M, Ohta Y, Bachmanova GI, Nishimoto Y, Archakov AI, Kawato S (1995) Dynamic interactions of rabbit liver cytochromes P450 IA2 and P450 IIB4 with cytochrome b_5 and NADPH-cytochrome P450 reductase in proteoliposomes. Biochemistry 34:10113–10119
341. Whitehouse CJC, Bell SG, Wong LL (2012) P450BM3 (CYP102A1): connecting the dots. Chem Soc Rev 41:1218–1260
342. Gustafsson MCU, Roitel O, Marshall KR, Noble MA, Chapman SK, Pessegueiro A, Fulco AJ, Cheesman MR, von Wachenfeldt C, Munro AW (2004) Expression, purification, and characterization of *Bacillus subtilis* cytochromes P450 CYP102A2 and CYP102A3: flavocytochrome homologues of P450BM3 from *Bacillus megaterium*. Biochemistry 43:5474–5487
343. Chowdhary PK, Alemseghed M, Haines DC (2007) Cloning, expression and characterization of a fast self-sufficient P450: CYP102A5 from *Bacillus cereus*. Arch Biochem Biophys 468:32–43
344. Dietrich M, Eiben S, Asta C, Do TA, Pleiss J, Urlacher VB (2008) Cloning, expression and characterization of CYP102A7, a self-sufficient P450 monooxygenase from *Bacillus licheniformis*. Appl Microbiol Biotechnol 79:931–940
345. Narhi LO, Fulco AJ (1987) Identification and characterization of two functional domains in cytochrome P-450BM-3, a catalytically self-sufficient monooxygenase induced by barbiturates in *Bacillus megaterium*. J Biol Chem 262:6683–6690
346. Joyce MG, Ekanem IS, Roitel O, Dunford AJ, Neeli R, Girvan HM, Bakler GJ, Curtis RA, Munro AW, Leys D (2012) The crystal structure of the FAD/NADPH-binding domain of flavocytochrome P450BM3. FEBS J 279:1694–1706
347. Neeli R, Roitel O, Scrutton NS, Munro AW (2005) Switching pyridine nucleotide specificity in P450BM3. Mechanistic analysis of the W1046H and W1046A enzymes. J Biol Chem 280:17634–17644
348. Kitazume T, Haines DC, Estabrook RW, Chen B, Peterson JA (2007) Obligatory intermolecular electron-transfer from FAD to FMN in dimeric P450BM-3. Biochemistry 46:11892–11901
349. Klein ML, Fulco AJ (1993) Critical residues involved in FMN binding and catalytic activity in cytochrome P450BM-3. J Biol Chem 268:7553–7561
350. Sevrioukova IF, Li H, Zhang H, Peterson JA, Poulos TL (1999) Structure of a cytochrome P450-redox partner electron-transfer complex. Proc Natl Acad Sci U S A 96:1863–1868
351. Hanley SC, Ost TWB, Daff S (2004) The unusual redox properties of flavocytochrome P450BM3

flavodoxin domain. Biochem Biophys Res Commun 325:1418–1423
352. Chen HC, Swenson RP (2008) Effect of the insertion of a glycine residue into the loop spanning residues 536–541 on the semiquinone state and redox properties of the flavin- mononucleotide-binding domain of flavocytochrome P450BM-3 from *Bacillus megaterium*. Biochemistry 47:13788–13799
353. Munro AW, Malarkey K, McKnight J, Thomson AJ, Kelly SM, Prince NC, Lindsay JG, Coggins JR, Miles JS (1994) The role of tryptophan 97 of cytochrome P450BM3 from *Bacillus megaterium* in catalytic function. Biochem J 303:423–428
354. Sevrioukova IF, Hazzard JT, Tollin G, Poulos TL (1999) The FMN to heme electron transfer in cytochrome P450BM-3. Effect of chemical modification of cysteines engineered at the FMN-heme domain interaction site. J Biol Chem 274:36097–36106
355. Noble MA, Girvan HM, Smith SJ, Smith WE, Murataliev M, Guzov VM, Feyereisen R, Munro AW (2007) Analysis of the interactions of cytochrome b_5 with flavocytochrome P450BM3 and its domains. Drug Metab Rev 39:599–617
356. Kitazume T, Takaya N, Nakayama N, Shoun H (2000) *Fusarium oxysporum* fatty-acid subterminal hydroxylase (CYP505) is a membrane-bound eukaryotic counterpart of *Bacillus megaterium* cytochrome P450BM3. J Biol Chem 275:39734–39740
357. Kitazume T, Tanaka A, Takaya N, Nakamura A, Matsuyama S, Suzuki T, Shoun H (2002) Kinetic analysis of hydroxylation of saturated fatty acids by recombinant $P450_{foxy}$ produced by an *Escherichia coli* expression system. Eur J Biochem 269:2075–2082
358. Nakayama N, Takemae A, Shoun H (1996) Cytochrome $P450_{foxy}$, a catalytically self-sufficient fatty acid hydroxylase of the fungus *Fusarium oxysporum*. J Biochem 119:435–440
359. Seo JA, Proctor RH, Plattner RD (2001) Characterization of four clustered and coregulated genes associated with fumonisin biosynthesis in *Fusarium verticillioides*. Fungal Genet Biol 34:155–165
360. Seth-Smith HMB, Rosser SJ, Basran A, Travis ER, Dabbs ER, Nicklin S, Bruce NC (2002) Cloning, sequencing, and characterization of the hexahydro-1,3,5-trinitro-1,3,5-triazine degradation gene cluster from *Rhodococcus rhodochrous*. Appl Environ Microbiol 68:4764–4771
361. Sabbadin F, Jackson R, Haider K, Tampi G, Turkenburg JP, Hart S, Bruce NC, Grogan G (2009) The 1.5-Å structure of XplA-heme, an unusual cytochrome P450 heme domain that catalyzes reductive biotransformation of royal demolition explosive. J Biol Chem 284:28467–28475
362. Rylott EL, Jackson RG, Sabbadin F, Seth-Smith HMB, Edwards J, Chong CS, Strand SE, Grogan G, Bruce NC (2011) The explosive-degrading cytochrome P450 XplA: biochemistry, structural features and prospects for bioremediation. Biochim Biophys Acta 1814:230–236
363. Bui SH, McLean KJ, Cheesman MR, Bradley JM, Rigby SEJ, Levy CW, Leys D, Munro AW (2012) Unusual spectroscopic and ligand binding properties of the cytochrome P450-flavodoxin fusion enzyme XplA. J Biol Chem 287:19699–19714
364. Rylott EL, Jackson RG, Edwards J, Womack GL, Seth-Smith HMB, Rathbone DA, Strand SE, Bruce NC (2006) An explosive-degrading cytochrome P450 activity and its targeted application for the phytoremediation of RDX. Nat Biotechnol 24:216–219
365. Gassner GT, Ludwig ML, Gatti DL, Correll CC, Ballou DP (1995) Structure and mechanism of the iron-sulfur flavoprotein phthalate dioxygenase reductase. FASEB J 9:1411–1418
366. Warman AJ, Robinson JW, Luciakova D, Lawrence AD, Marshall KR, Warren MJ, Cheesman MR, Rigby EJ, Munro AW, McLean KJ (2012) Characterization of *Cupriavidus metallidurans* CYP116B1 – a thiocarbamate herbicide oxygenating P450-phthalate dioxygenase reductase fusion protein. FEBS J 279:1675–1693
367. Roberts GA, Grogan G, Greter A, Flitsch SL, Turner NJ (2002) Identification of a new class of cytochrome P450 from a *Rhodococcus* sp. J Bacteriol 184:3898–3908
368. Roberts GA, Celik A, Hunter DJB, Ost TWB, White JH, Chapman SK, Turner NJ, Flitsch SL (2003) A self-sufficient cytochrome P450 with a primary structural organization that includes a flavin domain and a [2Fe-2S] redox center. J Biol Chem 278:48914–48920
369. Hunter DJB, Roberts GA, Ost TWB, White JH, Müller S, Turner NJ, Flitsch SL, Chapman SK (2005) Analysis of the domain properties of the novel cytochrome P450 RhF. FEBS Lett 579:2215–2220
370. Celik A, Roberts GA, White JH, Chapman SK, Turner NJ, Flitsch SL (2006) Probing the substrate specificity of the catalytically self-sufficient cytochrome P450 RhF from a *Rhodococcus* sp. Chem Commun 43:4492–4494
371. Liu L, Schmid RD, Urlacher VB (2006) Cloning, expression, and characterization of a self-sufficient cytochrome P450 monooxygenase from *Rhodococcus ruber* DSM 44319. Appl Microbiol Biotechnol 72:876–882
372. McLean KJ, Girvan HM, Munro AW (2007) Cytochrome P450/redox partner fusion enzymes: biotechnological and toxicological prospects. Expert Opin Drug Metab Toxicol 3:847–863
373. Gilardi G, Meharenna YT, Tsotsou GE, Sadeghi SJ, Fairhead M, Giannini S (2002) Molecular Lego: design of molecular assemblies of P450 enzymes for nanobiotechnology. Biosens Bioelectron 17:133–145
374. Sabbadin F, Hyde R, Robin A, Hilgarth EM, Delenne M, Flitsch S, Turner N, Grogan G, Bruce NC (2010) LICRED: a versatile drop-in vector for rapid generation of redox-self-sufficient cytochrome P450s. Chembiochem 11:987–994

375. Yabusaki Y (1995) Artificial P450/reductase fusion enzymes: what can we learn from their structures? Biochimie 77:594–603
376. Yamada M, Ohta Y, Sakaki T, Yabusaki Y, Ohkawa H, Kawato S (1999) Dynamic mobility of genetically expressed fusion protein between cytochrome P450 1A1 and NADPH- cytochrome P450 reductase in yeast microsomes. Biochemistry 38:9465–9470
377. Sakaki T, Kominami S, Takemori S, Ohkawa H, Akiyoshi-Shibata M, Yabusaki Y (1994) Kinetic studies on a genetically engineered fusion enzyme between rat cytochrome P450 1A1 and yeast NADPH-P450 reductase. Biochemistry 33:4933–4939
378. Chun YJ, Jeong TC, Roh JK, Guengerich FP (1997) Characterization of a fusion protein between human cytochrome P450 1A1 and rat NADPH-P450 oxidoreductase in *Escherichia coli*. Biochem Biophys Res Commun 230:211–214
379. Shiota N, Kodama S, Inui H, Ohkawa H (2000) Expression of human cytochromes P450 1A1 and P450 1A2 as fused enzymes with yeast NADPH-cytochrome P450 oxidoreductase in transgenic tobacco plants. Biosci Biotechnol Biochem 64:2025–2033
380. Harlow GR, Halpert JR (1996) Mutagenesis study of Asp-290 in cytochrome P450 2B11 using a fusion protein with rat NADPH-cytochrome P450 reductase. Arch Biochem Biophys 326:85–92
381. Helvig C, Capdevila JH (2000) Biochemical characterization of rat P450 2C11 fused to rat or bacterial NADPH-P450 reductase domains. Biochemistry 39:5196–5205
382. Deeni YY, Paine MJ, Ayrton AD, Clarke SE, Chenery R, Wolf CR (2001) Expression, purification, and biochemical characterization of a human cytochrome P450 CYP2D6-NADPH cytochrome P450 reductase fusion protein. Arch Biochem Biophys 396:16–24
383. Inui H, Maeda A, Ohkawa H (2007) Molecular characterization of specifically active recombinant fused enzymes consisting of CYP3A4, NADPH-cytochrome P450 oxidoreductase, and cytochrome b_5. Biochemistry 46:10213–10221
384. Chaurasia CS, Alterman MA, Lu P, Hanzlik RP (1995) Biochemical characterization of lauric acid ω-hydroxylation by a CYP4A1/NADPH-cytochrome P450 reductase fusion protein. Arch Biochem Biophys 317:161–169
385. Shet MS, Fisher CW, Holmans PL, Estabrook RW (1996) The ω-hydroxylation of lauric acid: oxidation of 12-hydroxylauric acid to dodecanedioic acid by a purified recombinant fusion protein containing P450 4A1 and NADPH-P450 reductase. Arch Biochem Biophys 330:199–208
386. Shet MS, Fisher CW, Arlotto MP, Shackleton CHL, Holmans PL, Martin-Wixtrom CA, Salki Y, Estabrook RW (1994) Purification and enzymatic properties of a recombinant fusion protein expressed in *Escherichia coli* containing the domains of bovine P450 17A and rat NADPH-P450 reductase. Arch Biochem Biophys 311:402–417
387. Shet MS, Fisher CW, Estabrook RW (1997) The function of recombinant cytochrome P450s in intact *Escherichia coli* cells: the 17α-hydroxylation of progesterone and pregnenolone by P450c17. Arch Biochem Biophys 339:218–225
388. Shibata M, Sakaki T, Yabusaki Y, Murakami H, Ohkawa H (1990) Genetically engineered P450 monooxygenases: construction of bovine P450c17/yeast reductase fused enzymes. DNA Cell Biol 9:27–36
389. Shet MS, Fisher CW, Tremblay Y, Belanger A, Conley AJ, Mason JI, Estabrook RW (2007) Comparison of the 17α-hydroxylase/C17,20-lyase activities of porcine, guinea pig and bovine P450c17 using purified recombinant fusion proteins containing P450c17 linked to NADPH-P450 reductase. Drug Metab Rev 39:289–307
390. Sakaki T, Shibata M, Yabusaki Y, Murakami H, Ohkawa H (1990) Expression of bovine cytochrome P450c21 and its fused enzymes with yeast NADPH-cytochrome P450 reductase in *Saccharomyces cerevisiae*. DNA Cell Biol 9:603–614
391. Sakaki T, Kominami S, Hayashi K, Akiyoshi-Shibata M, Yabusaki Y (1996) Molecular engineering study on electron transfer from NADPH-P450 reductase to rat mitochondrial P450c27 in yeast microsomes. J Biol Chem 271:26209–26213
392. Venkateswarlu K, Kelly DE, Kelly SL (1997) Characterization of *Saccharomyces cerevisiae* CYP51 and a CYP51 fusion protein with NADPH-cytochrome P-450 oxidoreductase expressed in *Escherichia coli*. Antimicrob Agents Chemother 41:776–780
393. Lamb SB, Lamb DC, Kelly SL, Stuckey DC (1998) Cytochrome P450 immobilization as a route to bioremediation/biocatalysis. FEBS Lett 431:343–346
394. Hotze M, Schröder G, Schröder J (1995) Cinnamate 4-hydroxylase from *Catharanthus roseus*, and a strategy for the functional expression of plant cytochrome P450 proteins as translational fusions with P450 reductase in *Escherichia coli*. FEBS Lett 374:345–350
395. Schückel J, Rylott EL, Grogan G, Bruce NC (2012) A gene-fusion approach to enabling plant cytochromes P450 for biocatalysis. Chembiochem 13:2758–2763
396. Didierjean L, Gondet L, Perkins R, Lau SMC, Schaller H, O'Keefe DP, Werck-Reichhart D (2002) Engineering herbicide metabolism in tobacco and Arabidopsis with CYP76B1, a cytochrome P450 enzyme from Jerusalem artichoke. Plant Physiol 130:179–189
397. Porter TD (1991) An unusual yet strongly conserved flavoprotein reductase in bacteria and mammals. Trends Biochem Sci 16:154–158
398. Dodhia VR, Fantuzzi A, Gilardi G (2006) Engineering human cytochrome P450 enzymes into

catalytically self-sufficient chimeras using molecular Lego. J Biol Inorg Chem 11:903–916
399. Rua F, Sadeghi SJ, Castrignano S, Di Nardo G, Gilardi G (2012) Engineering *Macaca fascicularis* cytochrome P450 2C20 to reduce animal testing for new drugs. J Inorg Biochem 117:277–284
400. Fairhead M, Giannini S, Gillam EMJ, Gilardi G (2005) Functional characterization of an engineered multidomain human P450 2E1 by molecular Lego. J Biol Inorg Chem 10:842–853
401. Degregorio D, Sadeghi SJ, Di Nardo G, Gilardi G, Solinas SP (2011) Understanding uncoupling in the multiredox centre P450 3A4-BMR model system. J Biol Inorg Chem 16:109–116
402. Fuziwara S, Sagami I, Rozhkova E, Craig D, Noble MA, Munro AW, Chapman SK, Shimizu T (2002) Catalytically functional flavocytochrome chimeras of P450BM3 and nitric oxide synthase. J Inorg Biochem 91:515–526
403. Choi KY, Jung E, Jung DH, An BR, Pandey BP, Yun H, Sung C, Park HY, Kim BG (2012) Engineering of daidzein 3′-hydroxylase P450 enzyme into catalytically self-sufficient cytochrome P450. Microb Cell Factories 11:81–90
404. Lacour T, Ohkawa H (1999) Engineering and biochemical characterization of the rat micro- somal cytochrome P450 1A1 fused to ferredoxin and ferredoxin-$NADP^+$ reductase from plant chloroplasts. Biochim Biophys Acta 1433:87–102
405. Harikrishna JA, Black SM, Szklarz GD, Miller WL (1993) Construction and function of fusion enzymes of the human cytochrome $P450_{scc}$ system. DNA Cell Biol 12:371–379
406. Cao P, Bülow H, Dumas B, Bernhardt R (2000) Construction and characterization of a catalytic fusion protein system: P-$450_{11\beta}$-adrenodoxin reductase-adrenodoxin. Biochim Biophys Acta 1476:253–264
407. Dilworth FJ, Black SM, Guo YD, Miller WL, Jones G (1996) Construction of a P450c27 fusion enzyme: a useful tool for analysis of vitamin D_3 25-hydroxylase activity. Biochem J 320:267–271
408. Hirakawa H, Kamiya N, Tanaka T, Nagamune T (2007) Intramolecular electron transfer in a cytochrome $P450_{cam}$ system with a site-specific branched structure. Protein Eng Des Sel 20:453–459
409. Hirakawa H, Nagamune T (2010) Molecular assembly of P450 with ferredoxin and ferredoxin reductase by fusion to PCNA. Chembiochem 11:1517–1520
410. Mandai T, Fujiwara S, Imaoka S (2009) Construction and engineering of a thermostable self-sufficient cytochrome P450. Biochem Biophys Res Commun 384:61–65
411. Kubota M, Nodate M, Yasumoto-Hirose M, Uchiyama T, Kagami O, Shizuri Y, Misawa N (2005) Isolation and functional analysis of cytochrome P450 CYP153A genes from various environments. Biosci Biotechnol Biochem 69:2421–2430
412. Bordeaux M, Galarneau A, Fajula F, Drone J (2011) A regioselective biocatalyst for alkane activation under mild conditions. Angew Chem Int Ed 50:2075–2079
413. Nodate M, Kubota M, Misawa N (2006) Functional expression system for cytochrome P450 genes using the reductase domain of self-sufficient P450RhF from *Rhodococcus* sp. NCIMB 9784. Appl Microbiol Biotechnol 71:455–462
414. Li S, Podust LM, Sherman DH (2007) Engineering and analysis of a self-sufficient biosynthetic cytochrome P450 PikC fused to the RhFRED reductase domain. J Am Chem Soc 129:12940–12941
415. Li S, Chaulagain M, Knauff AR, Podust LM, Montgomery J, Sherman DH (2009) Selective oxidation of carbolide C-H bonds by an engineered macrolide P450 mono-oxygenase. Proc Natl Acad Sci U S A 106:18463–18468
416. Choi KY, Jung EO, Jung DH, Pandey BP, Lee N, Yun H, Park H, Kim BG (2012) Novel iron-sulfur containing NADPH-reductase from *Nocardia farcinica* IFM 10152 and fusion construction with CYP51 lanosterol demethylase. Biotechnol Bioeng 109:630–636
417. Ortiz de Montellano PR (1995) Oxygen activation and reactivity. In: Ortiz de Montellano PR (ed) Cytochrome P450: structure, mechanism, and biochemistry, 2nd edn. Plenum Press, New York, pp 245–303
418. Fujishiro T, Shoji O, Nagano S, Sugimoto H, Shiro Y, Watanabe Y (2011) Crystal structure of H_2O_2-dependent cytochrome $P450_{SP\alpha}$ with its bound fatty acid substrate. Insight into the regioselective hydroxylation of fatty acids at the α-position. J Biol Chem 286:29941–29950
419. Matsunaga I, Yamada A, Lee DS, Obayashi E, Fujiwara N, Kobayashi K, Ogura H, Shiro Y (2002) Enzymatic reaction of hydrogen peroxide-dependent peroxygenase cytochrome P450s: kinetic deuterium isotope effects and analyses by resonance Raman spectroscopy. Biochemistry 41:1886–1892
420. Rude MA, Baron TS, Brubaker S, Alibhai M, Del Cardayre SB, Schirmer A (2011) Terminal olefin (1-alkene) biosynthesis by a novel P450 fatty acid decarboxylase from *Jeotgalicoccus* species. Appl Environ Microbiol 77:1718–1727
421. Niraula NP, Kanth BK, Sohng JK, Oh TJ (2011) Hydrogen peroxide-mediated dealkylation of 7-ethoxycoumarin by cytochrome P450 (CYP107AJ1) from *Streptomyces peucetius* ATCC 27952. Enzyme Microb Technol 48:181–186
422. Thompson CM, Capdevila JH, Strobel HW (2000) Recombinant cytochrome P450 2D18 metabolism of dopamine and arachidonic acid. J Pharmacol Exp Ther 294:1120–1130
423. Hlavica P, Golly I, Mietaschk J (1983) Comparative studies on the cumene hydroperoxide- and NADPH-supported N-oxidation of 4-chloroaniline. Biochem J 212:539–547

424. Golly I, Hlavica P, Wolf J (1984) The role of lipid peroxidation in the N-oxidation of 4-chloroaniline. Biochem J 224:415–421
425. Yoshigae Y, Kent UM, Hollenberg PF (2013) Role of the highly conserved threonine in cytochrome P450 2E1: prevention of H_2O_2-induced inactivation during electron transfer. Biochemistry 52:4636–4647
426. Chefson A, Zhao J, Auclair K (2006) Replacement of natural cofactors by selected hydrogen peroxide donors or organic peroxides results in improved activity for CYP3A4 and CYP2D6. Chembiochem 7:916–919
427. Kumar S, Liu H, Halpert JR (2006) Engineering of cytochrome P450 3A4 for enhanced peroxide-mediated substrate oxidation using directed evolution and site-directed mutagenesis. Drug Metab Dispos 34:1958–1965
428. Joo H, Lin Z, Arnold FH (1999) Laboratory evolution of peroxide-mediated cytochrome P450 hydroxylation. Nature 399:670–673
429. Cirino PC, Arnold FH (2002) Regioselectivity and activity of cytochrome P450BM-3 and mutant F87A in reactions driven by hydrogen peroxide. Adv Synth Catal 344:932–937
430. Cirino PC, Arnold FH (2003) A self-sufficient peroxide-driven hydroxylation biocatalyst. Angew Chem Int Ed 42:3299–3301
431. Vidal-Limon A, Aguila S, Ayala M, Batista CV, Vasquez-Duhalt R (2013) Peroxidase activity stabilization of cytochrome P450BM3 by rational analysis of intramolecular electron transfer. J Inorg Biochem 122:18–26
432. Salazar O, Cirino PC, Arnold FH (2003) Thermostabilization of a cytochrome P450 peroxygenase. Chembiochem 4:891–893
433. Holtmann D, Schrader J (2007) Approaches to recycling and substituting NAD(P)H as a CYP cofactor. In: Schmid RD, Urlacher VB (eds) Modern biooxidation: enzymes, reactions and applications. Wiley-VCH Verlag, Weinheim, pp 265–290
434. Li S, Wackett LP (1993) Reductive dehalogenation by cytochrome $P450_{cam}$: substrate binding and catalysis. Biochemistry 32:9355–9361
435. Tran NH, Huynh N, Chavez G, Nguyen A, Dwaraknath S, Nguyen TA, Nguyen M, Cheruzel L (2012) A series of hybrid P450BM3 enzymes with different catalytic activity in the light-initiated hydroxylation of lauric acid. J Inorg Biochem 115:50–56
436. Ipe BI, Lehnig M, Niemeyer CM (2005) On the generation of free radical species from quantum dots. Small 7:706–709
437. Ipe BI, Shukla A, Lu H, Zou B, Rehage H, Niemeyer CM (2006) Dynamic light-scattering analysis of the electrostatic interaction of hexahistidine-tagged cytochrome P450 enzyme with semiconductor quantum dots. Chemphyschem 7:1112–1118
438. Fruk L, Rajendran V, Spengler M, Niemeyer CM (2007) Light-induced triggering of peroxidase activity using quantum dots. Chembiochem 8:2195–2198
439. Gandubert VJ, Torres E, Niemeyer CM (2008) Investigation of cytochrome P450- modified cadmium sulfide quantum dots as photocatalysts. J Mater Chem 18:3824–3830
440. Sadeghi SJ, Fantuzzi A, Gilardi G (2011) Breakthrough in P450 bioelectrochemistry and future perspectives. Biochim Biophys Acta 1814:237–248
441. Shumyantseva VV, Bulko TV, Usanov SS, Schmid RD, Nicolini C, Archakov AI (2001) Construction and characterization of bioelectrocatalytic sensors based on cytochrome P450. J Inorg Biochem 87:185–190
442. Rudakov YO, Shumyantseva VV, Bulko TV, Suprun EV, Kuznetsova GP, Samenkova NF, Archakov AI (2008) Stoichiometry of electrocatalytic cycle of cytochrome P450 2B4. J Inorg Biochem 102:2020–2025
443. Shumyantseva VV, Ivanov YD, Bistolas N, Scheller FW, Archakov AI, Wollenberger U (2004) Direct electron transfer of cytochrome P450 2B4 at electrodes modified with nonionic detergent and colloidal clay nanoparticles. Anal Chem 76:6046–6052
444. Liu S, Peng L, Yang X, Wu Y, He L (2008) Electrochemistry of cytochrome P450 enzyme on nanoparticle-containing membrane-coated electrode and its applications for drug sensing. Anal Biochem 375:209–216
445. Zu X, Lu Z, Zhang Z, Schenkman JB, Rusling JF (1999) Electroenzyme-catalyzed oxidation of styrene and *cis*-β-methylstyrene using thin films of cytochrome $P450_{cam}$ and myoglobin. Langmuir 15:7372–7377
446. Estavillo C, Lu Z, Jansson I, Schenkman JB, Rusling JF (2003) Epoxidation of styrene by human cytochrome P450 1A2 by thin film electrolysis and peroxide activation compared to solution reactions. Biophys Chem 104:291–296
447. Fantuzzi A, Fairhead M, Gilardi G (2004) Direct electrochemistry of immobilized human cytochrome P450 2E1. J Am Chem Soc 126:5040–5041
448. Joseph S, Rusling JF, Lvov YM, Friedberg T, Fuhr U (2003) An amperometric biosensor with human CYP3A4 as a novel drug screening tool. Biochem Pharmacol 65:1817–1826
449. Yang M, Kabulski JL, Wollenberg L, Chen X, Subramanian M, Tracy TS, Lederman D, Gannett PM, Wu N (2009) Electrocatalytic drug metabolism by CYP2C9 bonded to a self-assembled monolayer-modified electrode. Drug Metab Dispos 37:892–899
450. Urlacher VB, Girhard M (2012) Cytochrome P450 monooxygenases: an update on perspectives for synthetic application. Trends Biotechnol 30:26–36
451. Julsing MK, Cornelissen S, Bühler B, Schmid A (2008) Heme-iron oxygenases: powerful industrial biocatalysts? Curr Opin Chem Biol 12:177–186
452. Bureik M, Bernhardt R (2007) Steroid hydroxylation: microbial steroid biotransformations using cytochrome P450 enzymes. In: Schmid RD,

Urlacher VB (eds) Modern biooxidation: enzymes, reactions and applications. Wiley-VCH Verlag, Weinheim, pp 155–176
453. Park JW, Lee JK, Kwon TJ, Yi DH, Kim YJ, Moon SH, Suh HH, Kang SM, Park YI (2003) Bioconversion of compactin into pravastatin by *Streptomyces* sp. Biotechnol Lett 25:1827–1831
454. Ro DK, Paradise EM, Ouellet M, Fisher KJ, Newman KL, Ndungu JM, Ho KA, Eachus RA, Ham TS, Kirby J, Chang CY, Withers ST, Shiba Y, Sarpong R, Keasling JD (2006) Production of the antimalarial drug precursor artemisinic acid in engineered yeast. Nature 440:940–943
455. Liu S, Li C, Fang X, Cao Z (2004) Optimal pH control strategy for high-level production of long-chain α, ω-dicarboxylic acid by Candida tropicalis. Enzym Microb Technol 34:73–77
456. Roy P, Waxman DJ (2006) Activation of oxazaphosphorines by cytochrome P450: application to gene-directed enzyme prodrug therapy of cancer. Toxicol In Vitro 20:176–186
457. Kumar S, Chen CS, Waxman DJ, Halpert JR (2005) Directed evolution of mammalian cytochrome P450 2B1. Mutations outside of the active site enhance the metabolism of several substrates, including the anticancer prodrugs cyclophosphamide and ifosfamide. J Biol Chem 280:19569–19575
458. Sun L, Chen CS, Waxman DJ, Liu H, Halpert JR, Kumar S (2007) Re-engineering cytochrome P450 2B11dH for enhanced metabolism of several substrates including anti-cancer prodrugs cyclophosphamide and ifosfamide. Arch Biochem Biophys 458:167–174
459. Nguyen TA, Tychpoulos M, Bichat F, Zimmermann C, Flinois JP, Diry M, Ahlberg E, Delaforge M, Corcos L, Beaune P, Dansette P, Andre F, de Waziers I (2008) Improvement of cyclophosphamide activation by CYP2B6 mutants: from in silico to ex vivo. Mol Pharmacol 73:1122–1133
460. Tychopoulos M, Corcos L, Genne P, Beaune P, de Waziers I (2005) A virus-directed enzyme prodrug therapy (VDEPT) strategy for lung cancer using a CYP2B6/NADPH-cytochrome P450 reductase fusion protein. Cancer Gene Ther 12:497–508
461. Kawahigashi H, Hirose S, Ohkawa H, Ohkawa Y (2006) Phytoremediation of the herbicides atrazine and metolachlor by transgenic rice plants expressing human CYP1A1, CYP2B6, and CYP2C19. J Agric Food Chem 54:2985–2991
462. Jackson RG, Rylott EL, Fournier D, Hawari J, Bruce NC (2007) Exploring the biochemical properties and remediation applications of the unusual explosive-degrading P450 system XplA/B. Proc Natl Acad Sci U S A 104:16822–16827
463. Chun YJ, Shimada T, Guengerich FP (1996) Construction of a human cytochrome P450 1A1–rat NADPH-cytochrome P450 reductase fusion protein cDNA and expression in *Escherichia coli*, purification, and catalytic properties of the enzyme in bacterial cells and after purification. Arch Biochem Biophys 330:48–58
464. Carmichael AB, Wong LL (2001) Protein engineering of *Bacillus megaterium* CYP102. The oxidation of polycyclic aromatic hydrocarbons. Eur J Biochem 268:3117–3125
465. Syed K, Porollo A, Miller D, Yadav JS (2013) Rational engineering of the fungal P450 monooxygenase CYP5136A3 to improve its oxidizing activity toward polycyclic aromatic hydrocarbons. Protein Eng Des Sel 26:553–557
466. Kanaly RA, Harayama S (2000) Biodegradation of high-molecular-weight polycyclic aromatic hydrocarbons by bacteria. J Bacteriol 182:2059–2067
467. Bistolas N, Wollenberger U, Jung C, Scheller FW (2005) Cytochrome P450 biosensors – a review. Biosens Bioelectron 20:2408–2423
468. Wang Y, Xu H, Zhang J, Li G (2008) Electrochemical sensors for clinic analysis. Sensors 8:2043–2081
469. Ansede JH, Thakker DR (2004) High-throughput screening for stability and inhibitory activity of compounds toward cytochrome P450-mediated metabolism. J Pharm Sci 93:239–255